Aligning point clouds and topographic change detection

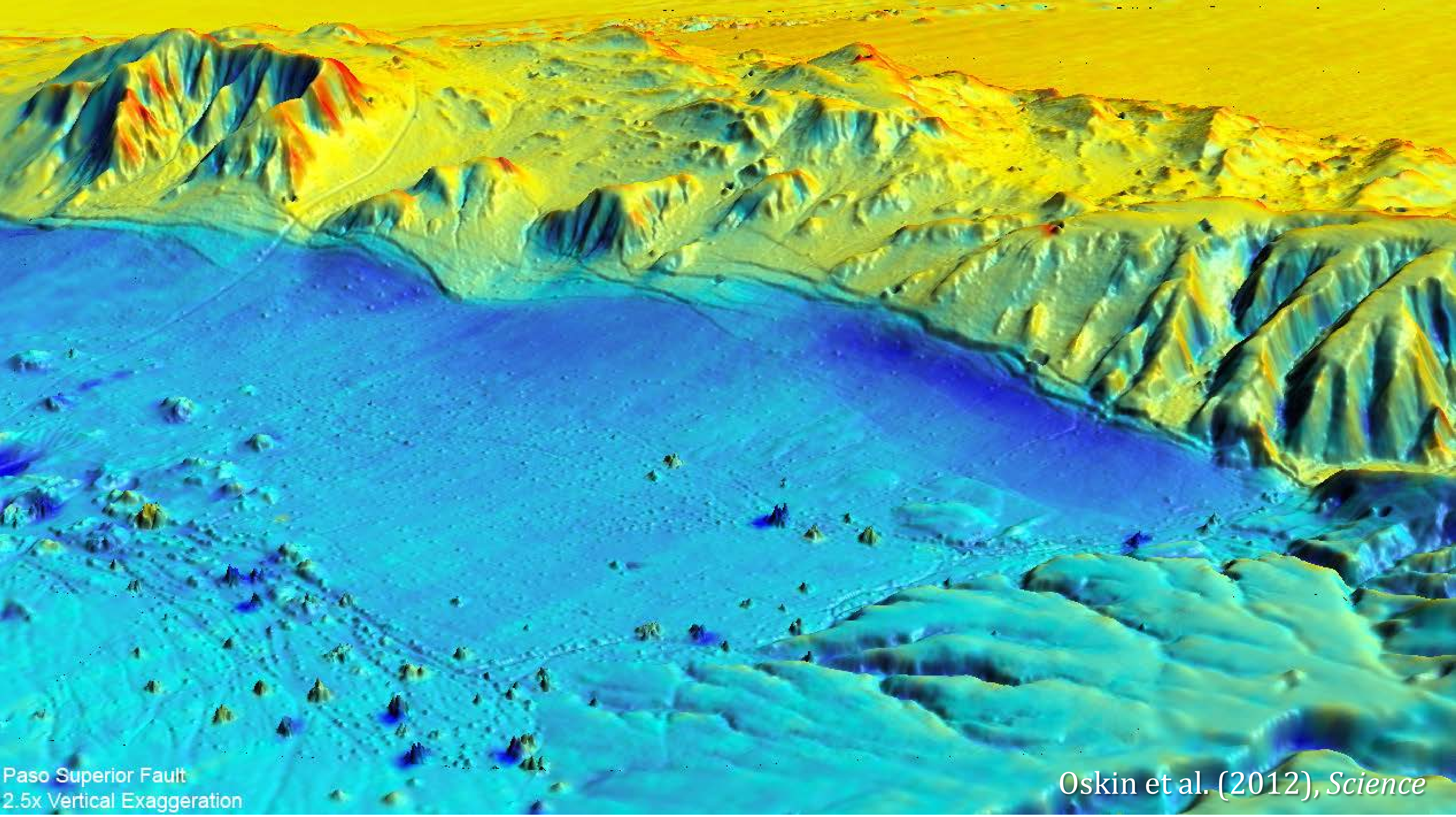

Edwin Nissen (Colorado School of Mines)

Thanks to: Ramon Arrowsmith, Srikanth Saripalli, Aravindhan Krishnan (ASU), Adrian Borsa (Scripps), Craig Glennie (Houston), Alejandro Hinojosa-Corona (CICESE), Tadashi Maruyama (AIST), Austin Elliott, Mike Oskin (UC Davis)

Aligning point clouds and topographic change detection

- Multi-temporal topography
- Earthquake examples:
  - scientific motivation
  - aligning (registering) topography data with ICP
  - 2008 Iwate earthquake (Japan)
  - 2011 Fukushima earthquake (Japan)
  - 2010 El Mayor Cucapah earthquake (Mexico)
- Other applications

Paso Superior Fault
2.5x Vertical Exaggeration

Aligning point clouds and topographic change detection

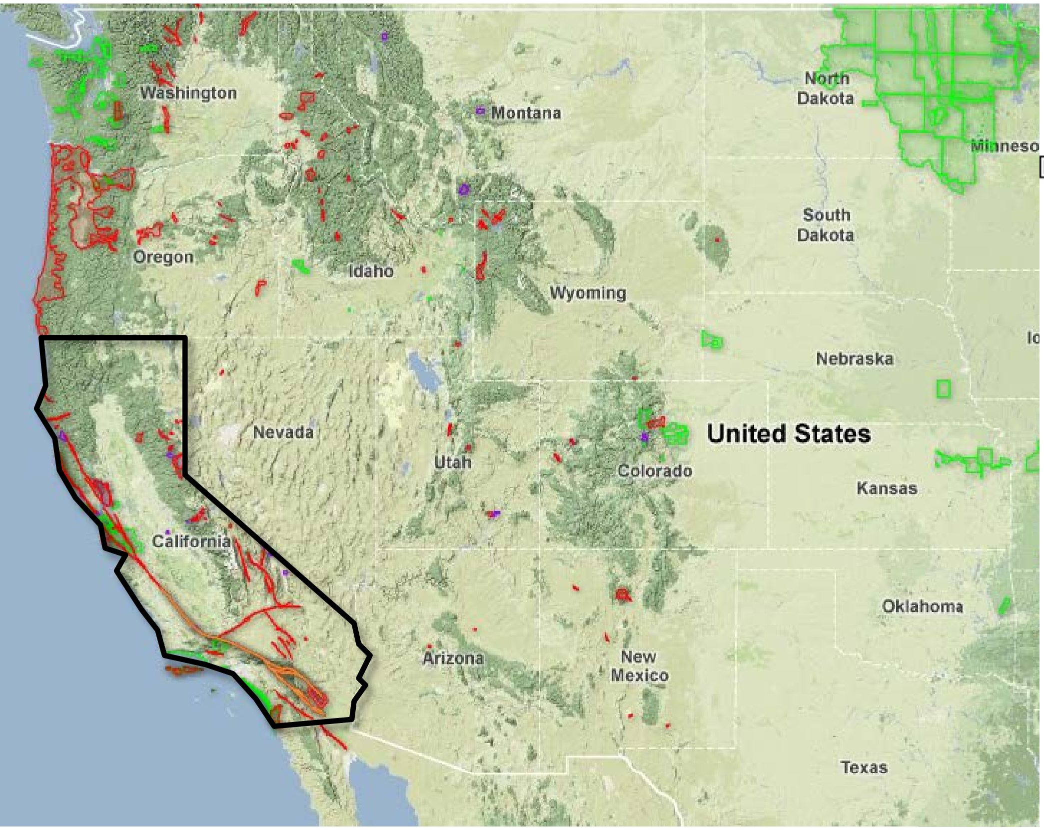

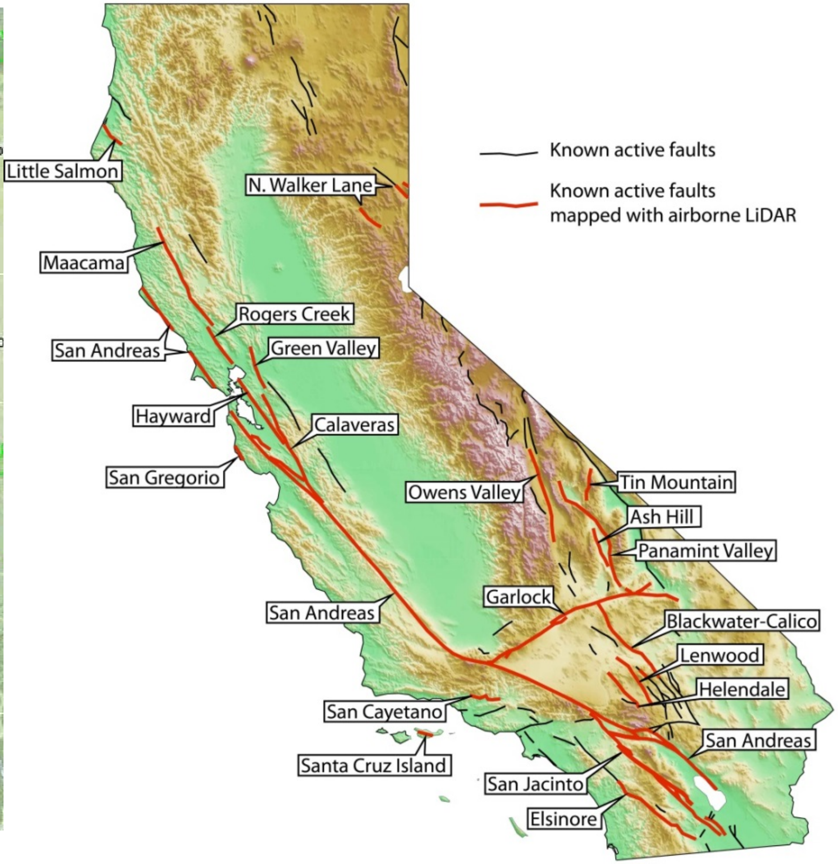

www.opentopography.org

- There is now a “baseline” of lidar topography on many active faults in the western US
- After an earthquake, repeat lidar data can be collected and differenced

Measuring fault slip – far field

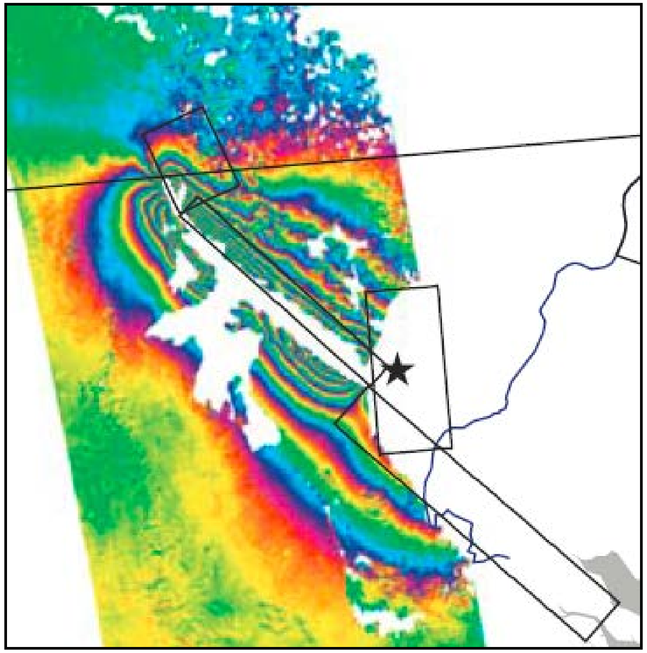

Wei et al. (2011), *Nat. Geosci.*

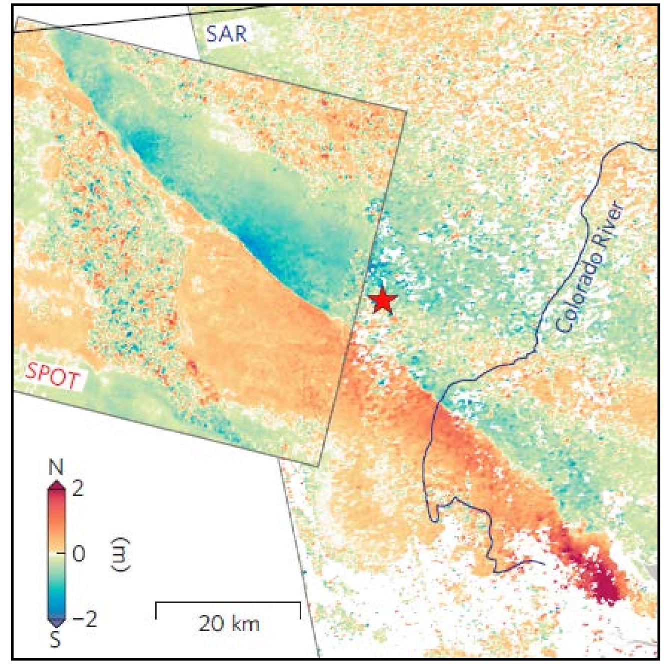

Radar interferometry (InSAR)

- Precise (sub-centimetric) line-of-sight displacements over wide areas
- Breaks down amongst dense vegetation and steep deformation gradients (e.g. along surface ruptures)

Pixel cross-correlation

- Horizontal displacements over wide areas
- Decorrelates in dense vegetation and with changes in surface reflectance (e.g. agriculture, seasonal change)

Measuring fault slip – far field

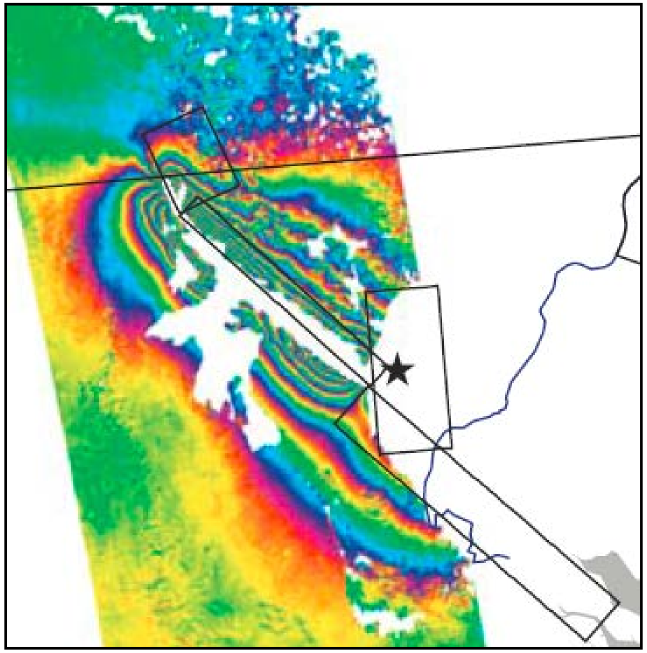

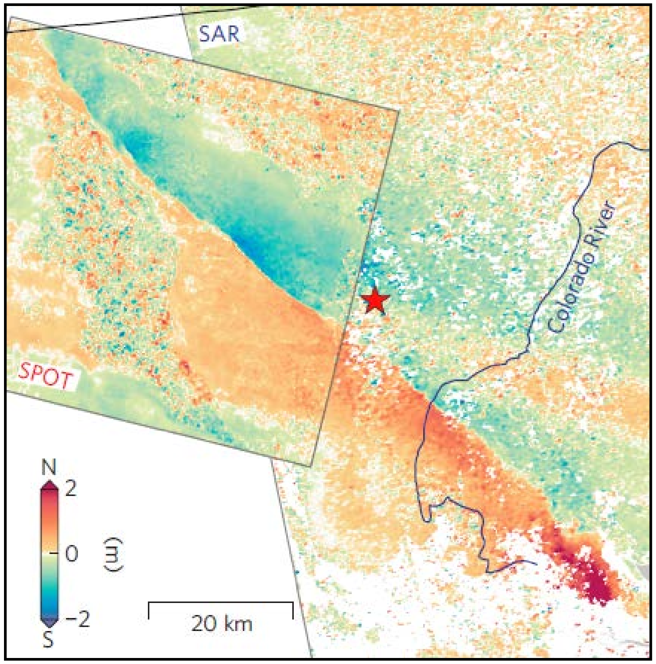

Wei et al. (2011), *Nat. Geosci.*

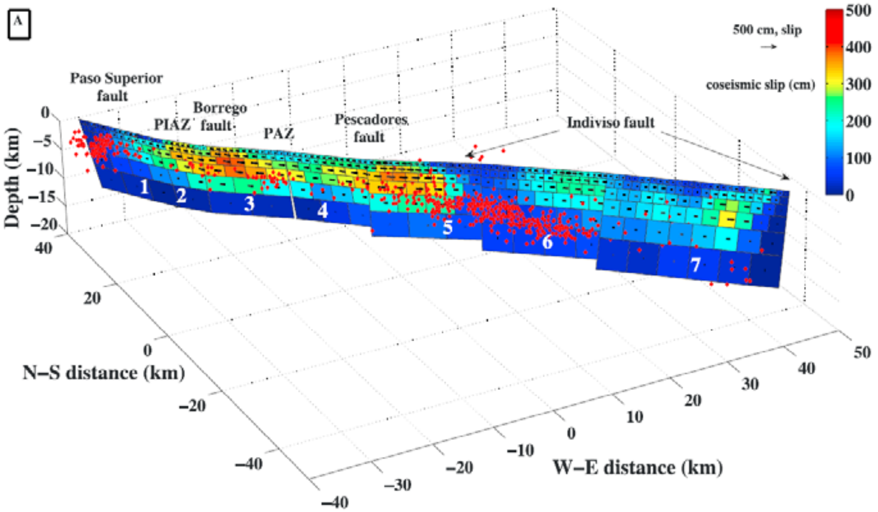

Fialko *et al.* (2010), *AGU Fall Meeting*

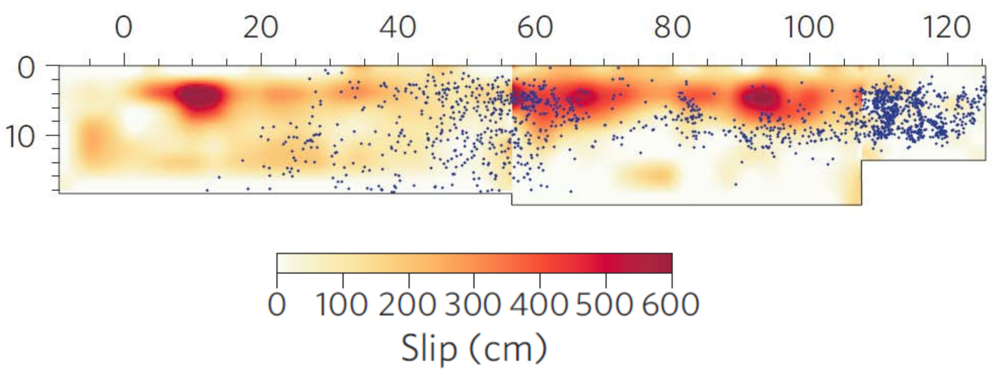

Wei *et al.* (2011), *Nat. Geosci.*

Measuring fault slip – near field

- Time consuming and subject to measurement error and misinterpretation
- Typically shows high scatter – genuine slip heterogeneity or not?

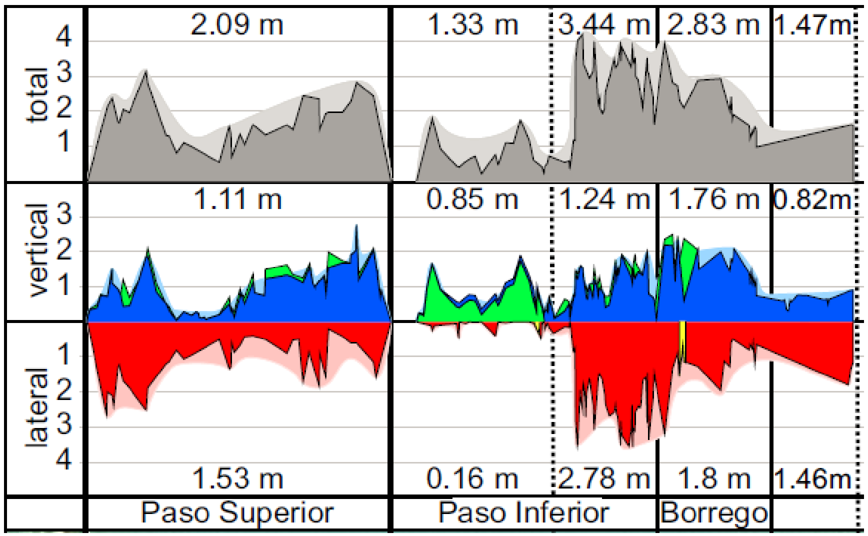

Fletcher *et al.* (2014), *Geosphere*

Teran *et al.* (2015), *Geosphere*

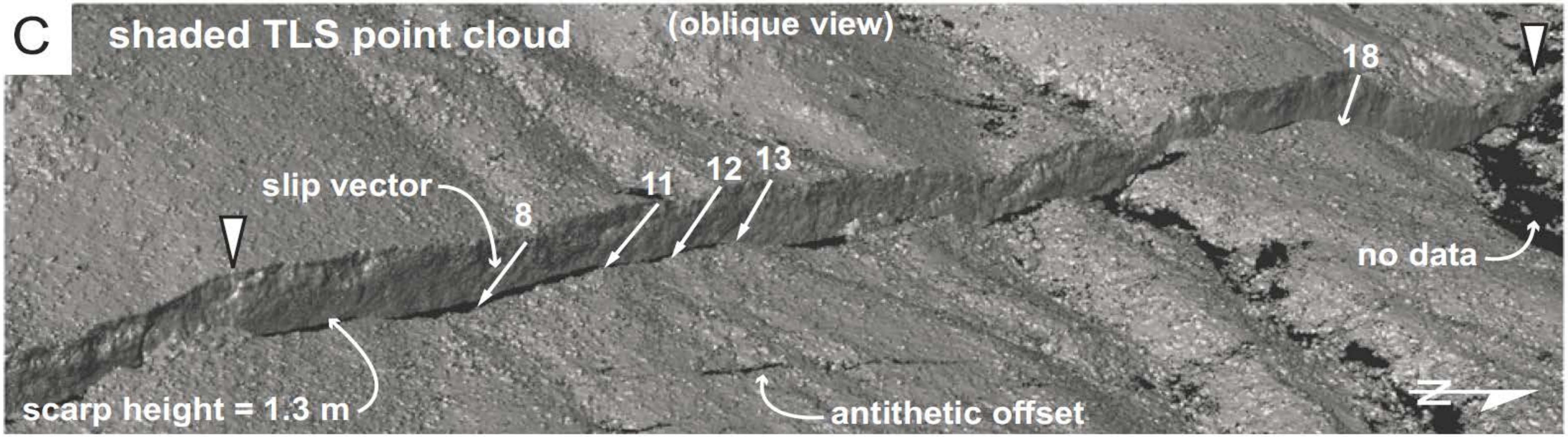

Gold *et al.* (2013), *EPSL*

Shallow slip deficit

• The observation that in large, ground-rupturing earthquakes, slip at depths of 100s to 1000s of meters commonly exceeds surface offsets surveyed at the fault scarp

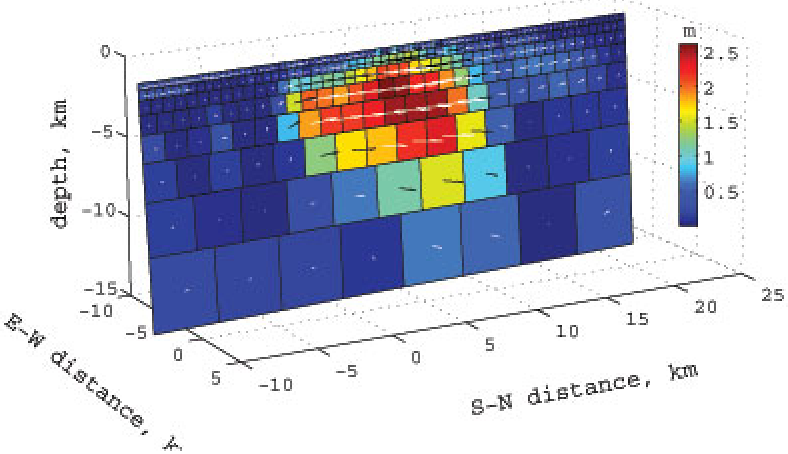

Fialko *et al.* (2005), *Nature*

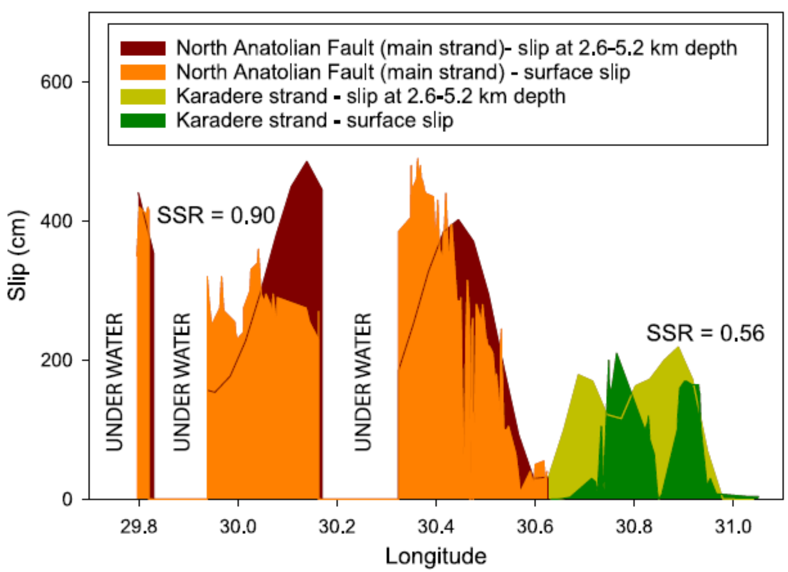

Dolan & Haravitch (2014), *EPSL*

Reflects:

• Genuine loss of slip made up during other parts of the earthquake cycle (e.g. afterslip)?

• Redistribution of slip in near-surface onto subsidiary small faults and fractures?

• artifacts that arise when InSAR data with poor correlation near the surface rupture are inverted for slip at depth?

Controlled by:

• Material properties?

• Fault structural maturity?

• Fault geometry?

• Earthquake magnitude?

Measuring fault slip – near field

Far-field

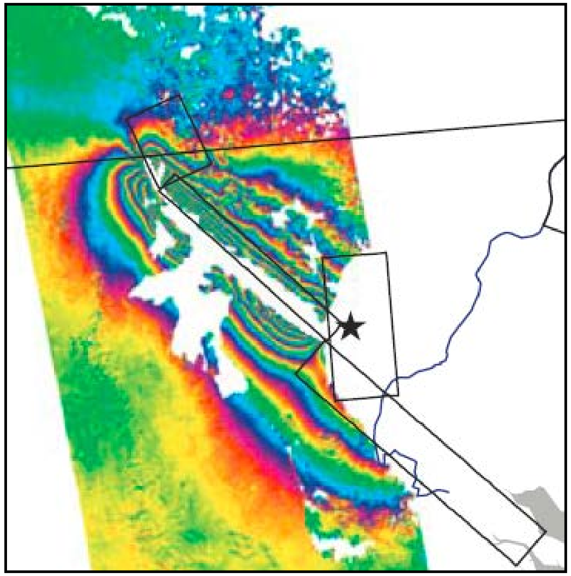

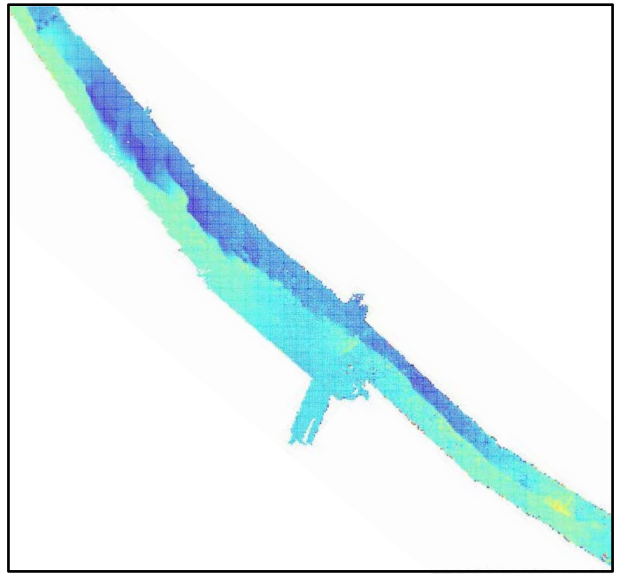

Near-field

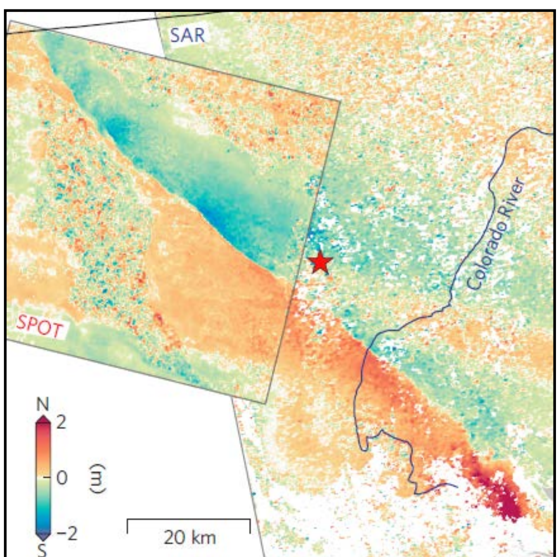

Differential lidar

- 3-D displacements within narrow fault zone swaths
- Shallow slip and mechanical behavior of the interior fault zone
- Remains coherent over long time-spans and in dense vegetation

Wei *et al.* (2011), *Nat. Geosci.*

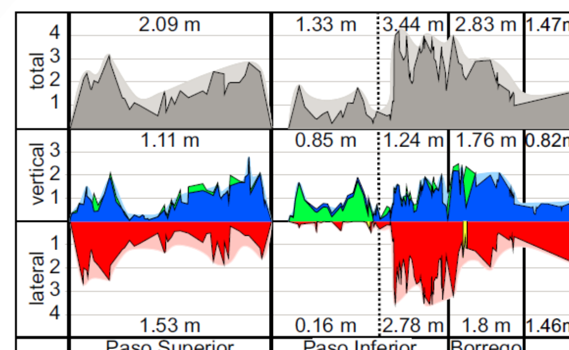

Teran *et al.* (2014), *Geosphere*

Fletcher *et al.* (2014), *Geosphere*

3-D earthquake deformation from repeat lidar

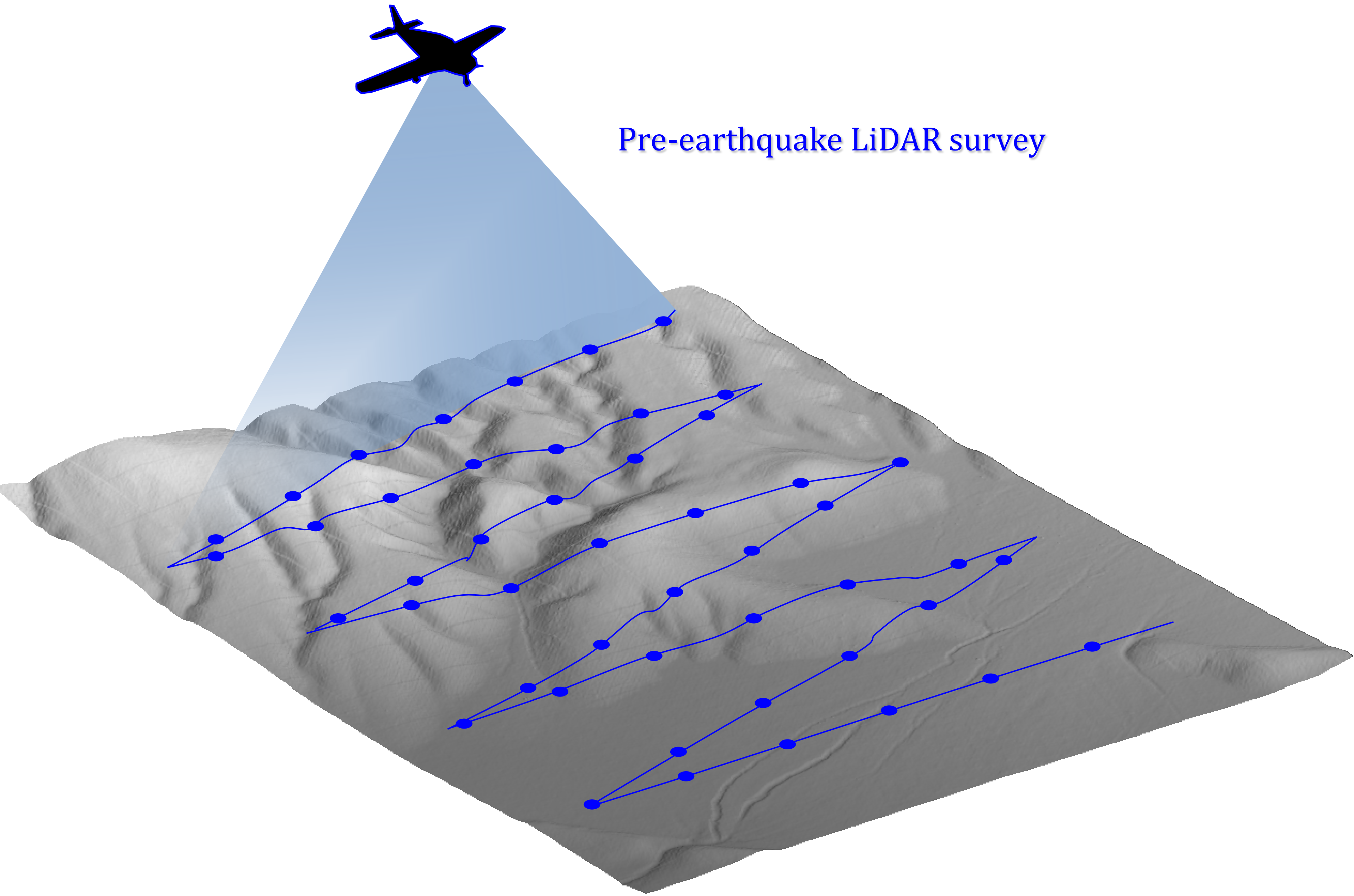

3-D earthquake deformation from repeat lidar

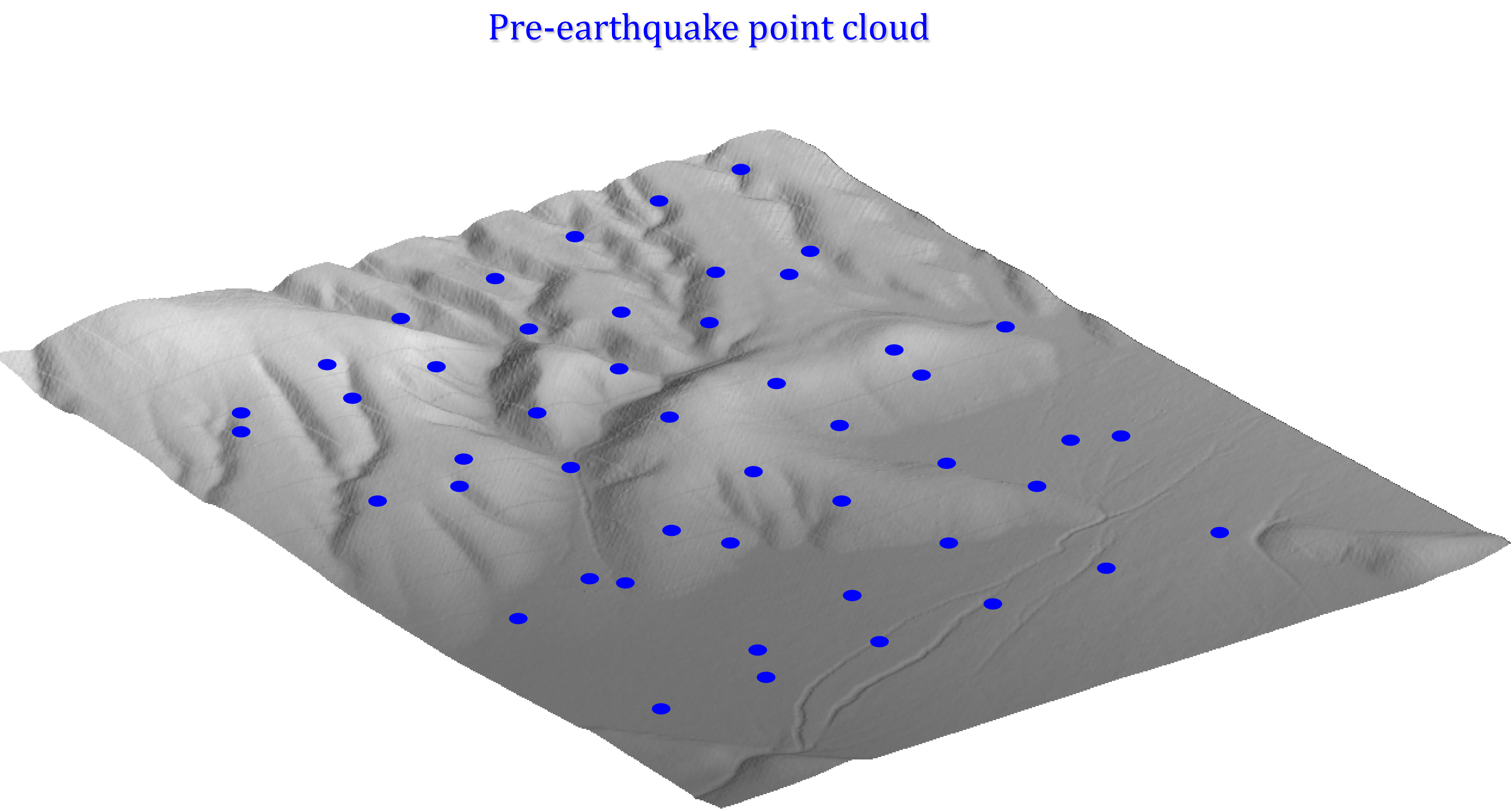

3-D earthquake deformation from repeat lidar

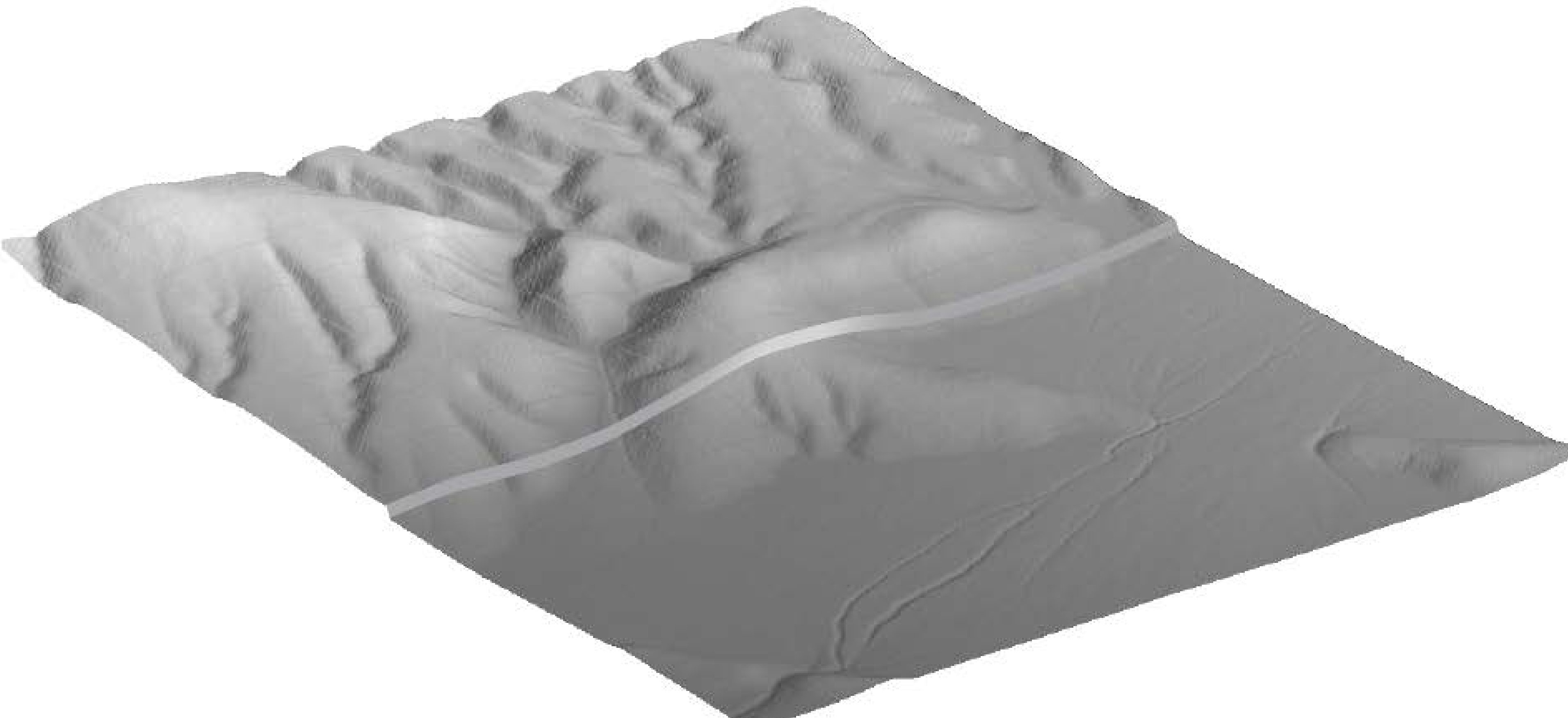

3-D earthquake deformation from repeat lidar

Post-earthquake LiDAR survey

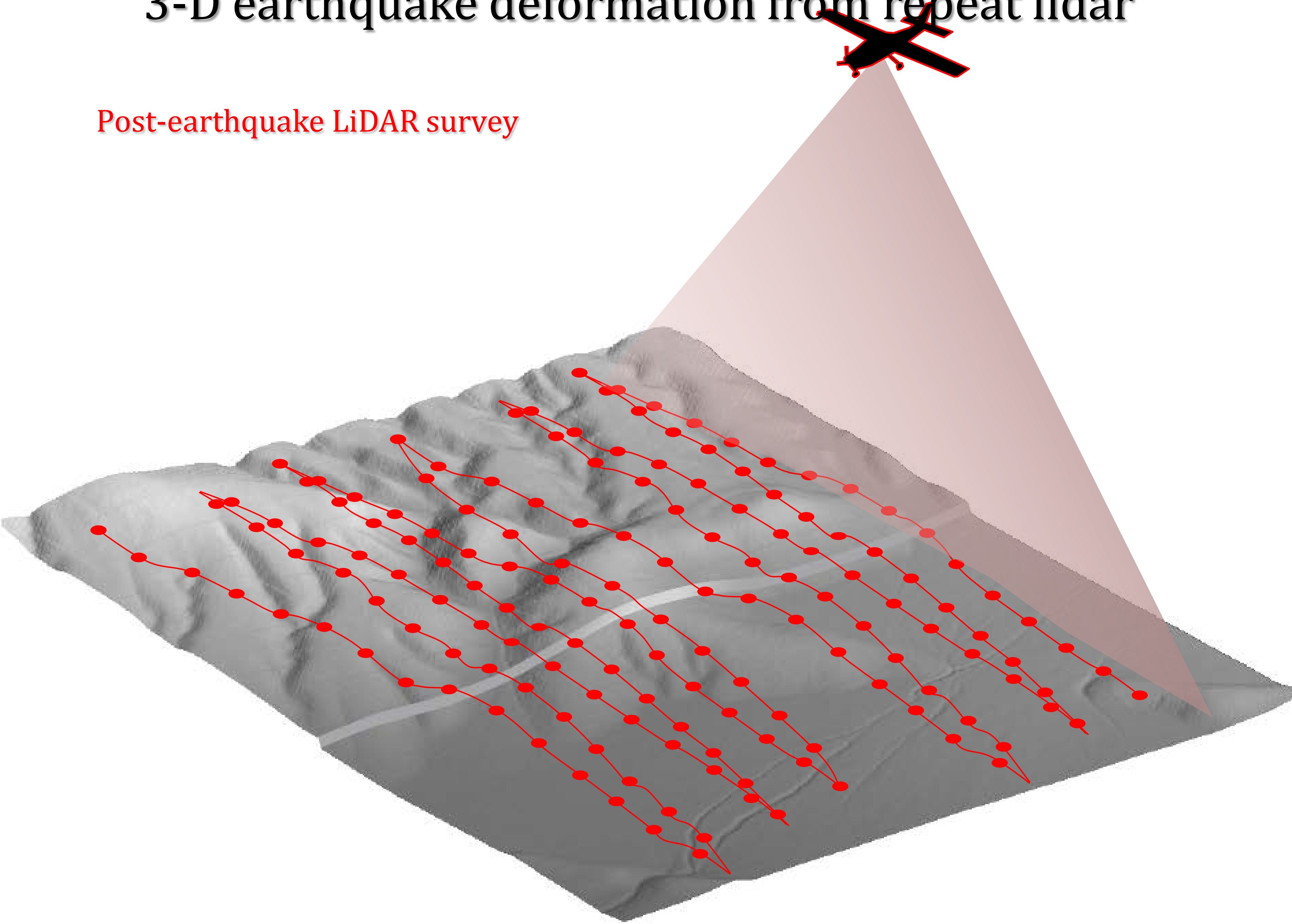

3-D earthquake deformation from repeat lidar

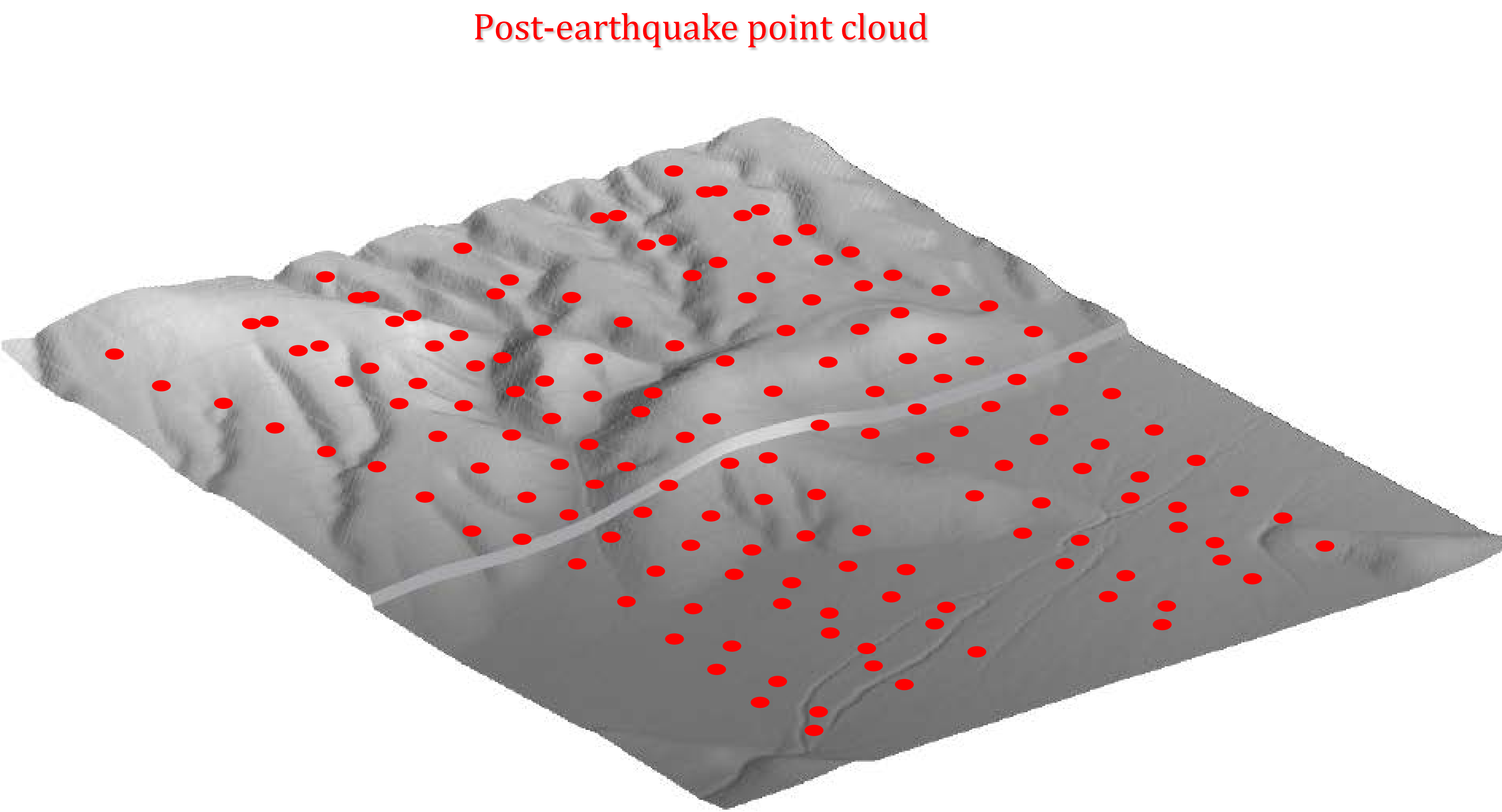

3-D earthquake deformation from repeat lidar

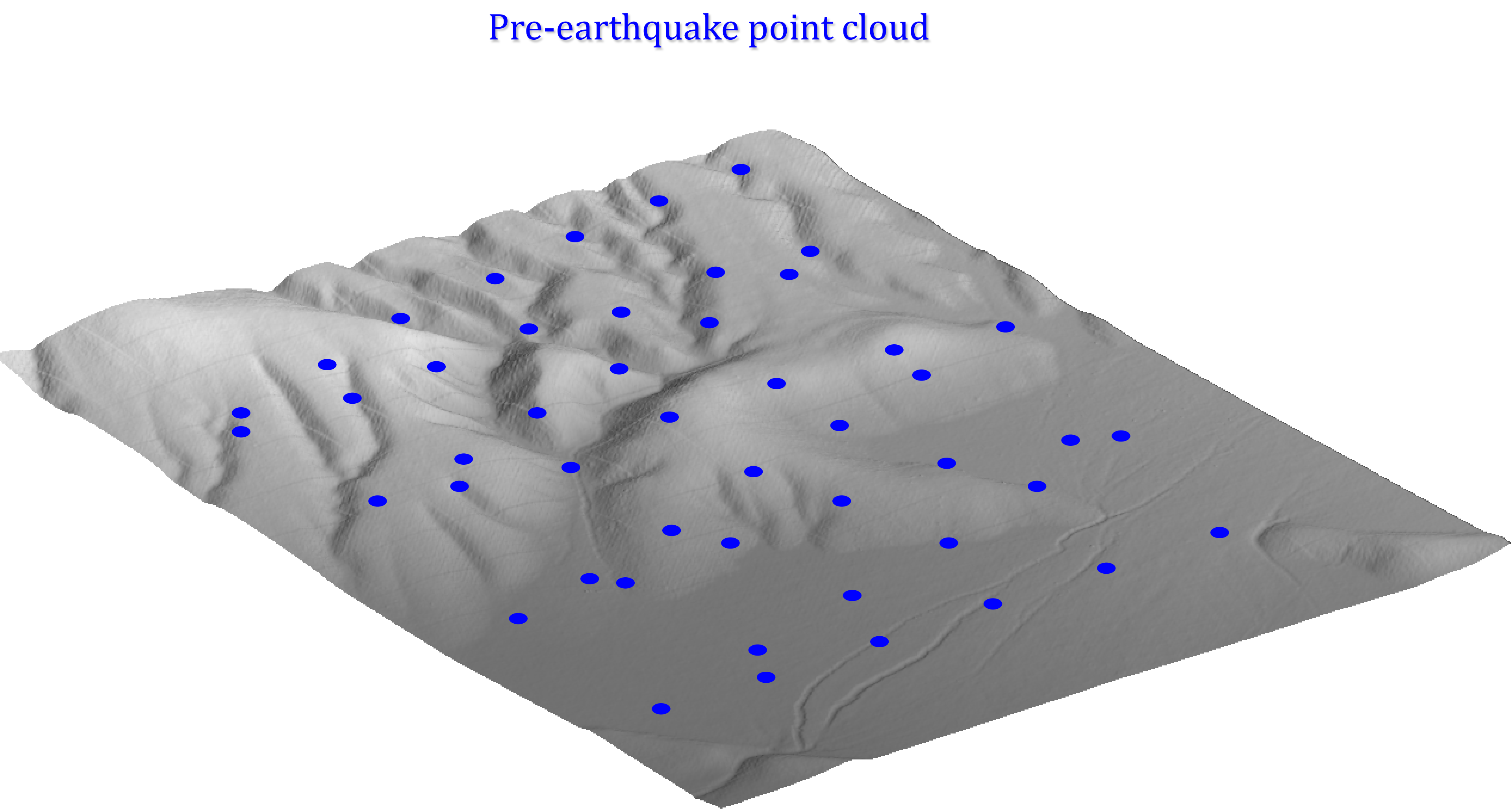

3-D earthquake deformation from repeat lidar

Pre-earthquake point cloud

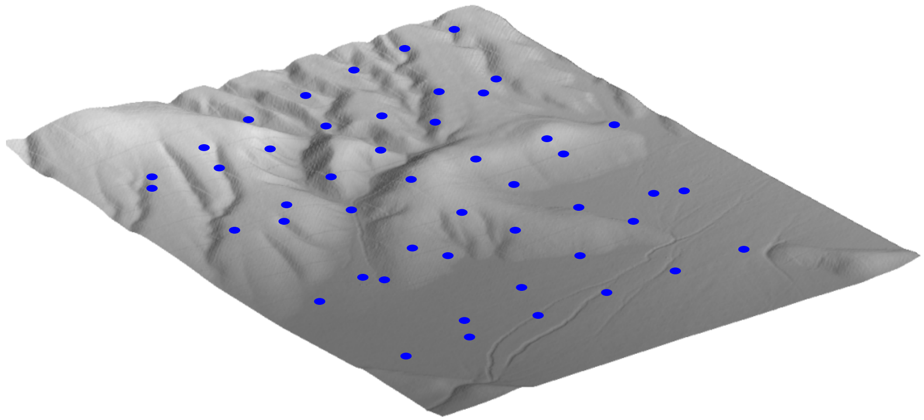

Post-earthquake point cloud

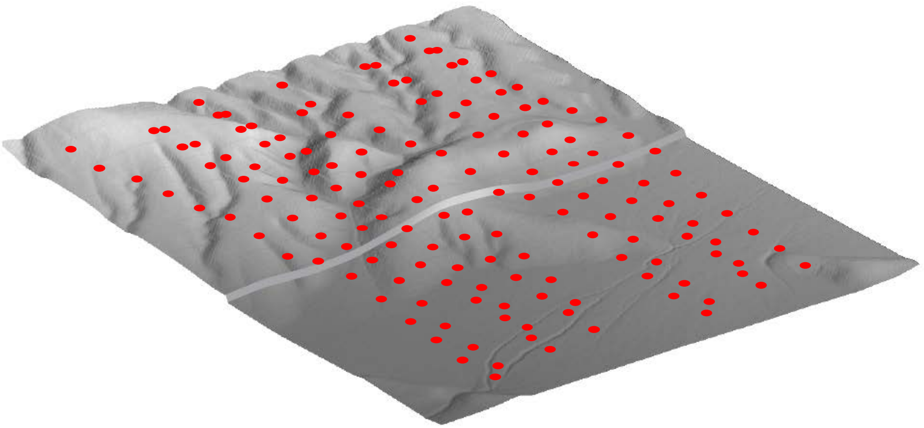

The Challenges of LiDAR differencing

- Data are irregularly spaced (we can rasterize them, but lose information doing so)
- There can be large mismatches in point density (legacy datasets vs modern surveys)
- … and mismatches in data quality and metrics (third party vs research-grade)
- Treatment of vegetation returns in forested areas

3-D earthquake deformation from repeat lidar

- The **iterative closest point** algorithm (ICP) is a method for registering (aligning) irregular point clouds, well known in computer vision and medical imaging
- ICP minimizes closest point pair distances using iterative **rigid-body transformations,** each one comprising a **translation** [$\boldsymbol{t_x\ t_y\ t_z}$] and a **rotation** [$\boldsymbol{\alpha\ \beta\ \gamma}$]

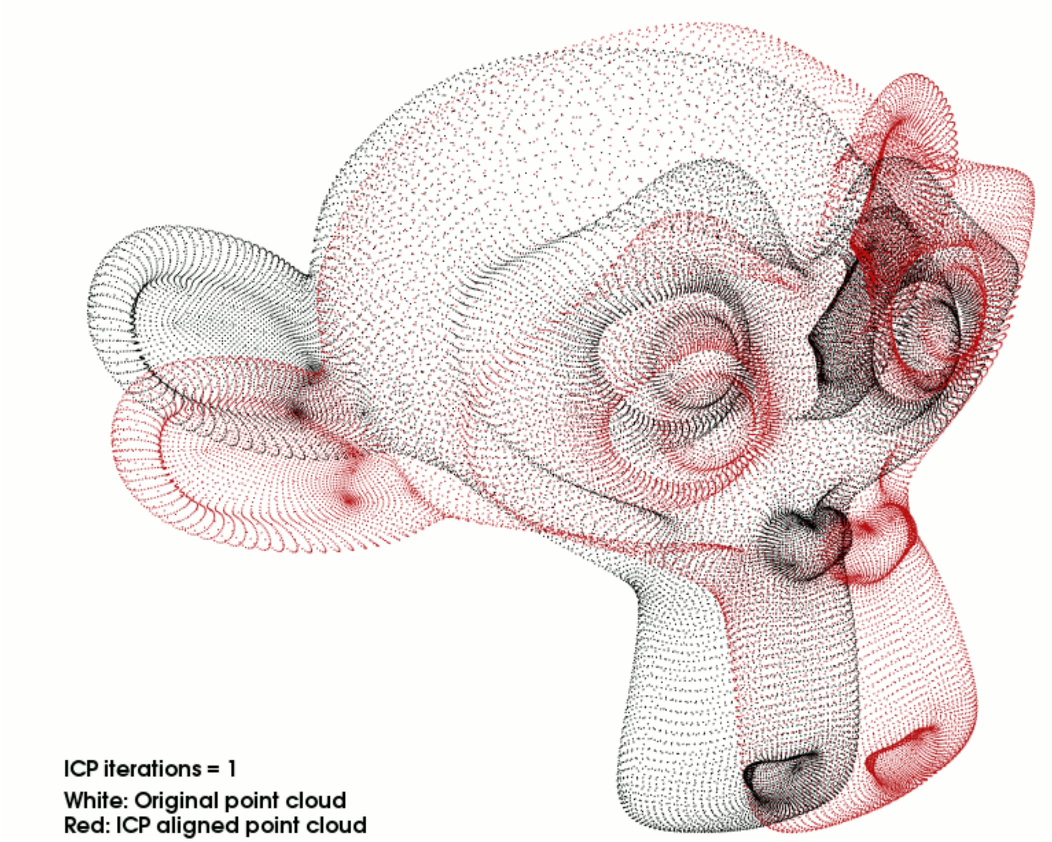

$$\Phi = \begin{pmatrix} 1 & -\gamma & \beta & t_x \\ \gamma & 1 & -\alpha & t_y \\ -\beta & \alpha & 1 & t_z \\ 0 & 0 & 0 & 1 \end{pmatrix}$$

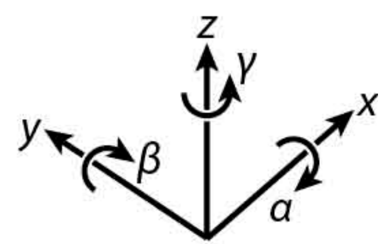

pointclouds.org/documentation/tutorials/interactive_icp.php

3-D earthquake deformation from repeat lidar

- The **iterative closest point** algorithm (ICP) is a method for registering (aligning) irregular point clouds, well known in computer vision and medical imaging
- ICP minimizes closest point pair distances using iterative **rigid-body transformations,** each one comprising a **translation** [t_x t_y t_z] and a **rotation** [α β γ]

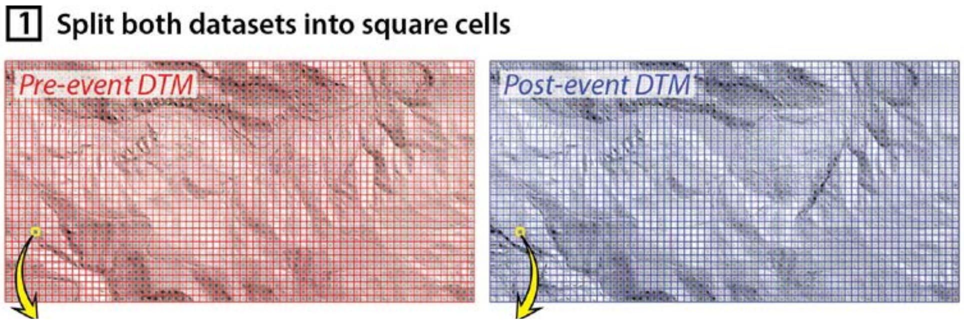

- (1) the two LiDAR datasets are first split into square "cells"
- (2) ICP is run on each equivalent pair of cells. The **translation** [t_x t_y t_z] corresponds to the cell displacement
- (3) this is repeated for the next pair of cells

Nissen *et al.* (2012), *Geophys. Res. Lett.*

Iterative Closest Point algorithm (ICP)

Pre-earthquake cell

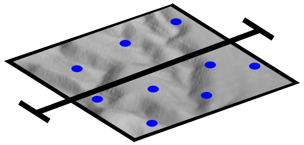

Post-earthquake cell

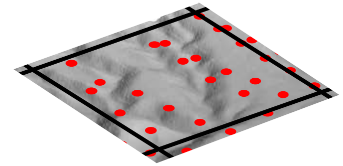

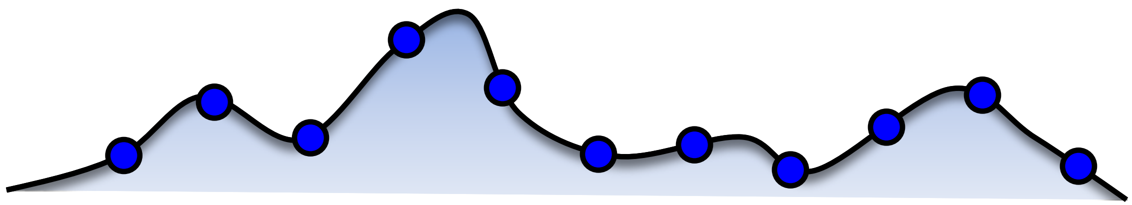

Iterative Closest Point algorithm (ICP)

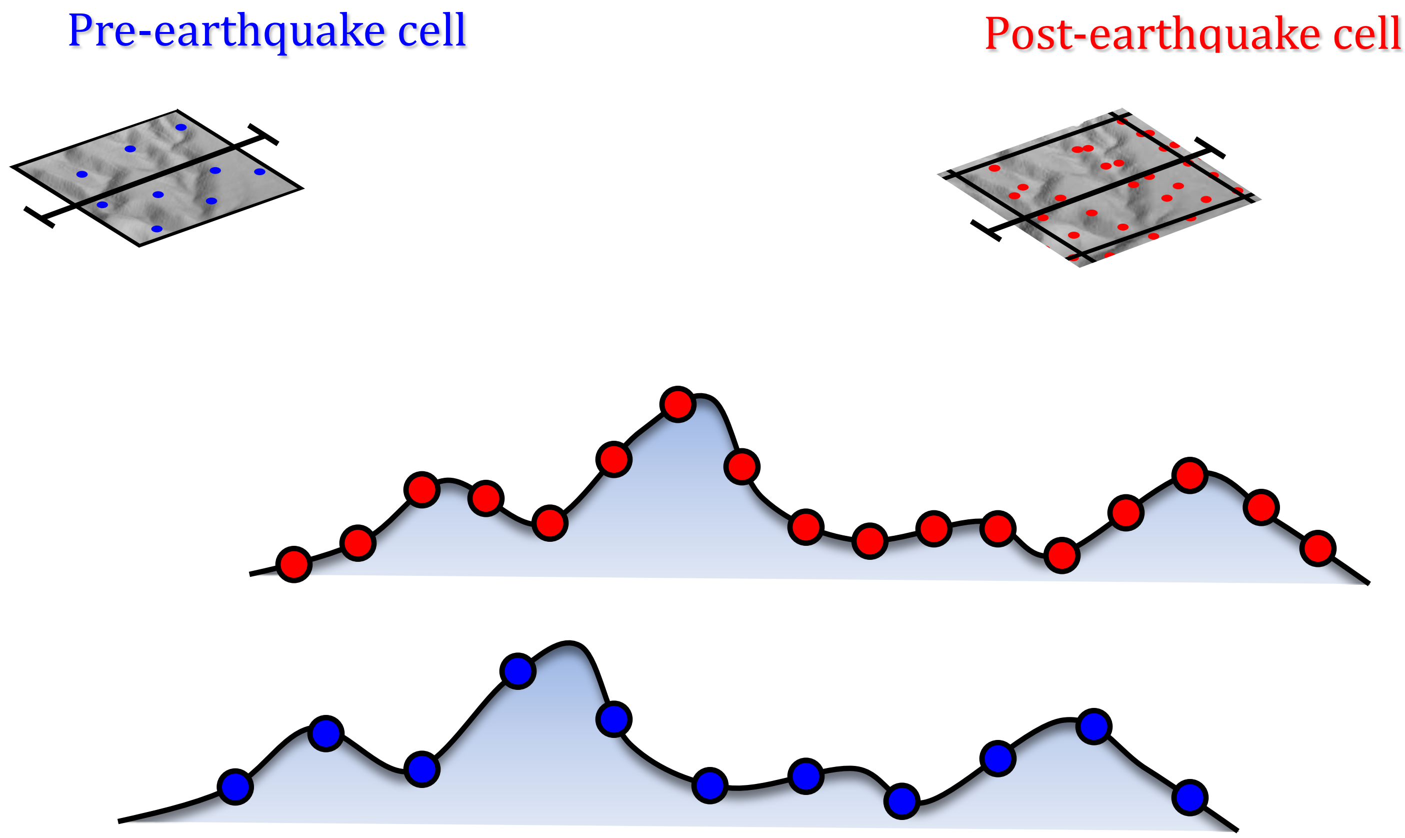

Iterative Closest Point algorithm (ICP)

Pre-earthquake cell

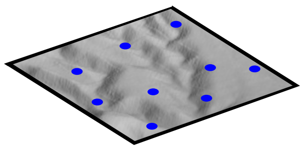

Post-earthquake cell

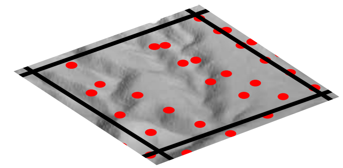

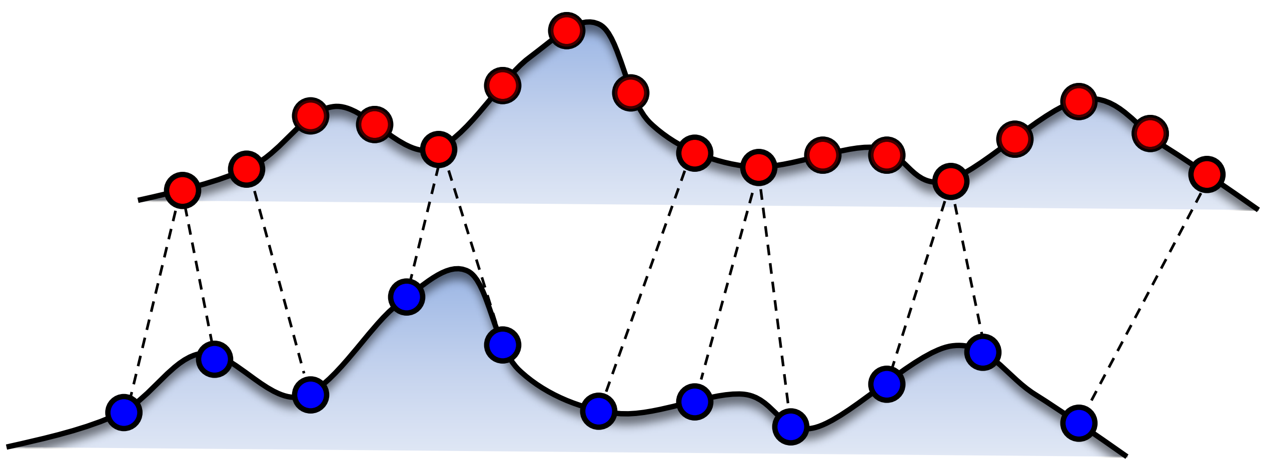

Find closest points

Iterative Closest Point algorithm (ICP)

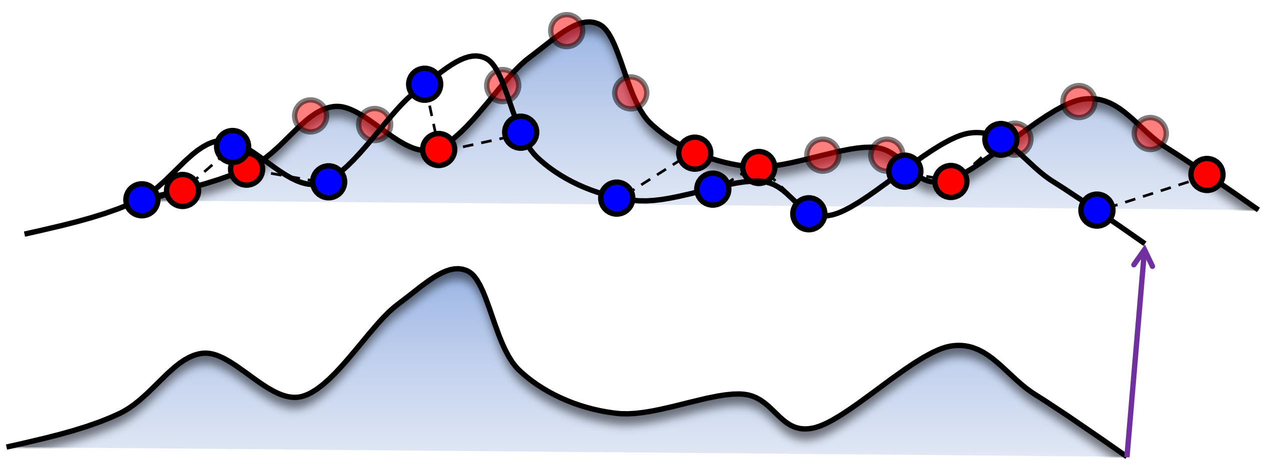

Iterate
Find closest points
Transform point cloud

$$\phi = \begin{pmatrix} 1 & -\gamma & \beta & t_x \\ \gamma & 1 & -\alpha & t_y \\ -\beta & \alpha & 1 & t_z \\ 0 & 0 & 0 & 1 \end{pmatrix}$$

Iterative Closest Point algorithm (ICP)

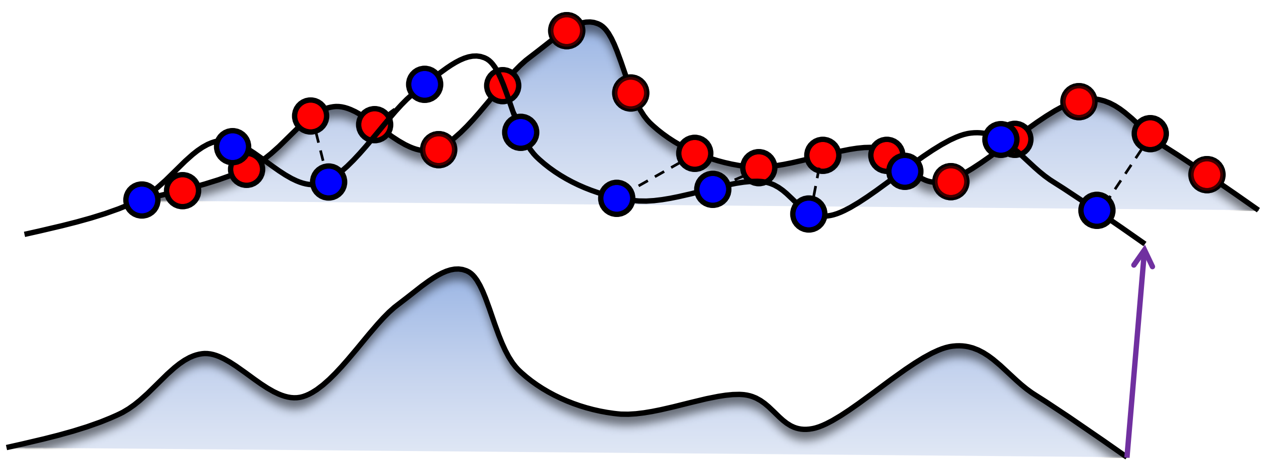

Find closest points

Transform point cloud

Iterative Closest Point algorithm (ICP)

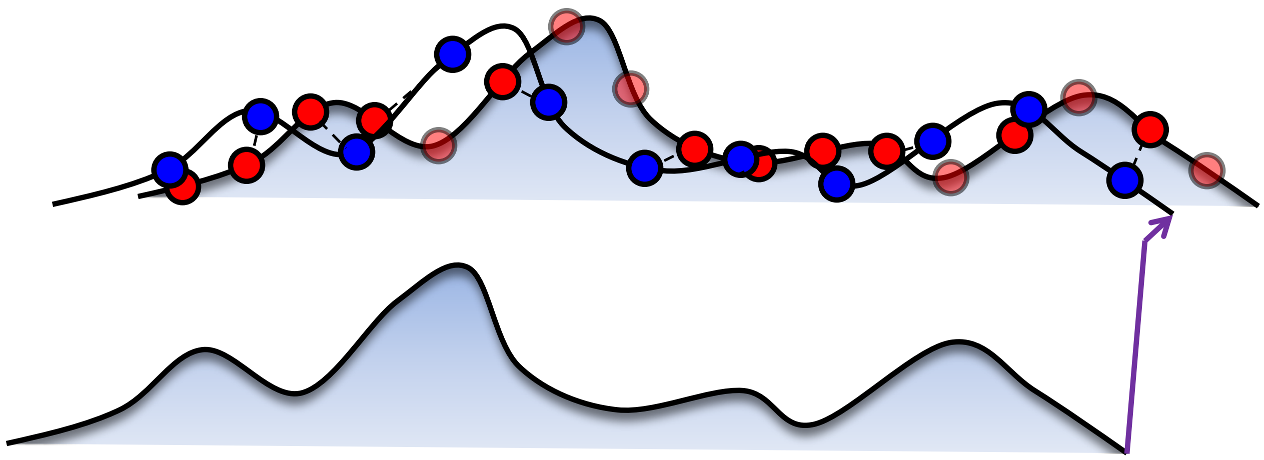

Find closest points

Transform point cloud

Iterative Closest Point algorithm (ICP)

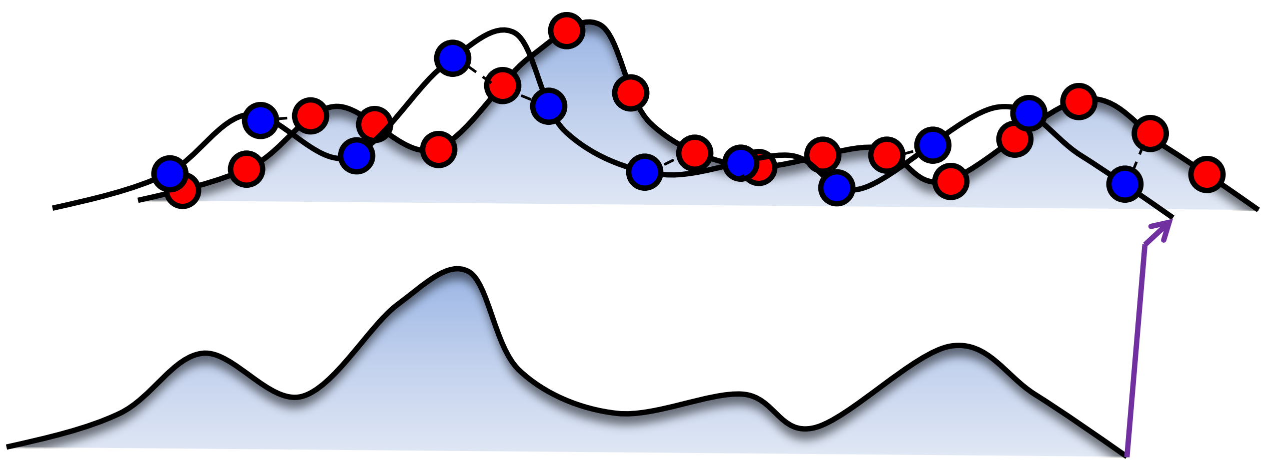

Find closest points

Transform point cloud

Iterative Closest Point algorithm (ICP)

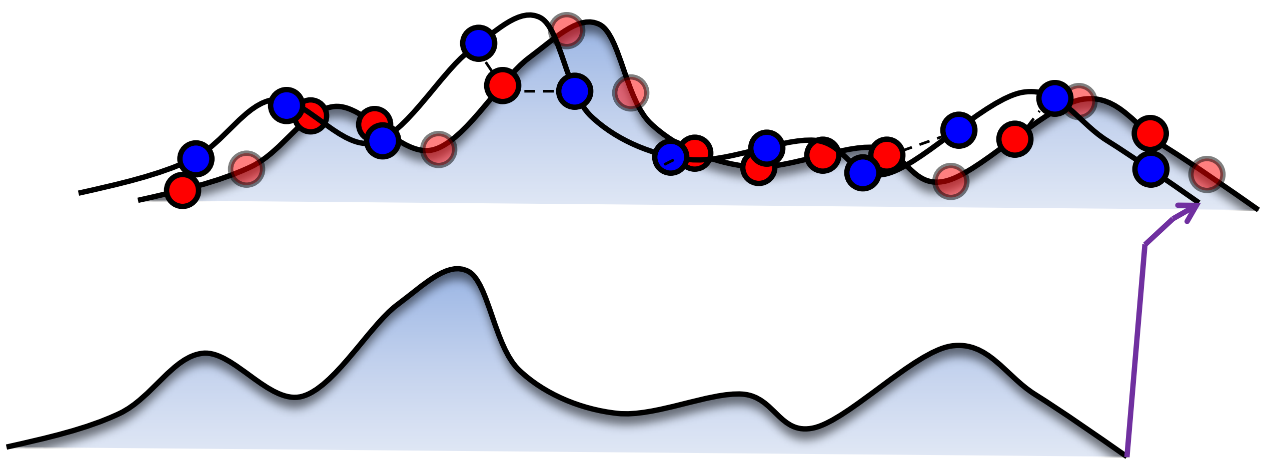

Find closest points

Transform point cloud

Iterative Closest Point algorithm (ICP)

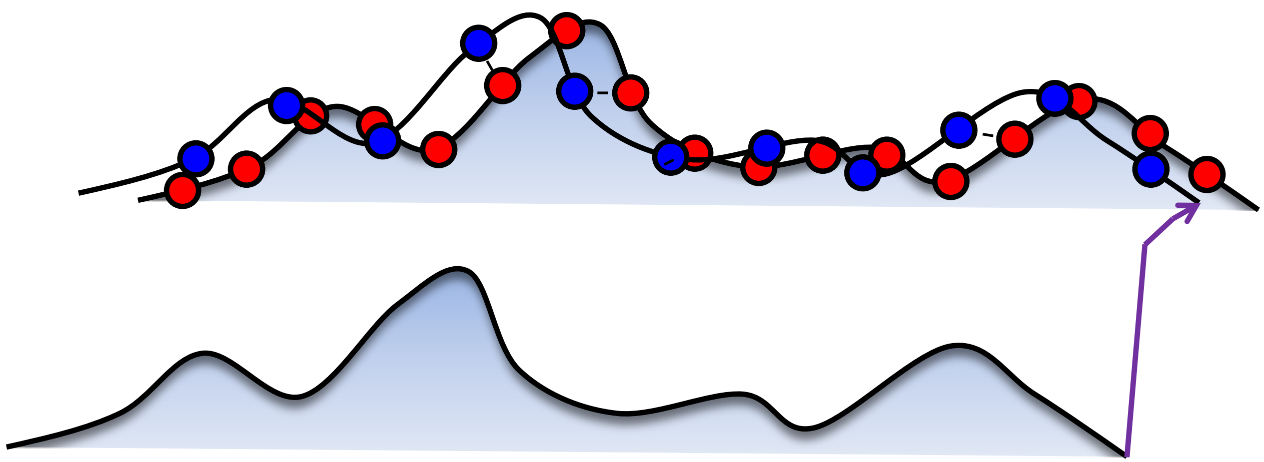

Find closest points

Transform point cloud

Iterative Closest Point algorithm (ICP)

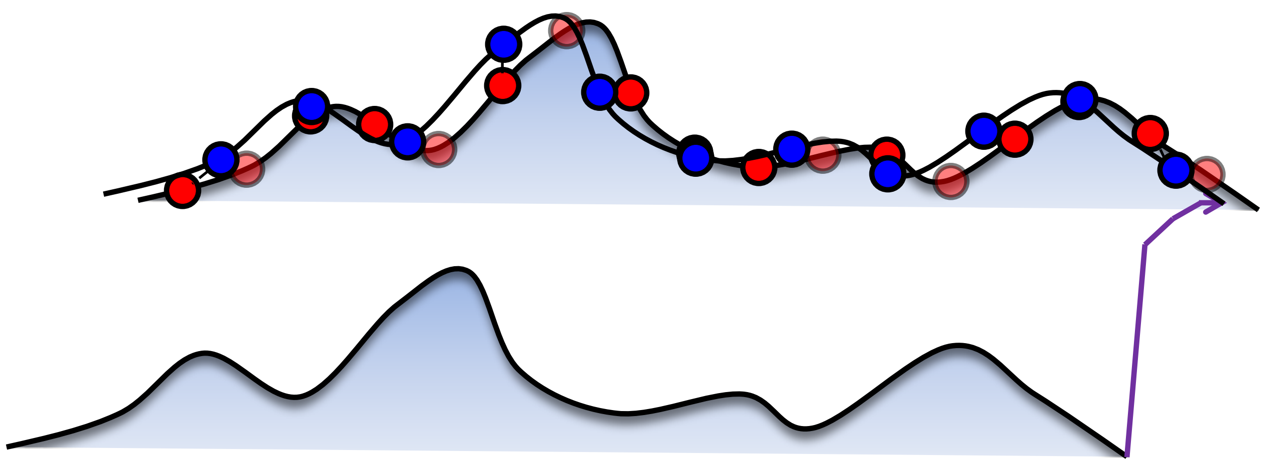

Find closest points

Transform point cloud

Iterative Closest Point algorithm (ICP)

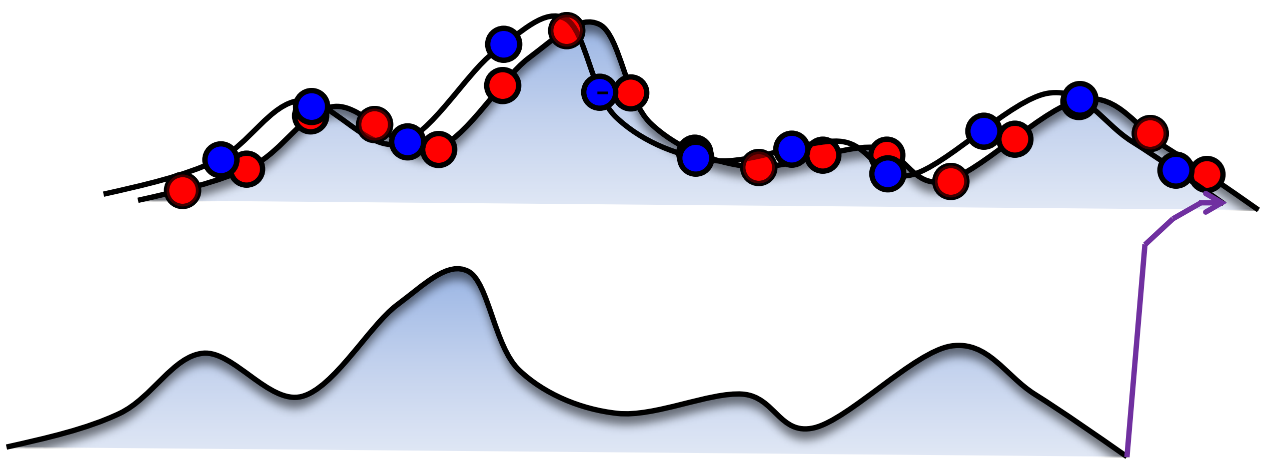

Find closest points

Transform point cloud

Iterative Closest Point algorithm (ICP)

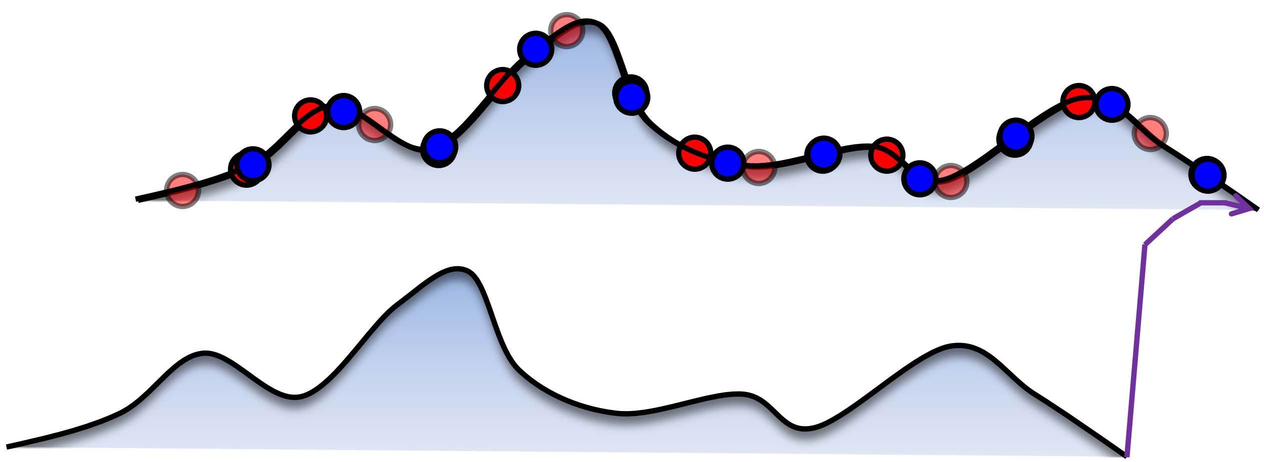

Find closest points

Transform point cloud

Iterative Closest Point algorithm (ICP)

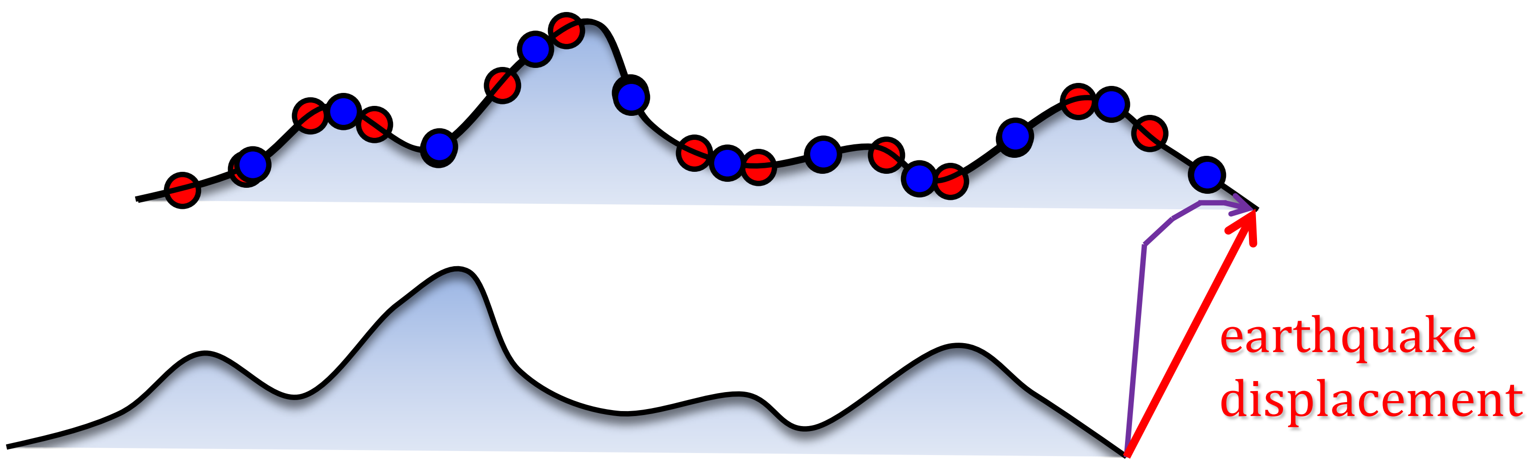

Find closest points

Transform point cloud

3-D earthquake deformation from repeat LiDAR point clouds

Caveats

• ICP will not work if there are large changes to the shape of the cell, e.g. through landsliding

• ICP will generate spurious results in areas that are very planar

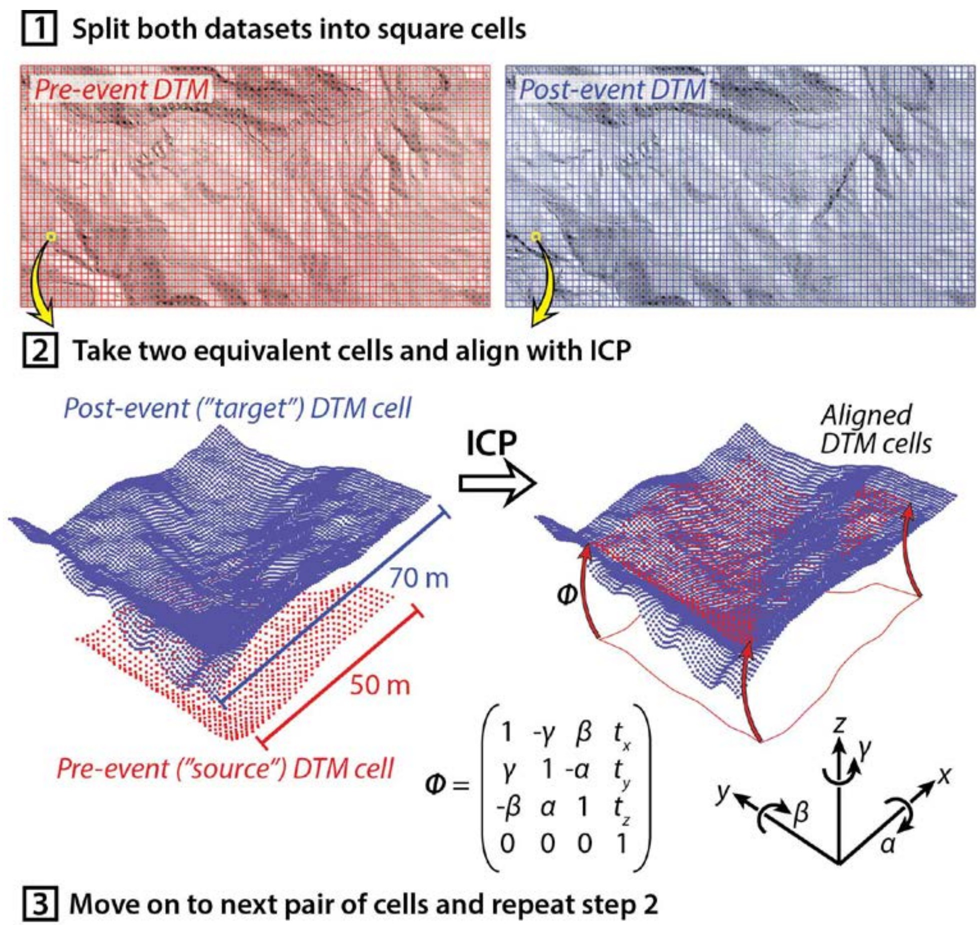

Nissen *et al.* (2012), *Geophys. Res. Lett.*

14 June 2008 Iwate-Miyagi earthquake

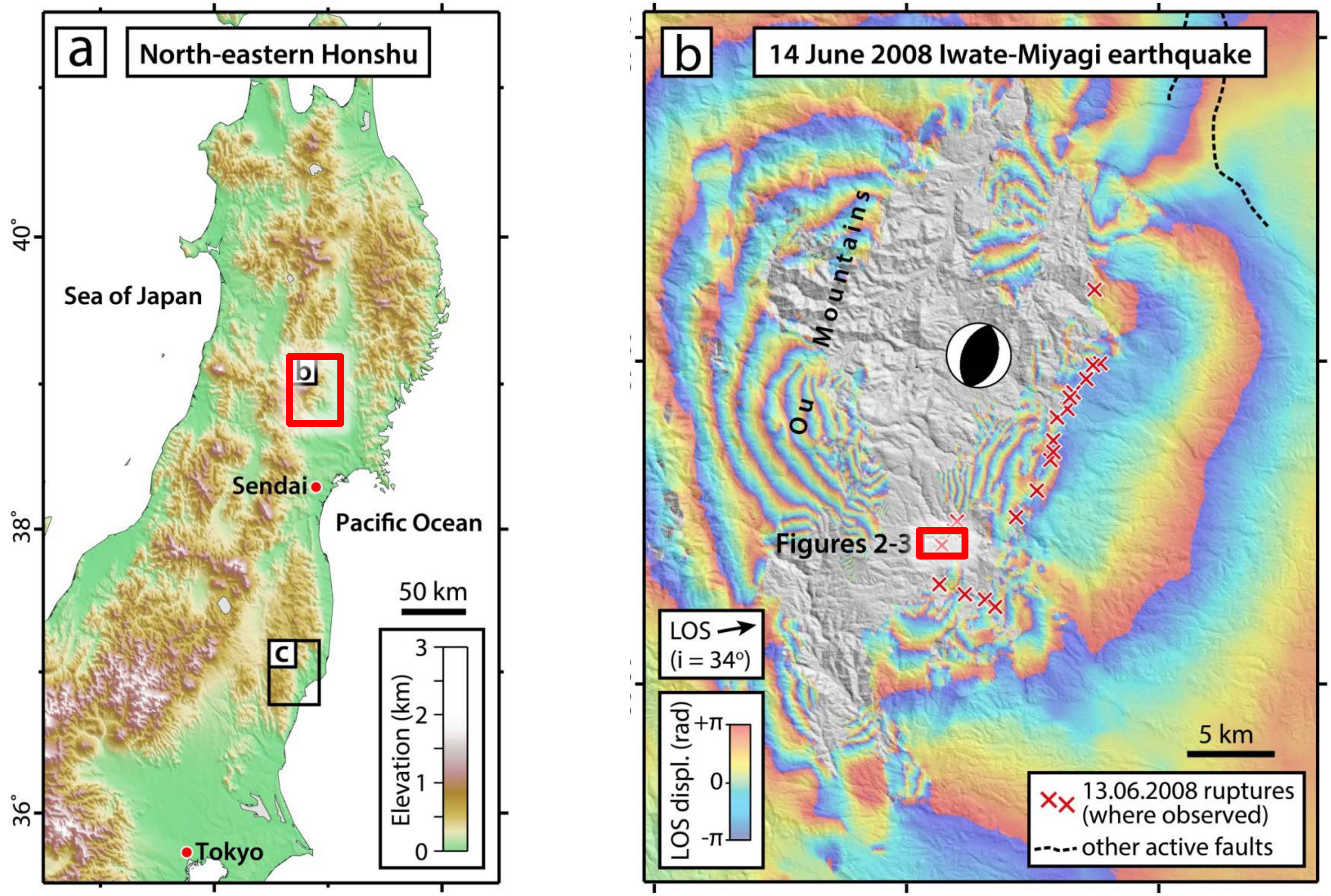

Nissen *et al.* (2014), *EPSL*

- First ever partial earthquake rupture with pre-event lidar coverage
- Pre- and post-event lidar flown by commercial surveying firms
- InSAR and pixel tracking limited by dense vegetation and steep phase gradients

14 June 2008 Iwate-Miyagi earthquake

Photos: Tadashi Maruyama

14 June 2008 Iwate-Miyagi earthquake

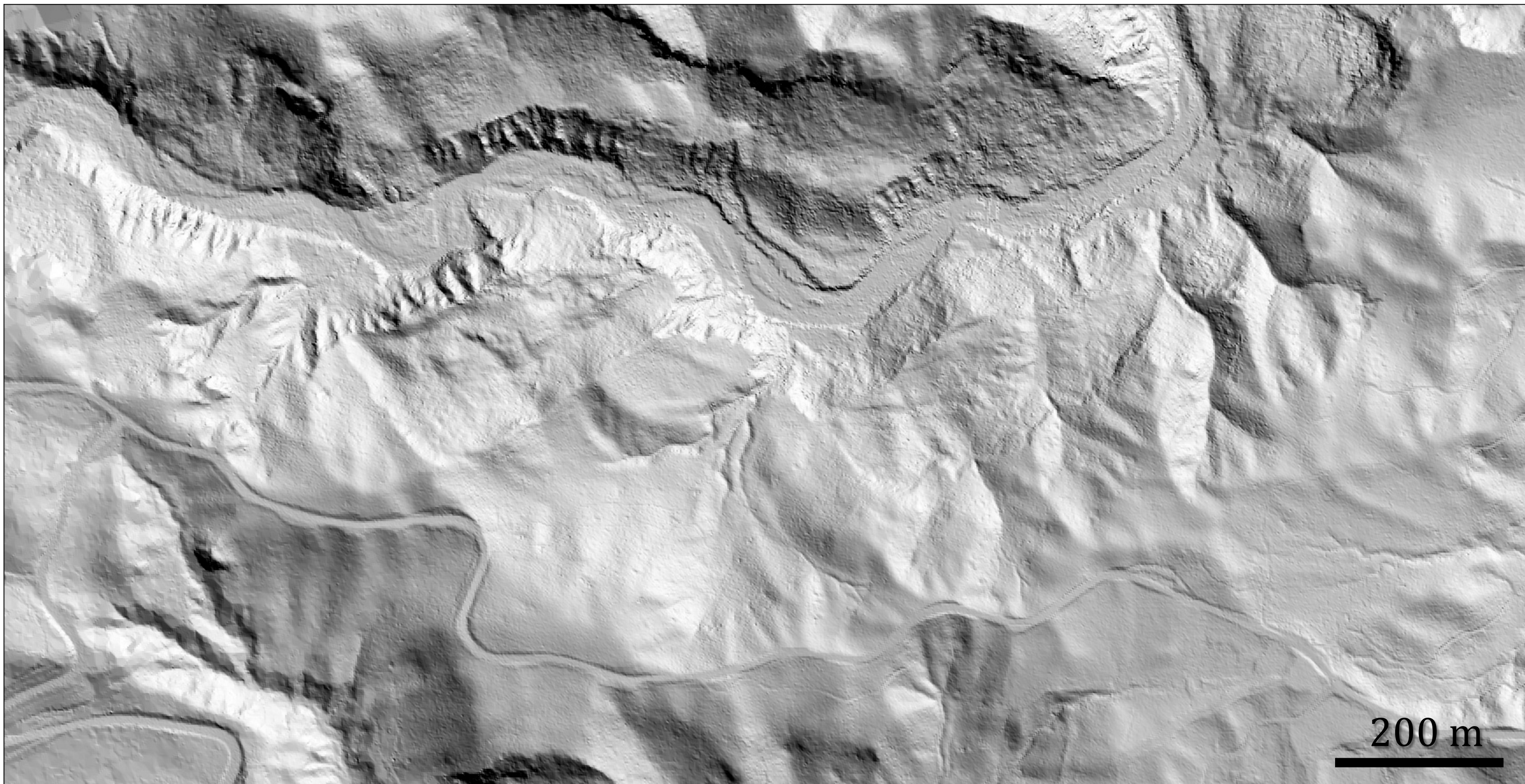

2006 pre-earthquake bare Earth DTM (2m)

KOKUSAI KOGYO GROUP

14 June 2008 Iwate-Miyagi earthquake

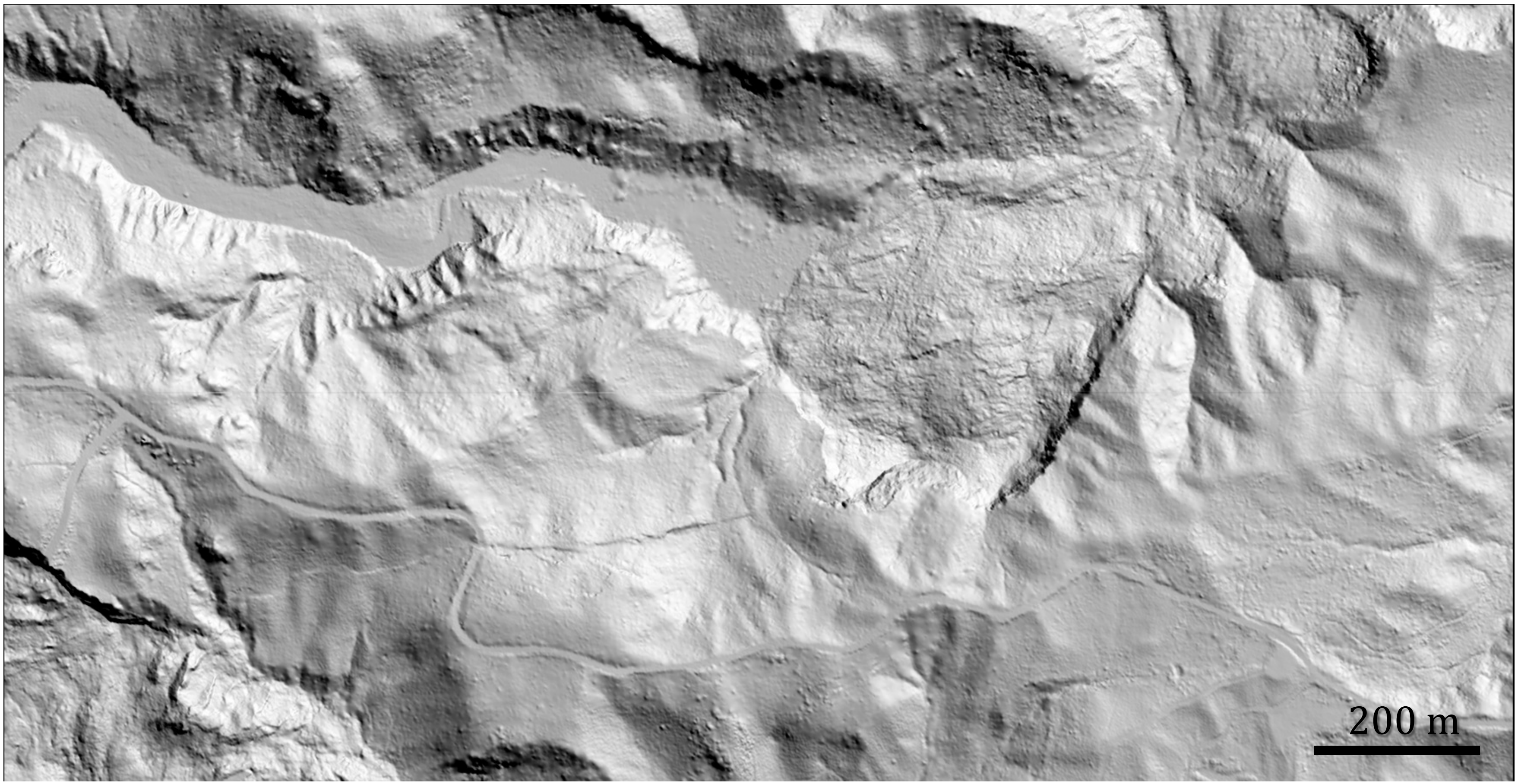

2008 post-earthquake bare Earth DTM (1m)

AERO ASAHI CORPORATION

14 June 2008 Iwate-Miyagi earthquake

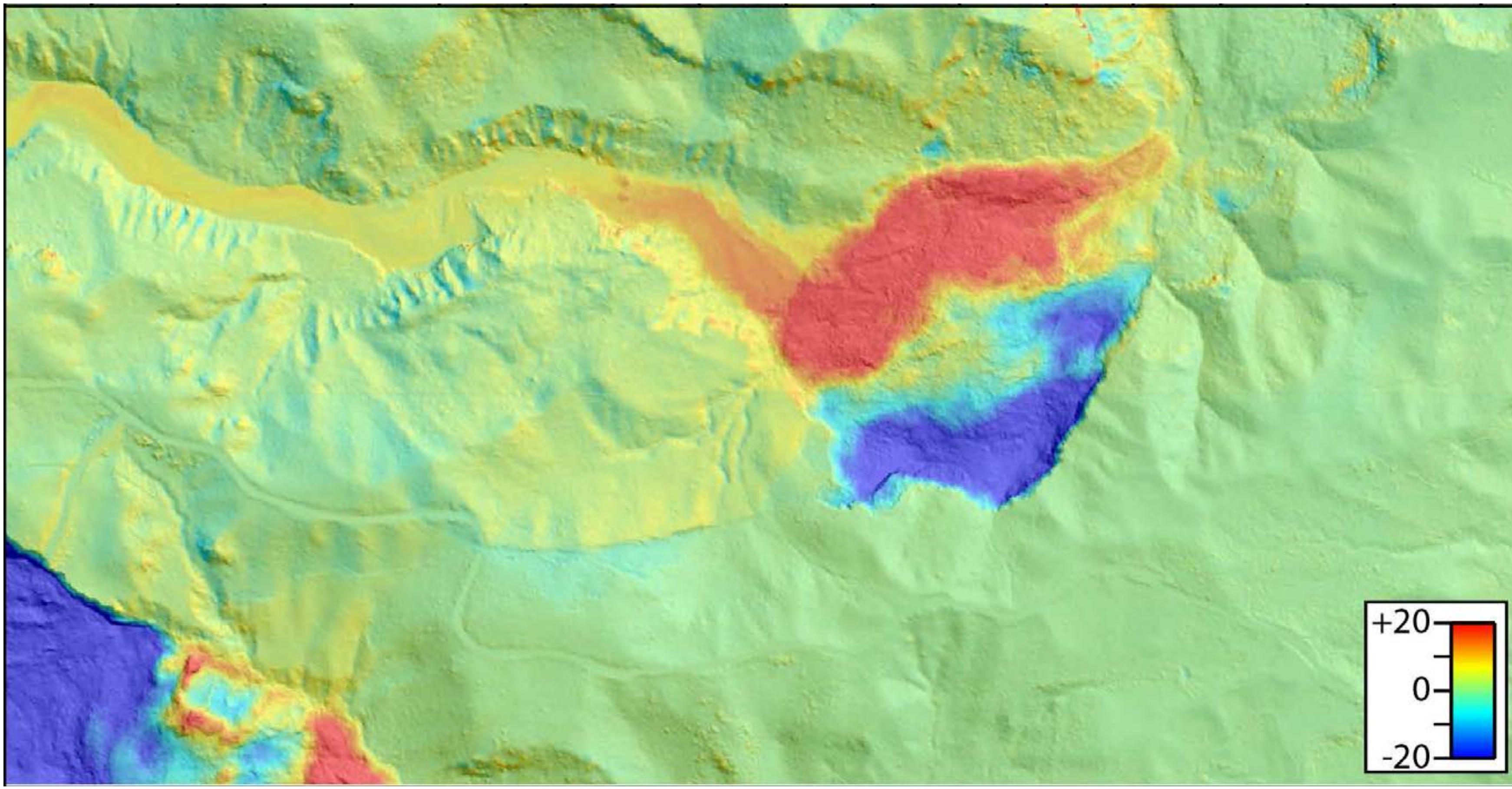

2006-2008 DoD (m)

14 June 2008 Iwate-Miyagi earthquake

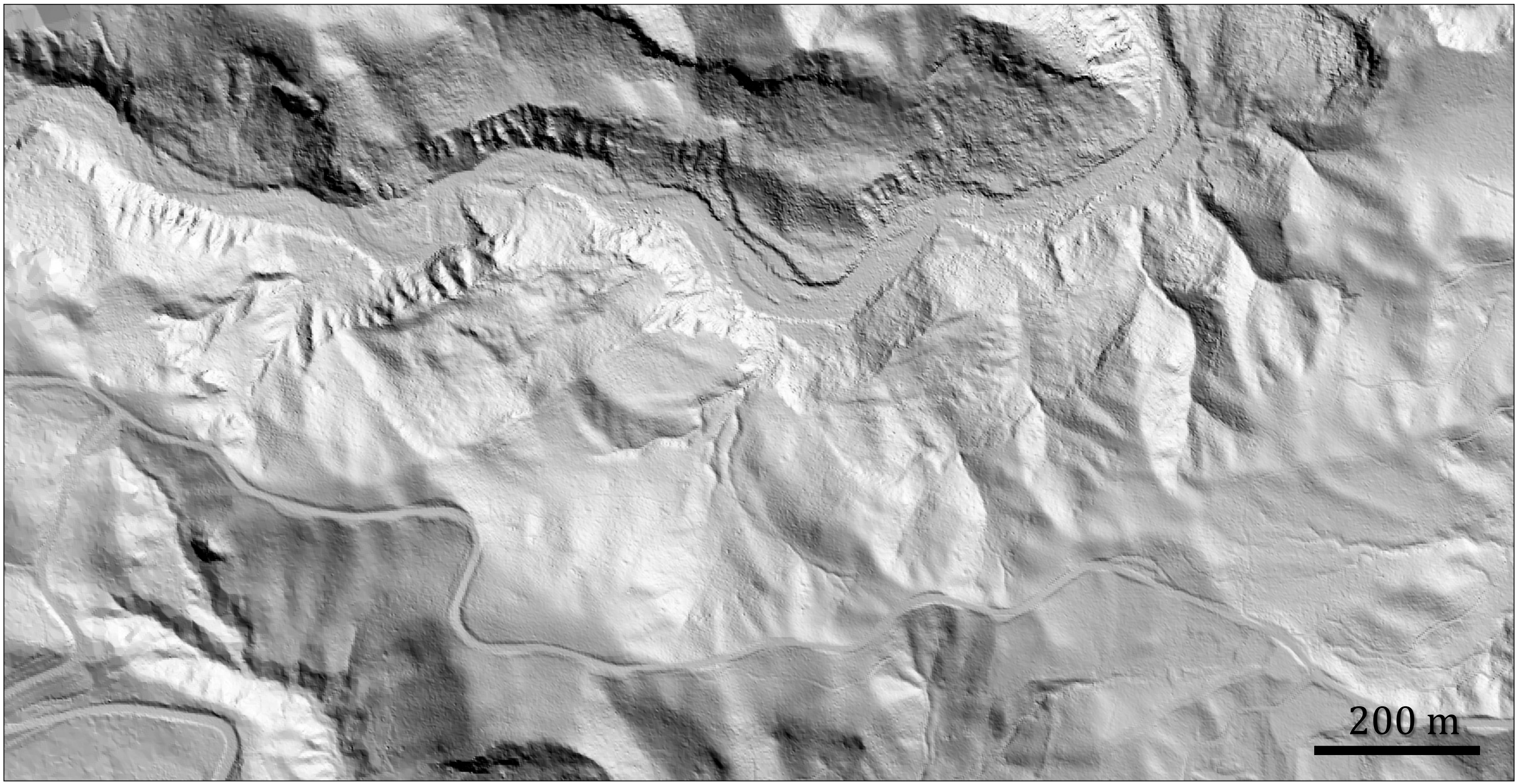

2006 pre-earthquake DEM (2m)

14 June 2008 Iwate-Miyagi earthquake

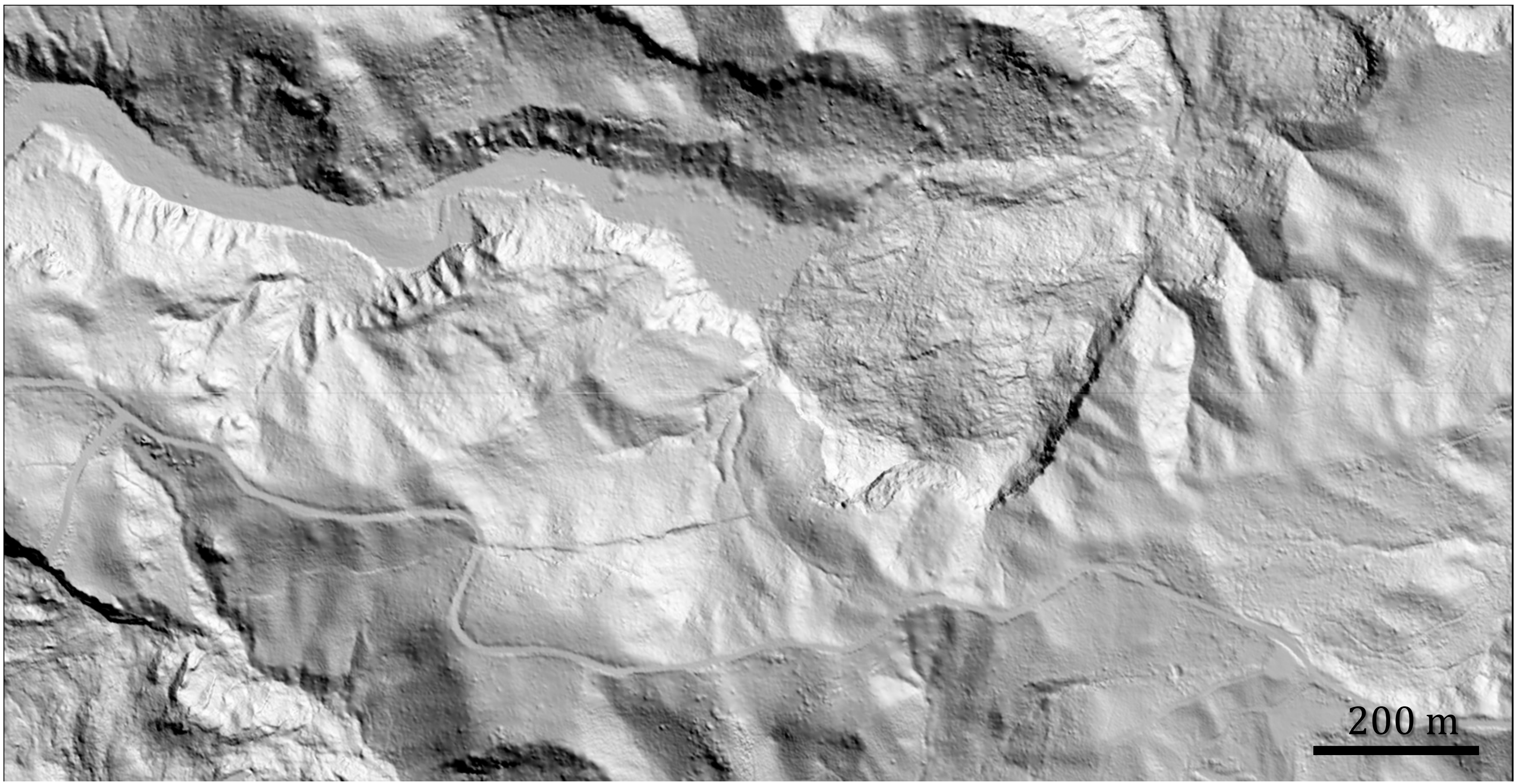

2008 post-earthquake DEM (1m)

14 June 2008 Iwate-Miyagi earthquake

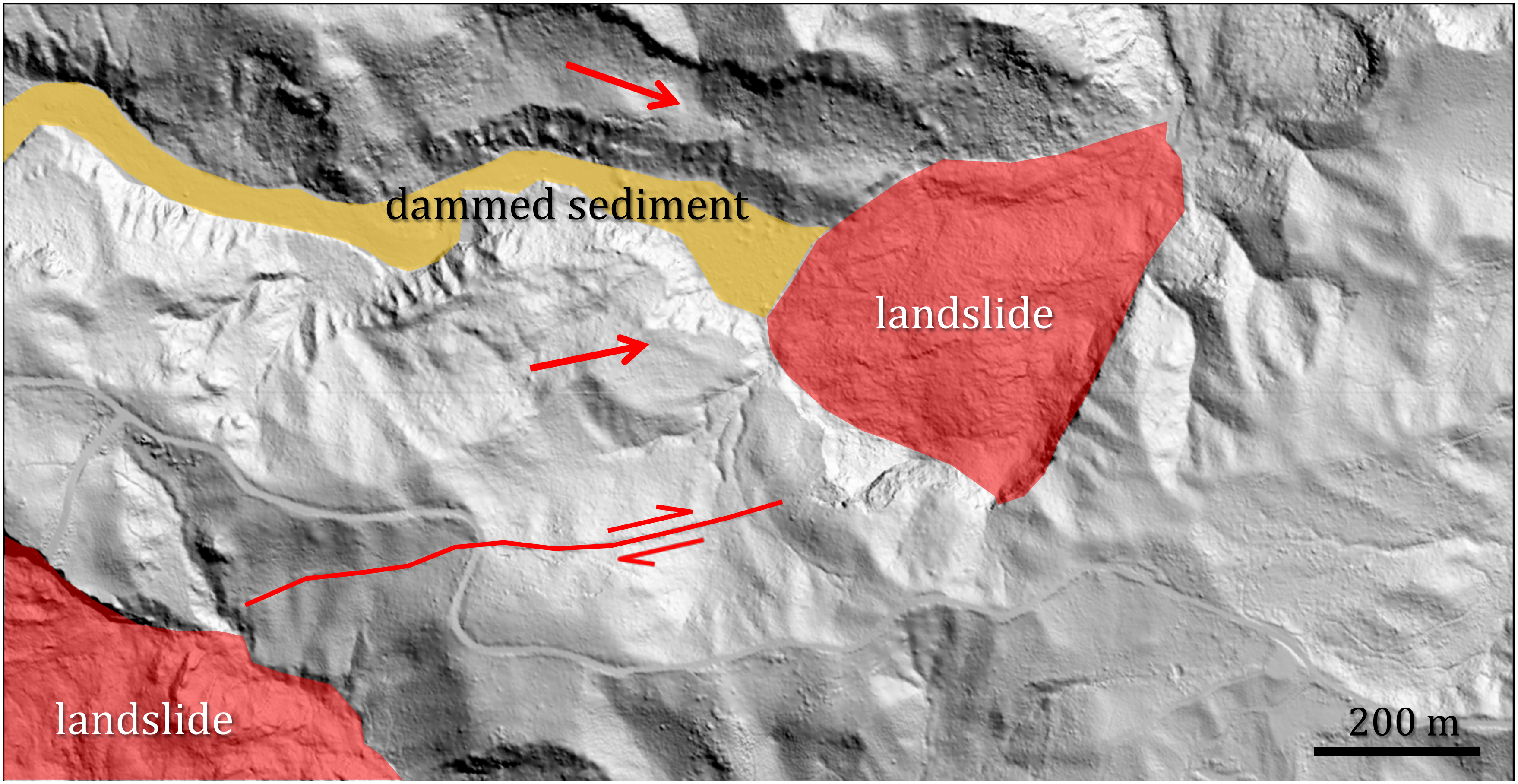

14 June 2008 Iwate-Miyagi earthquake

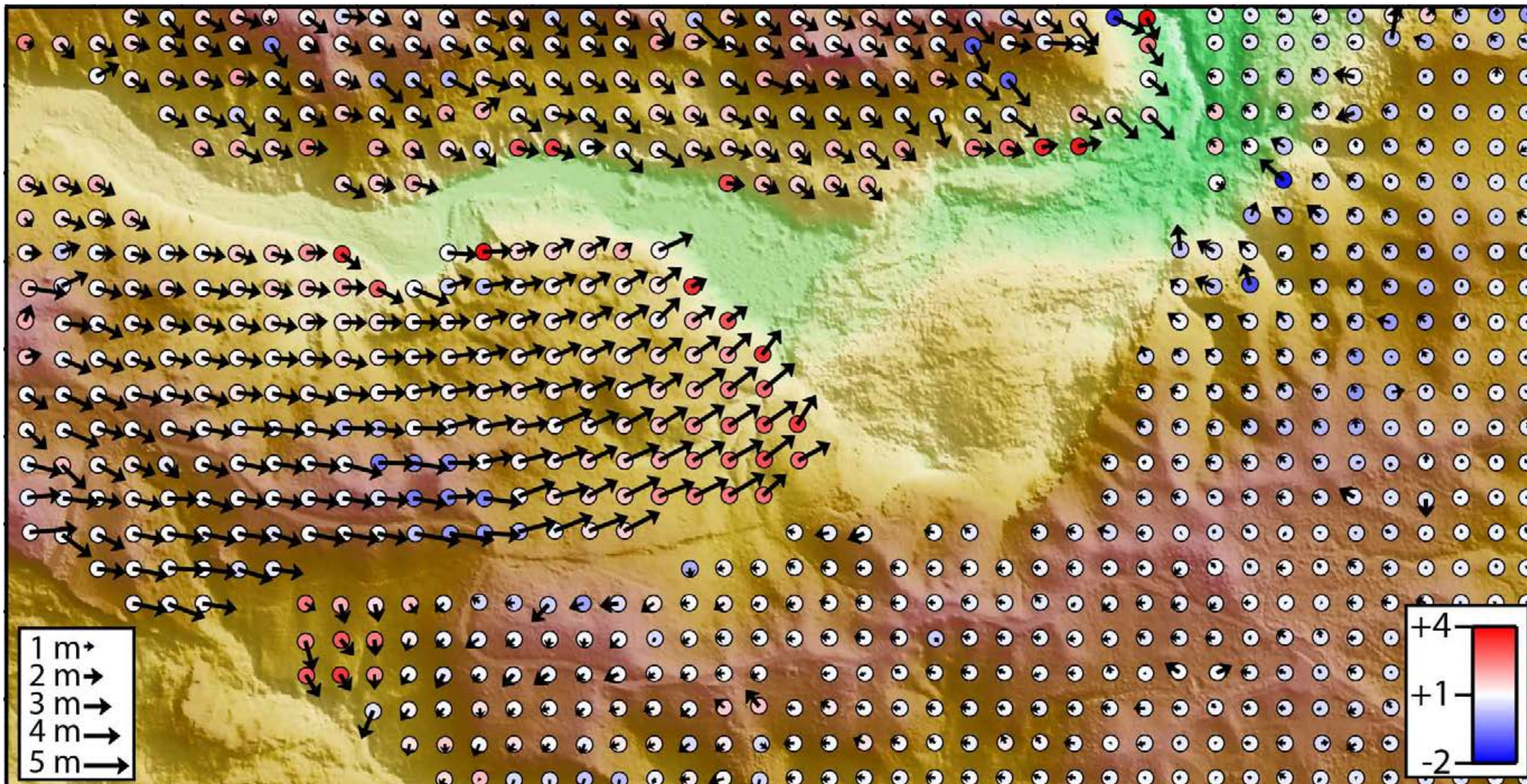

2006-2008 3-D displacements

11 April 2011 Fukushima-Hamadori earthquake

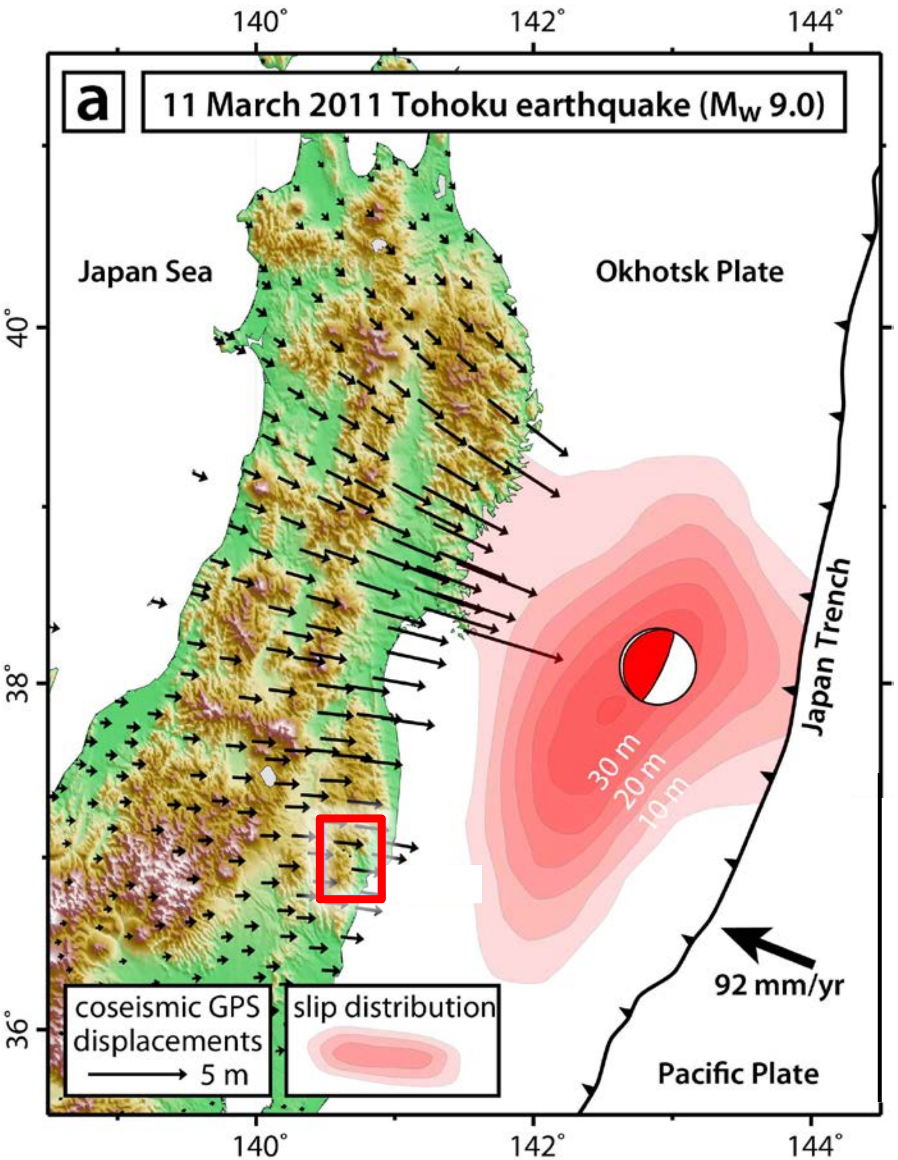

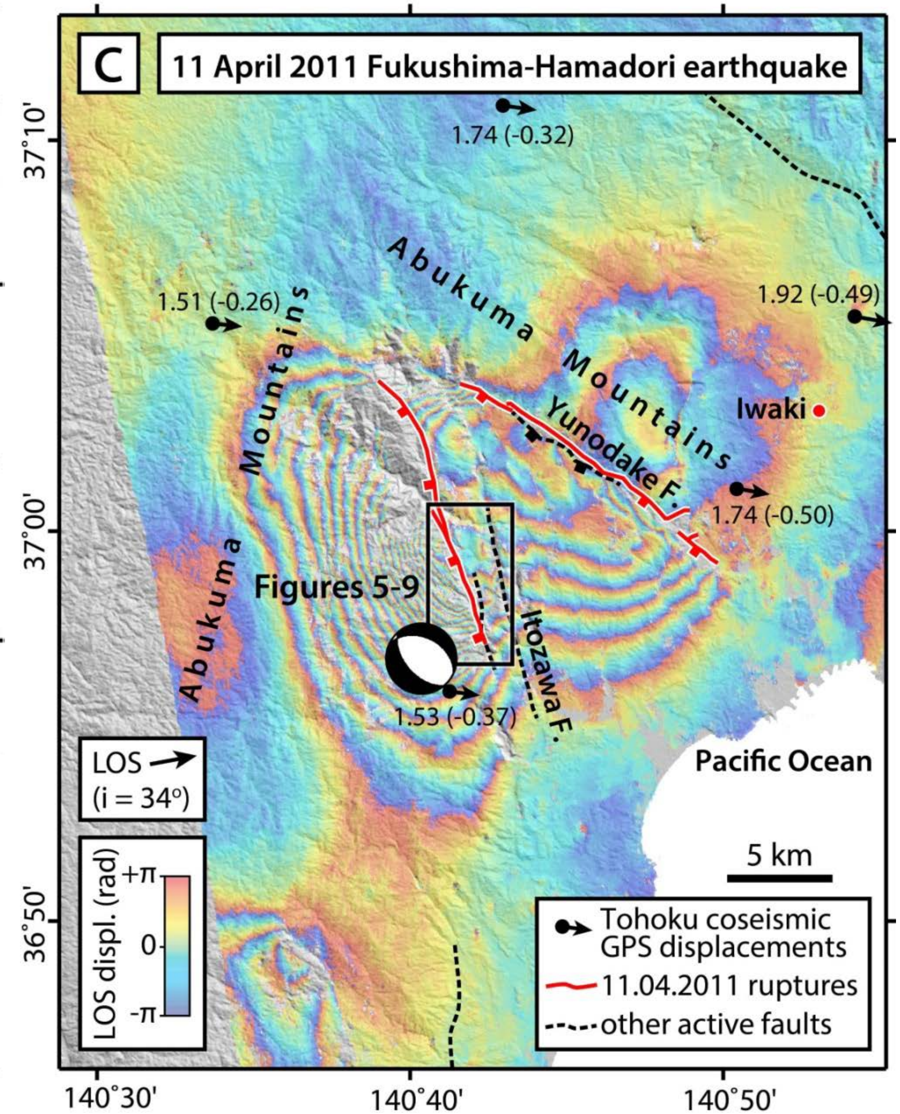

Nissen *et al.* (2014), *Earth Planet. Sci. Lett.*

11 April 2011 Fukushima-Hamadori earthquake

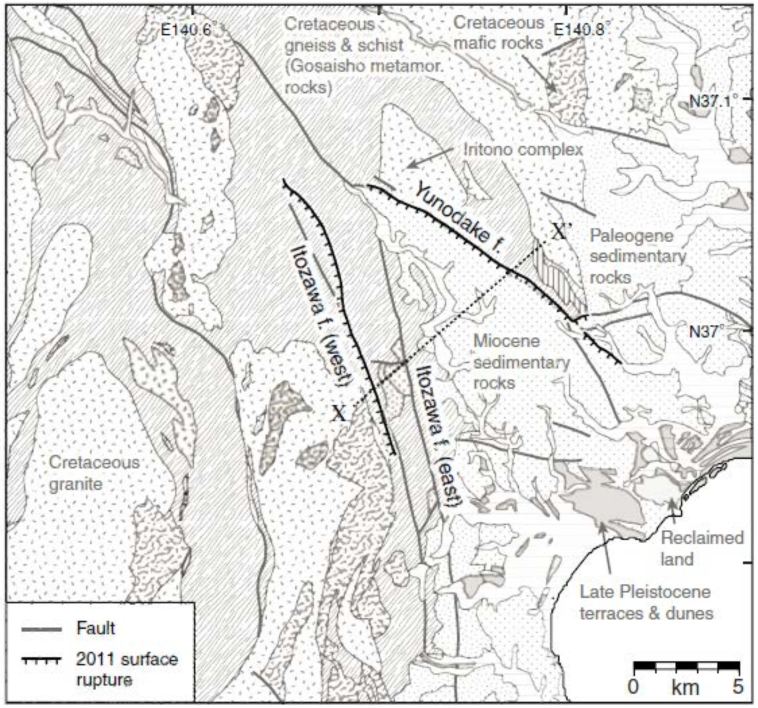

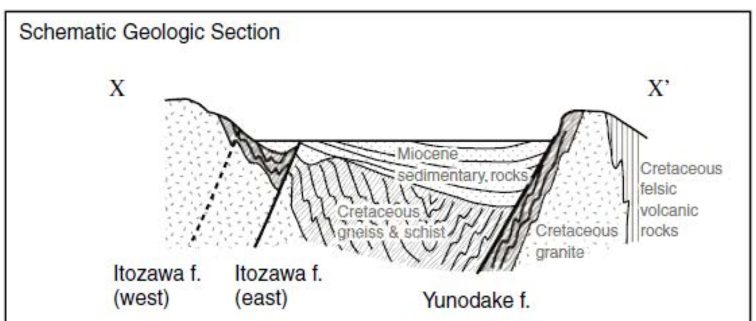

Toda & Tsutsumi (2013), *BSSA*

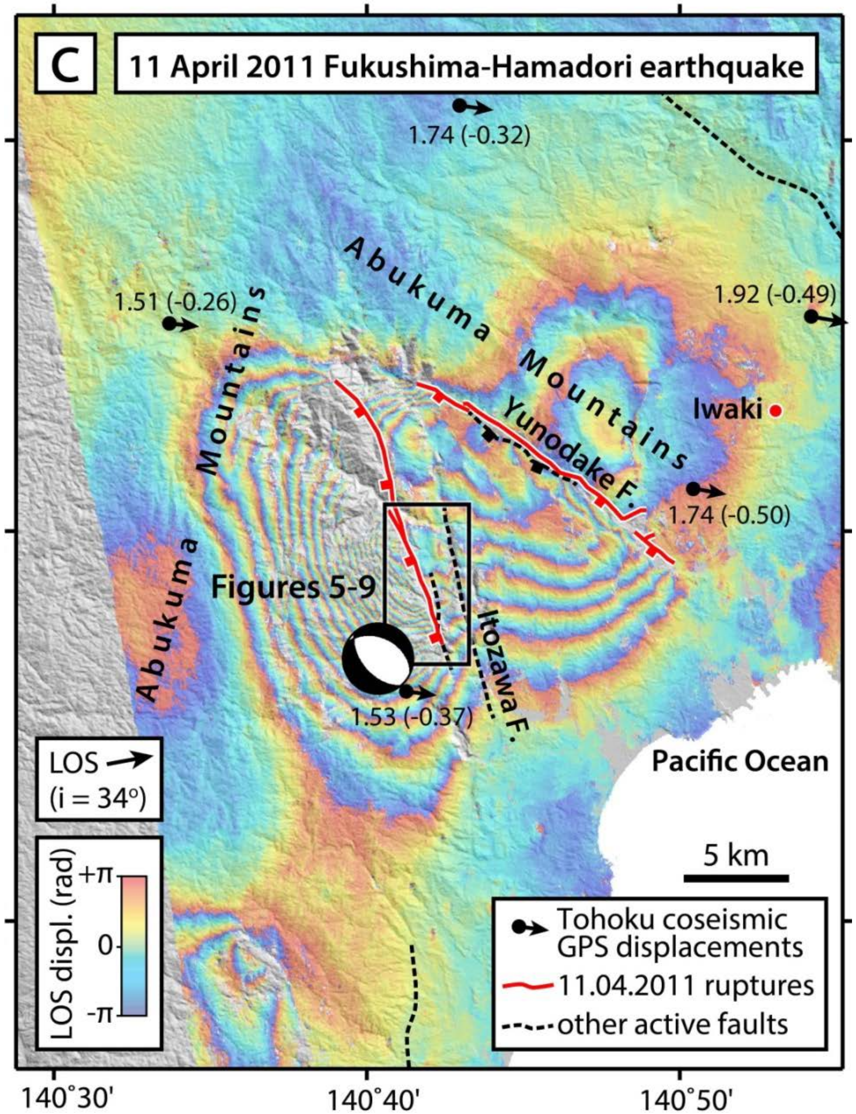

11 April 2011 Fukushima-Hamadori earthquake

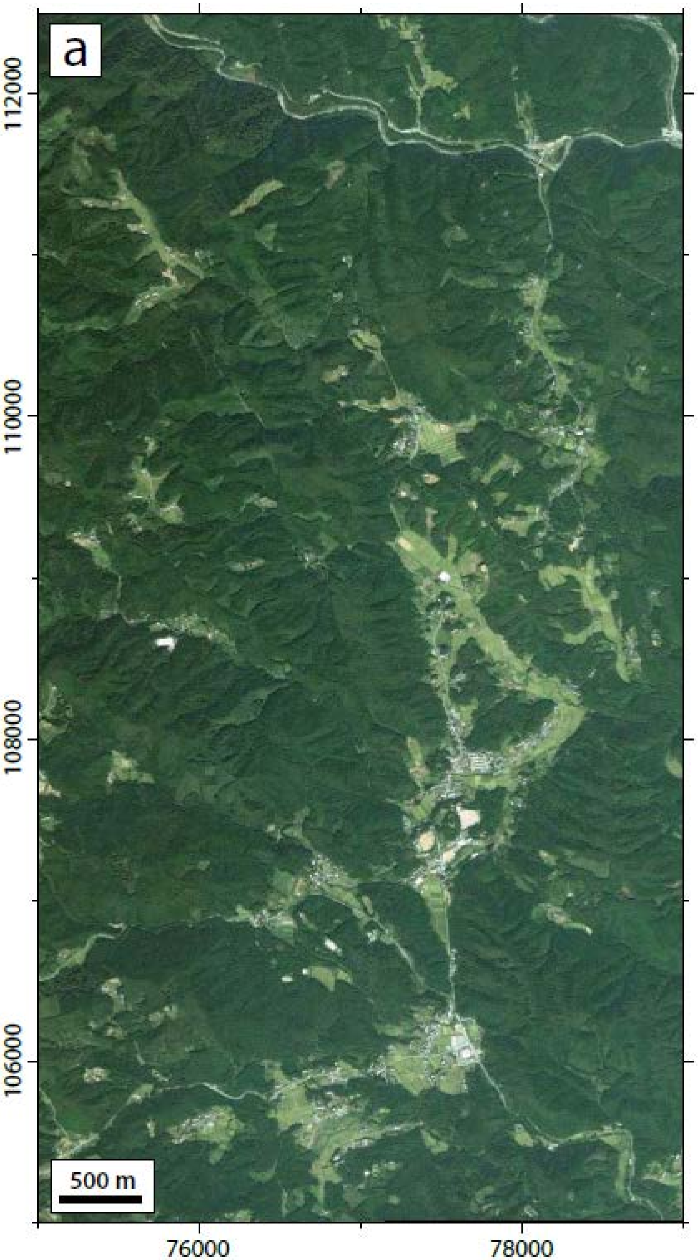

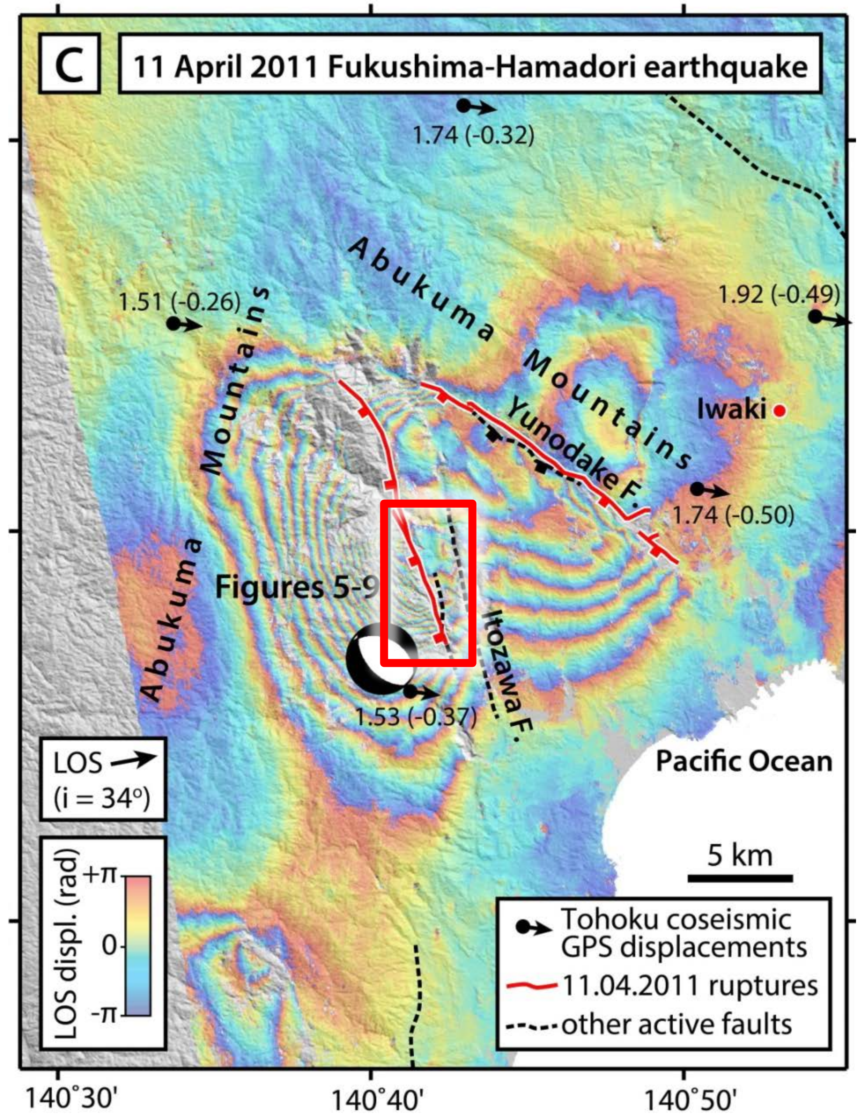

11 April 2011 Fukushima-Hamadori earthquake

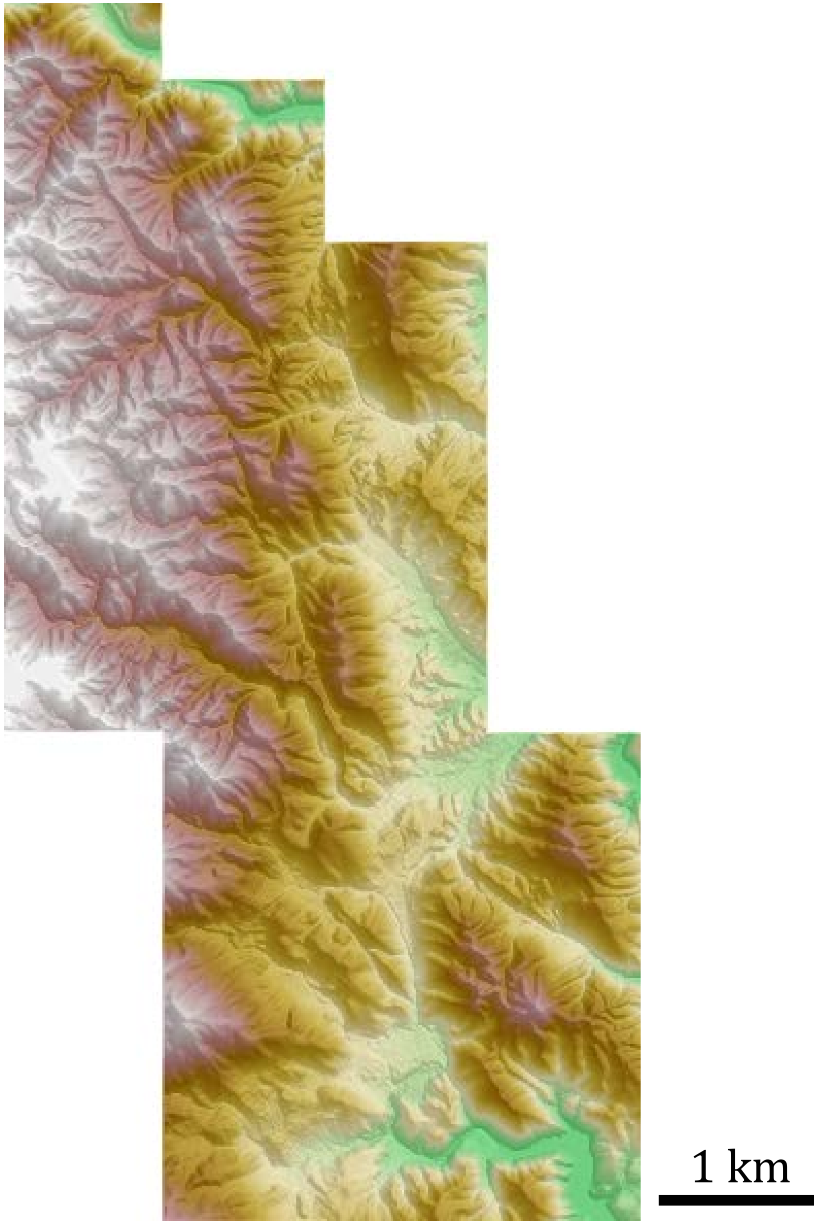

2006 pre-event 2 m DEM KOKUSAI KOGYO GROUP

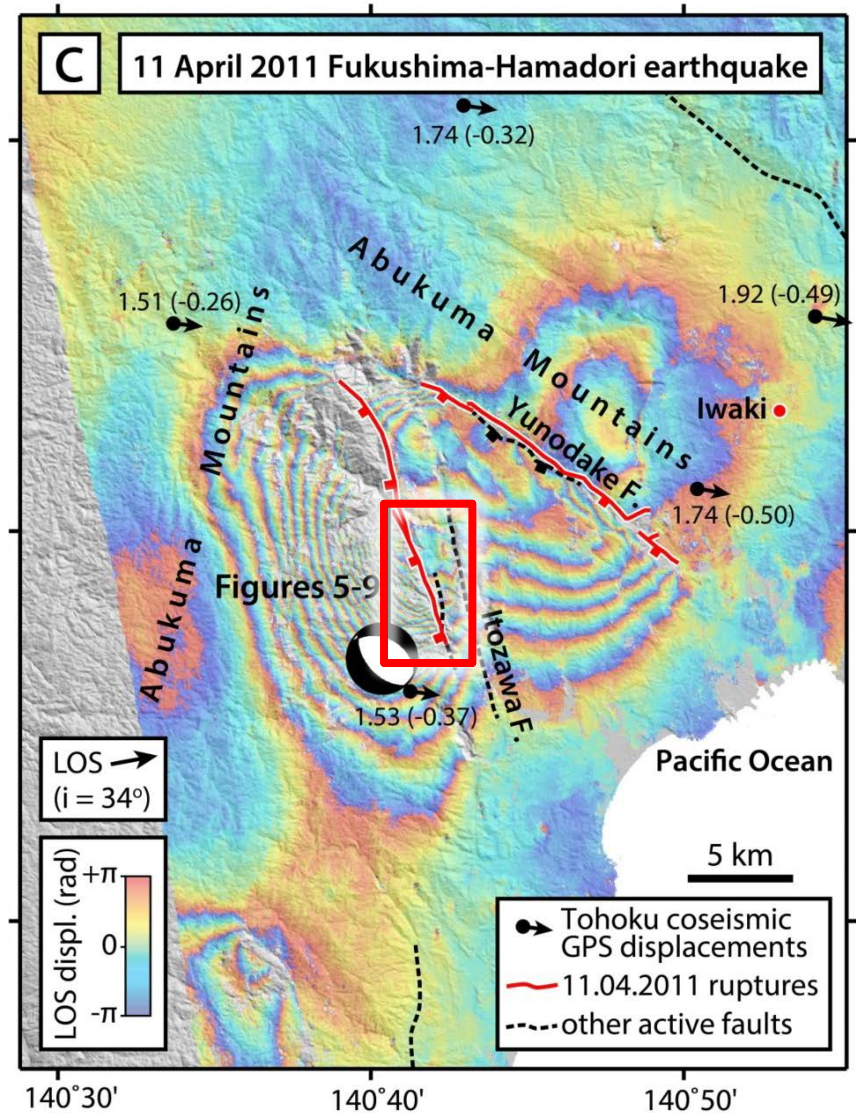

11 April 2011 Fukushima-Hamadori earthquake

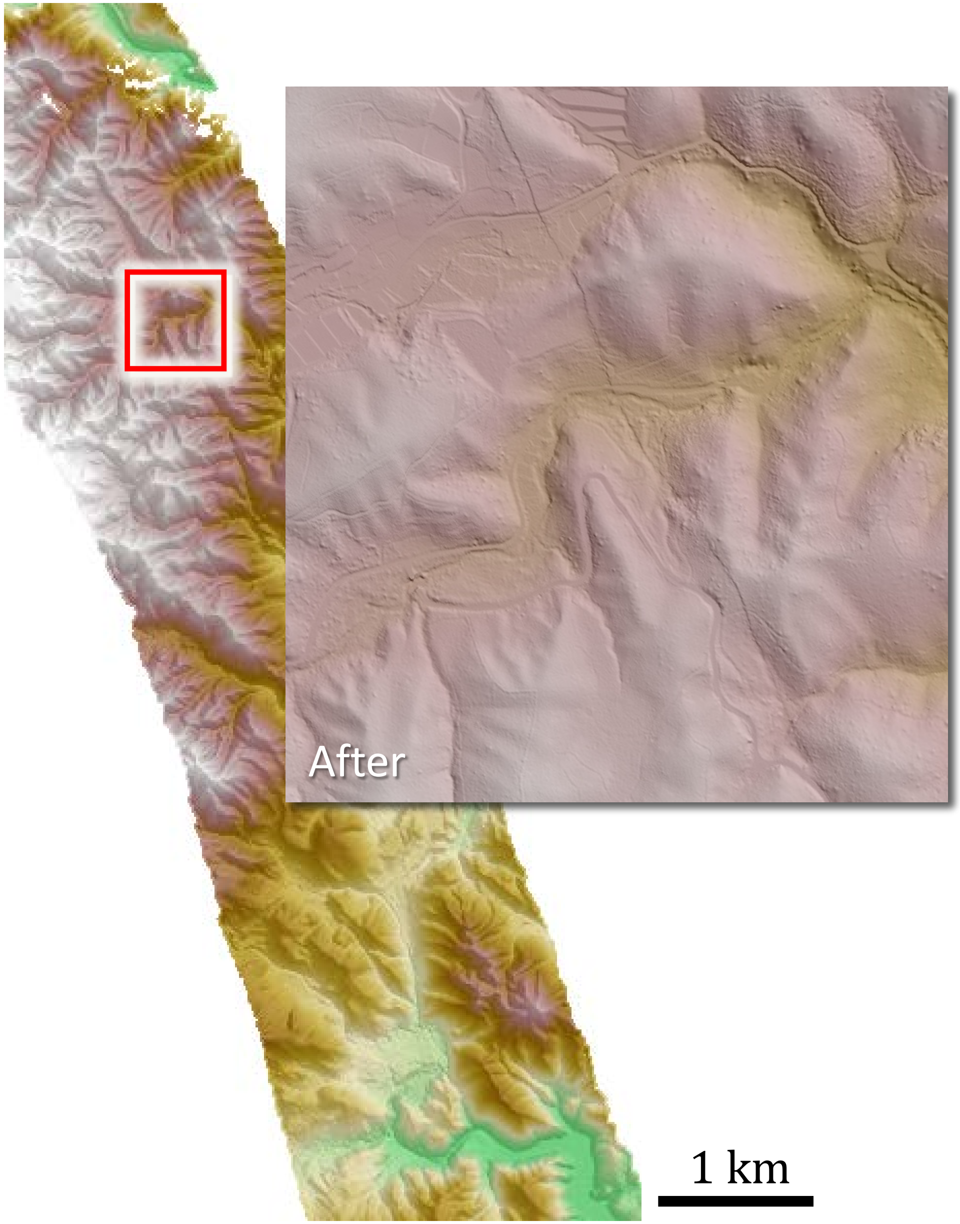

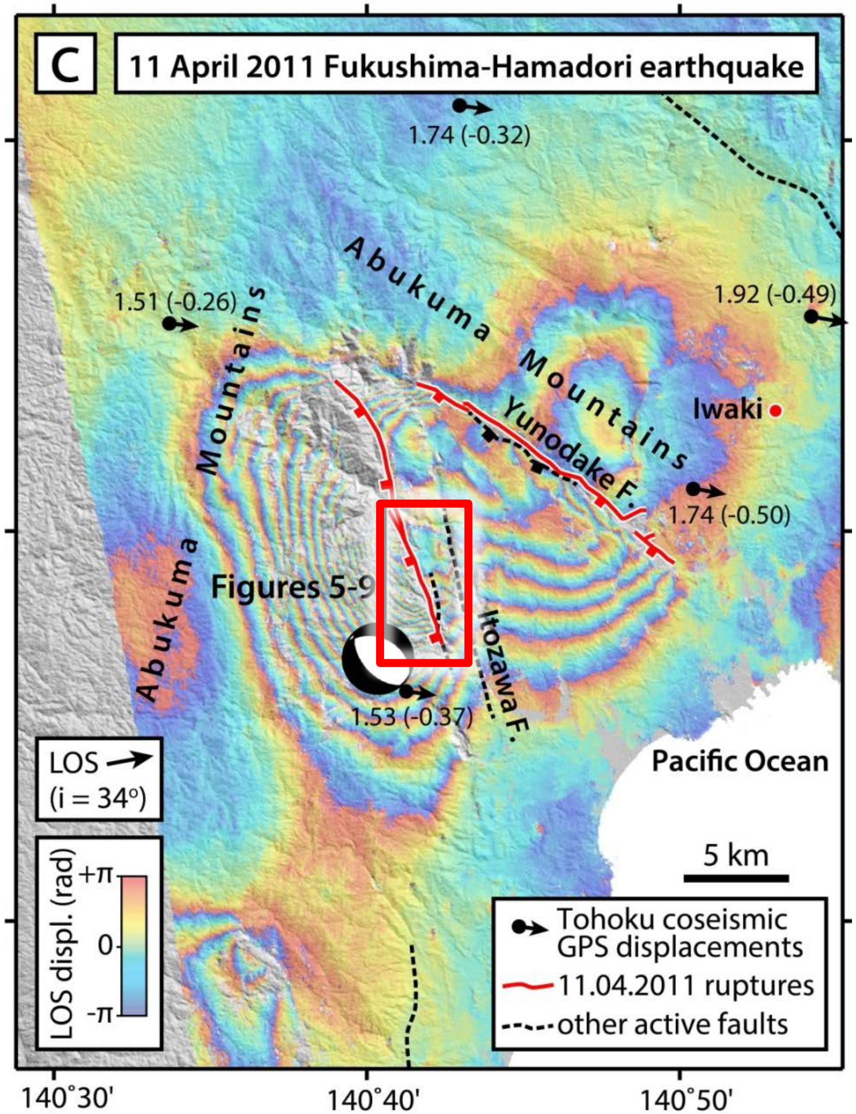

2011 post-event 1 m DEM AERO ASAHI CORPORATION

11 April 2011 Fukushima-Hamadori earthquake

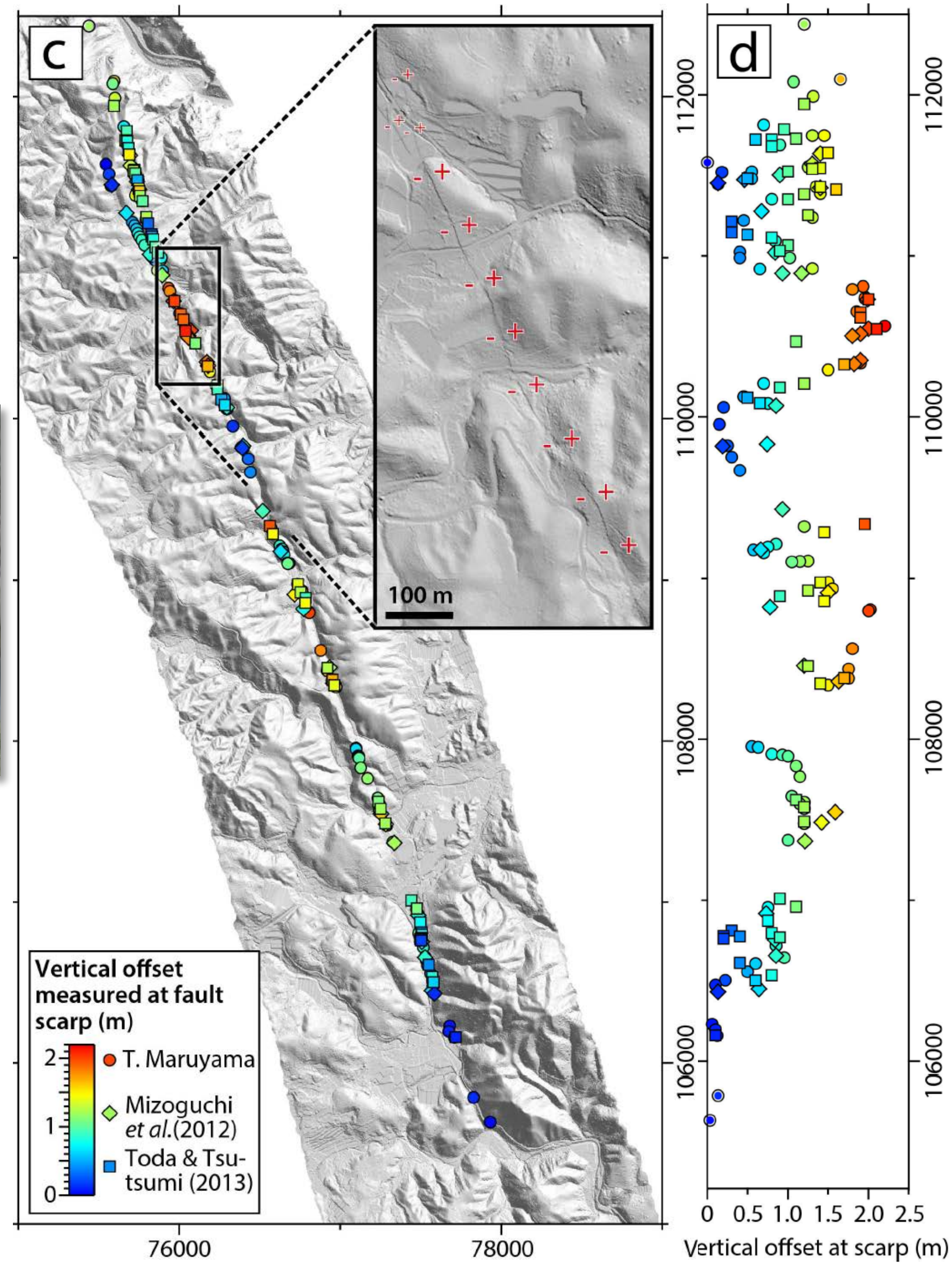

Photos from Toda & Tsutsumi (2013), *BSSA*

2005-2011 vertical displacements

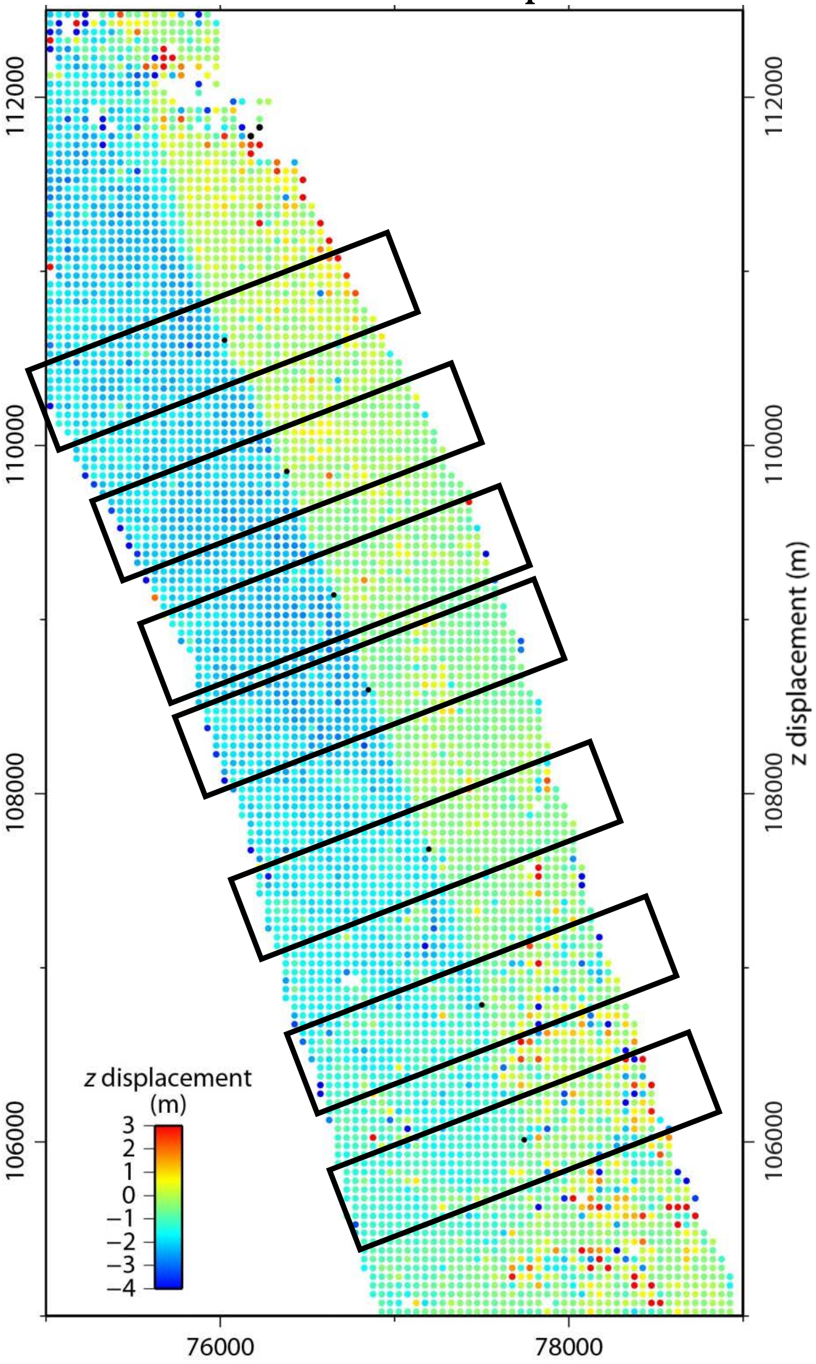

2005-2011 vertical displacements

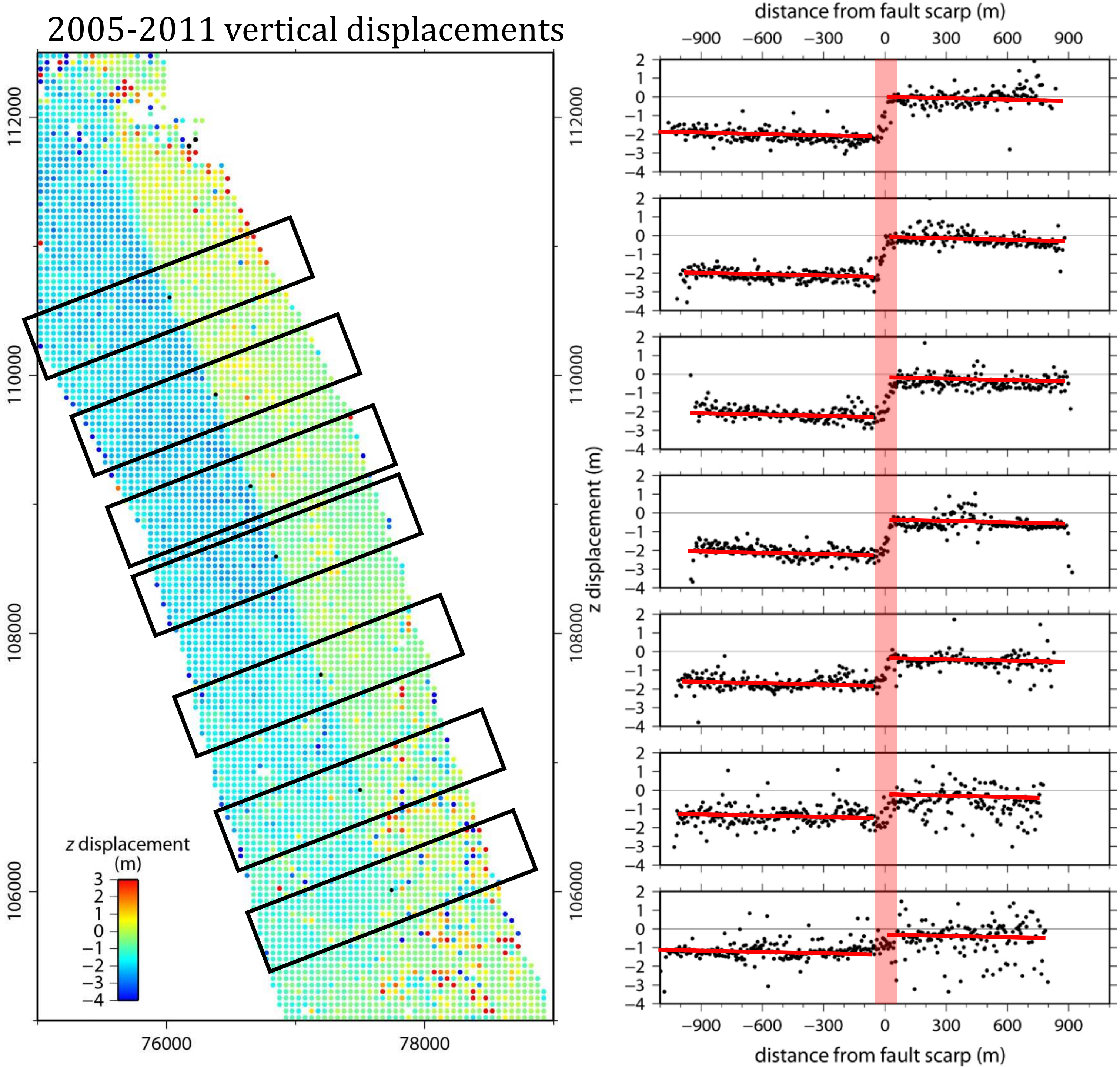

2005-2011 vertical displacements

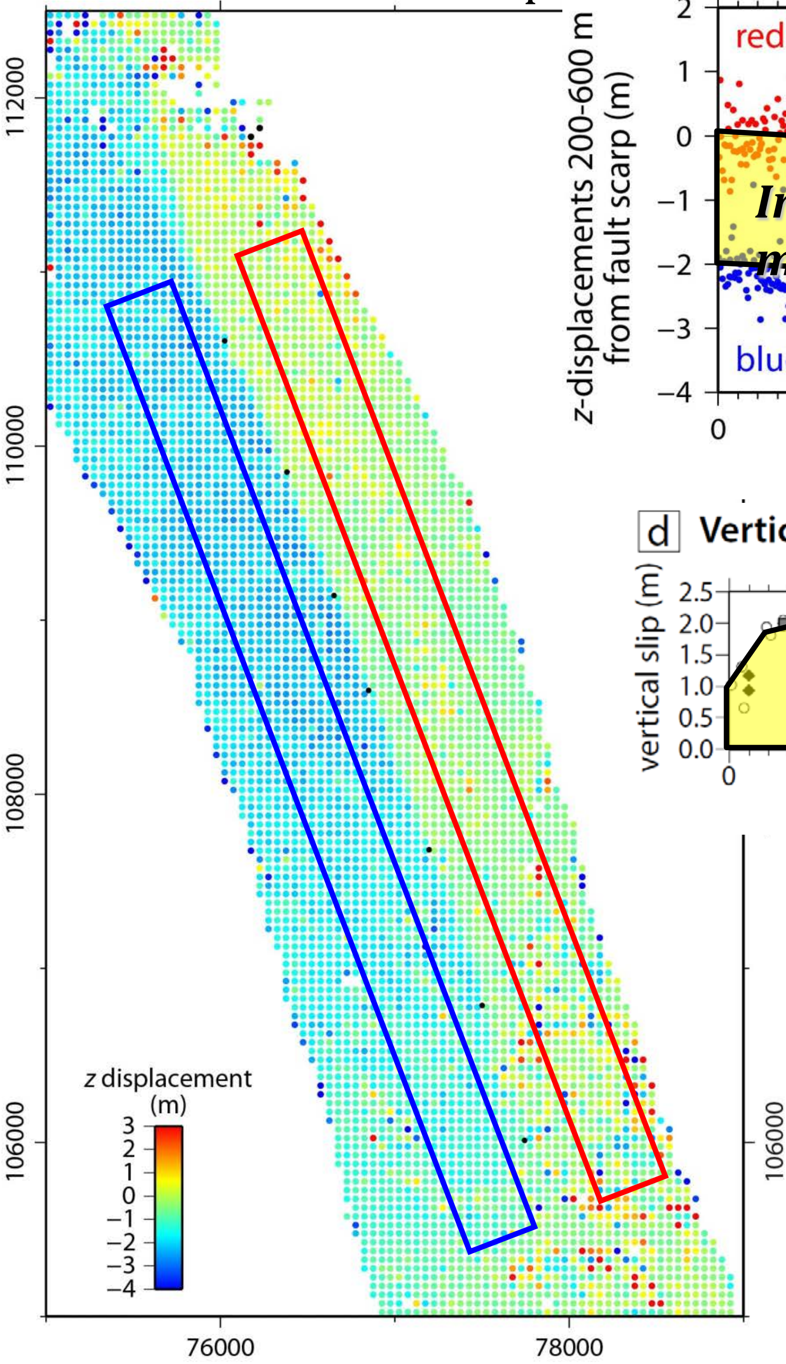

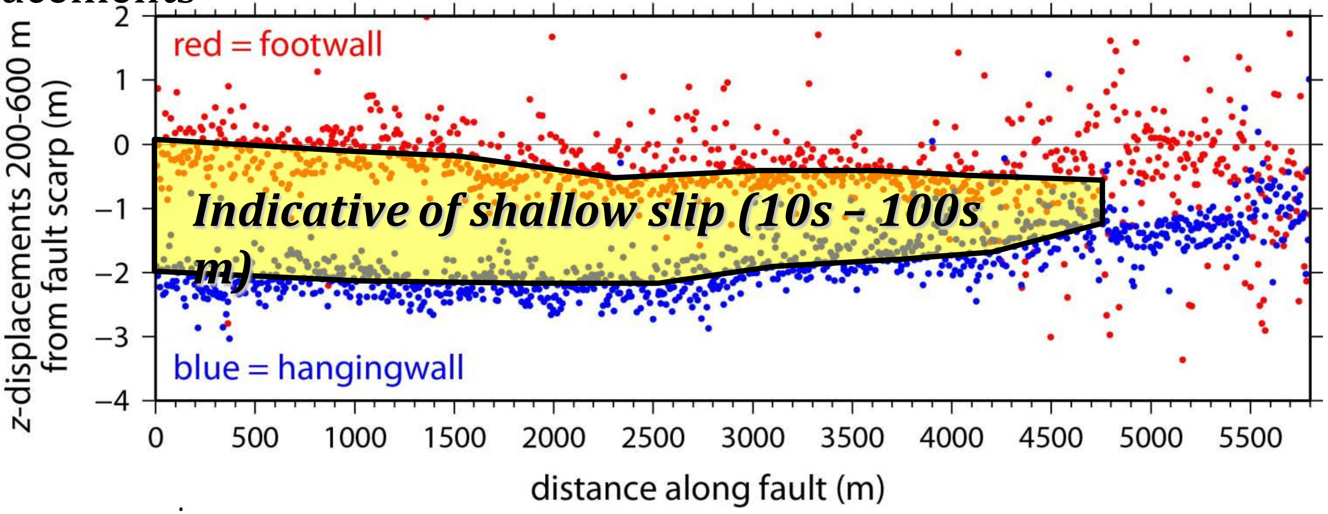

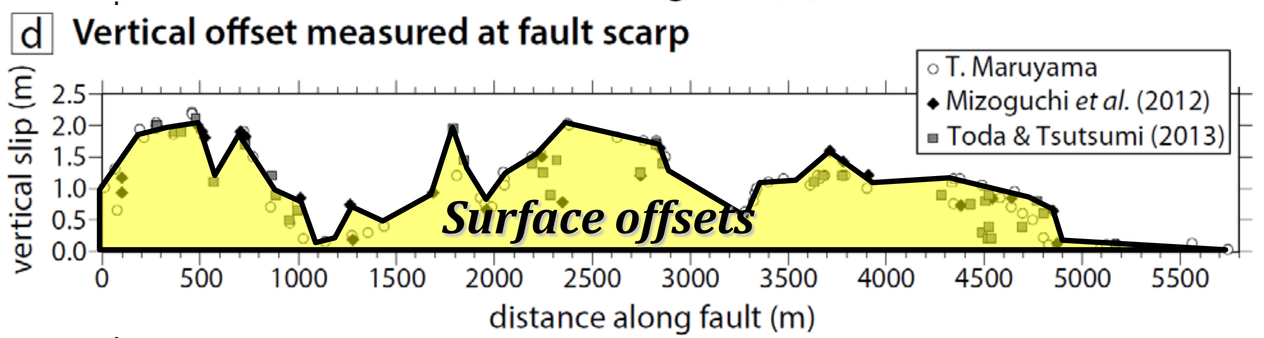

- Slip at depths of a few hundred meters appears to vary smoothly
- In many places, only a small proportion of the slip makes it to the surface

2005-2011 *y*-axis rotations

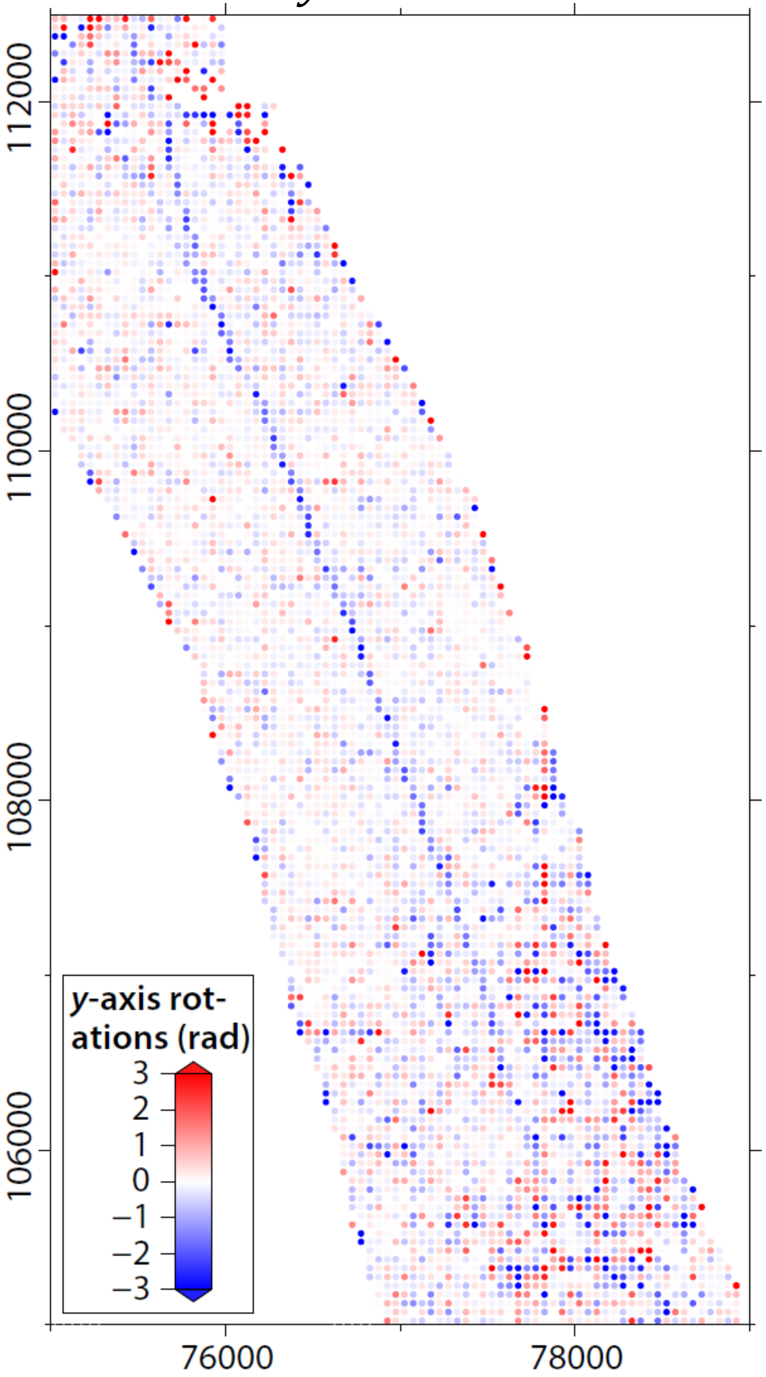

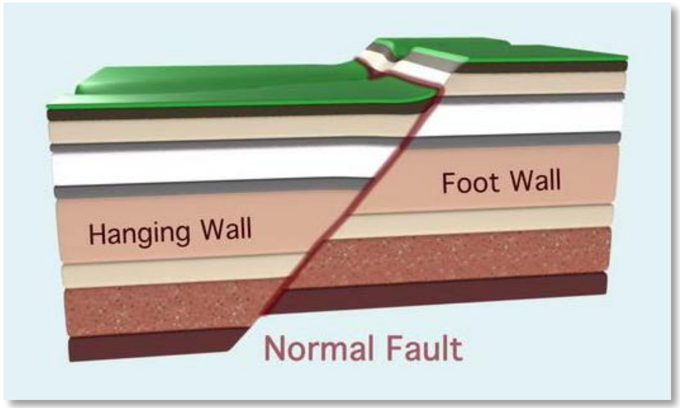

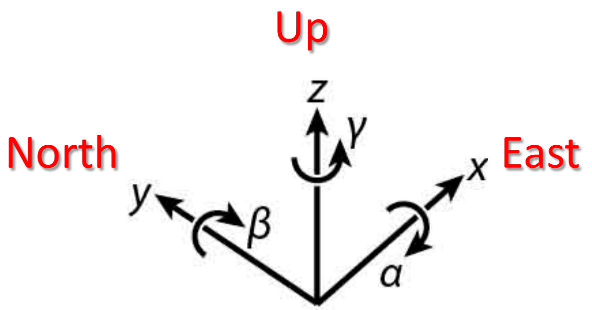

2005-2011 *y*-axis rotations

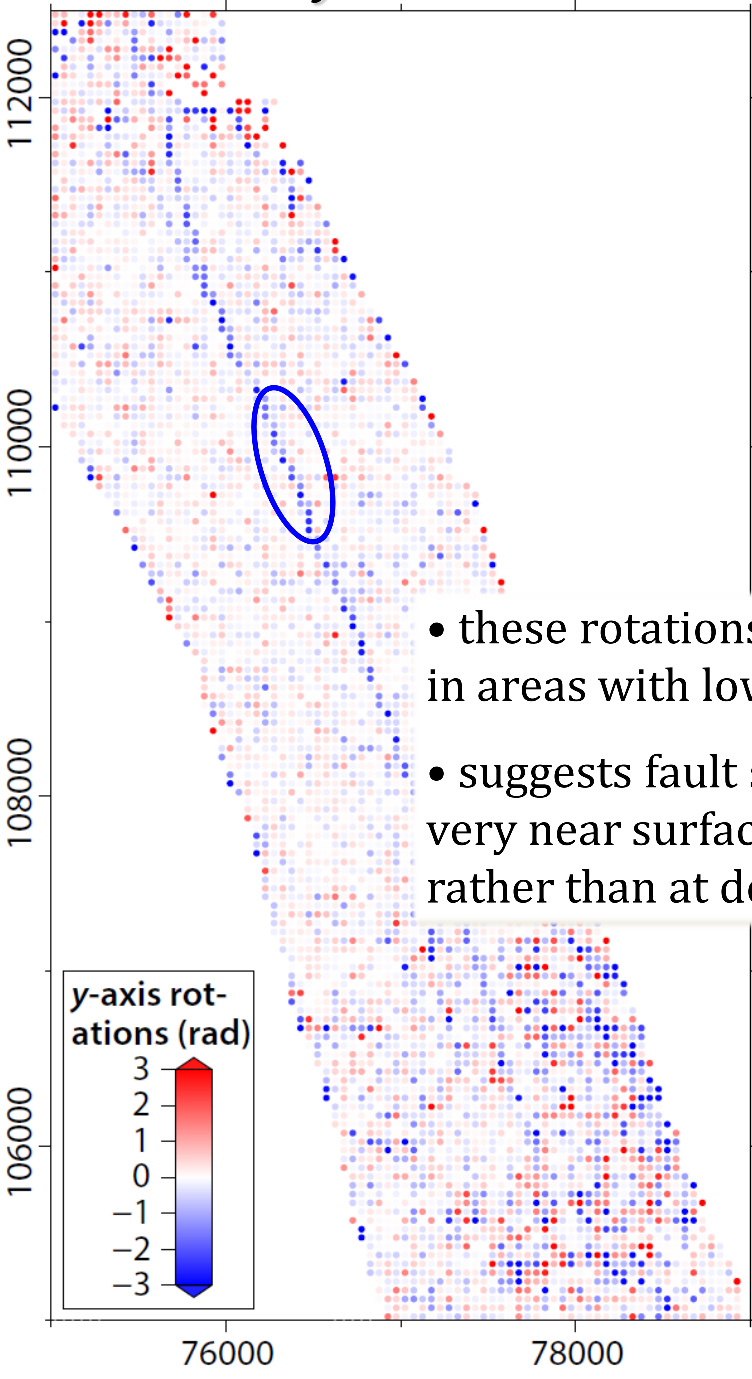

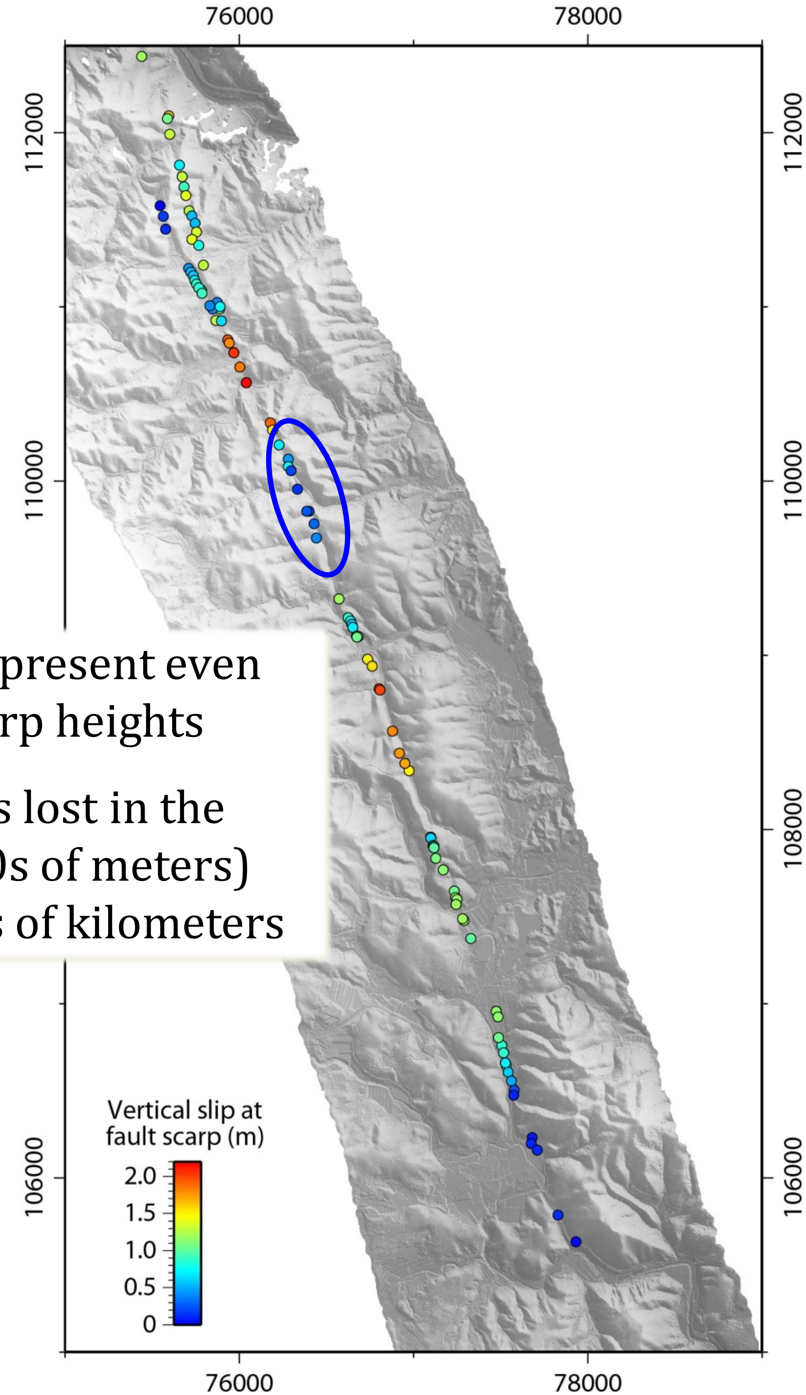

- these rotations are present even in areas with low scarp heights
- suggests fault slip is lost in the very near surface (10s of meters) rather than at depths of kilometers

Darfield rupture (Quigley *et al.* 2010)

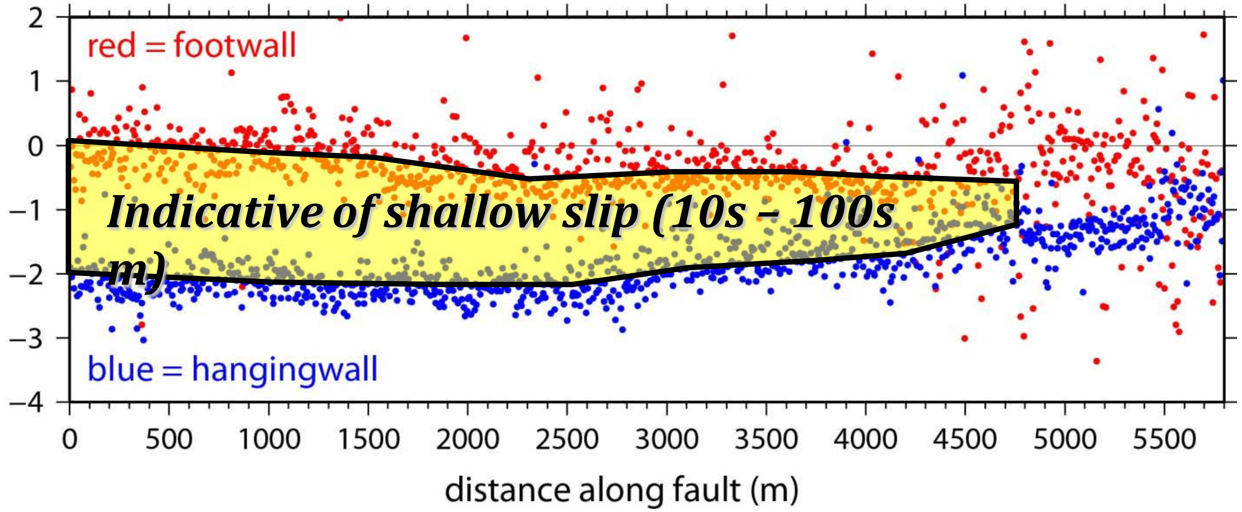

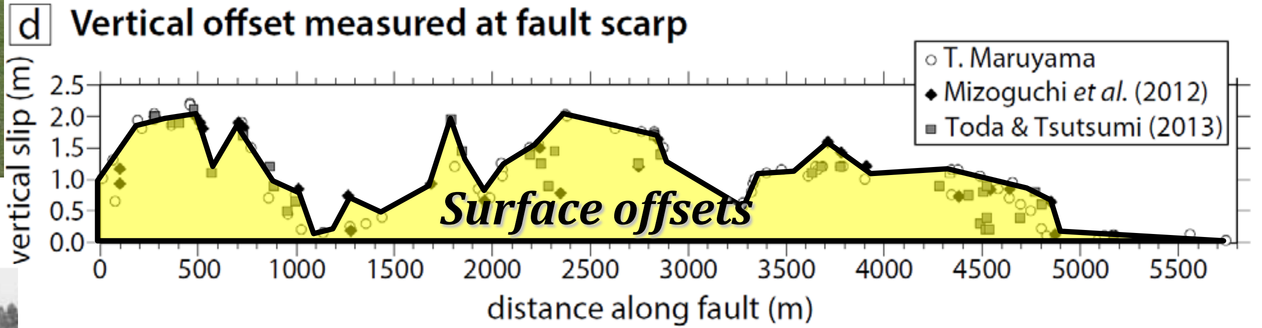

Izmit rupture (Rockwell *et al.* 2002)

- Slip at depths of a few hundred meters appears to vary smoothly
- In many places, only a small proportion of the slip makes it to the surface
- Reflects off-fault deformation in the shallow subsurface?

4 April 2010 El-Mayor-Cucapah earthquake

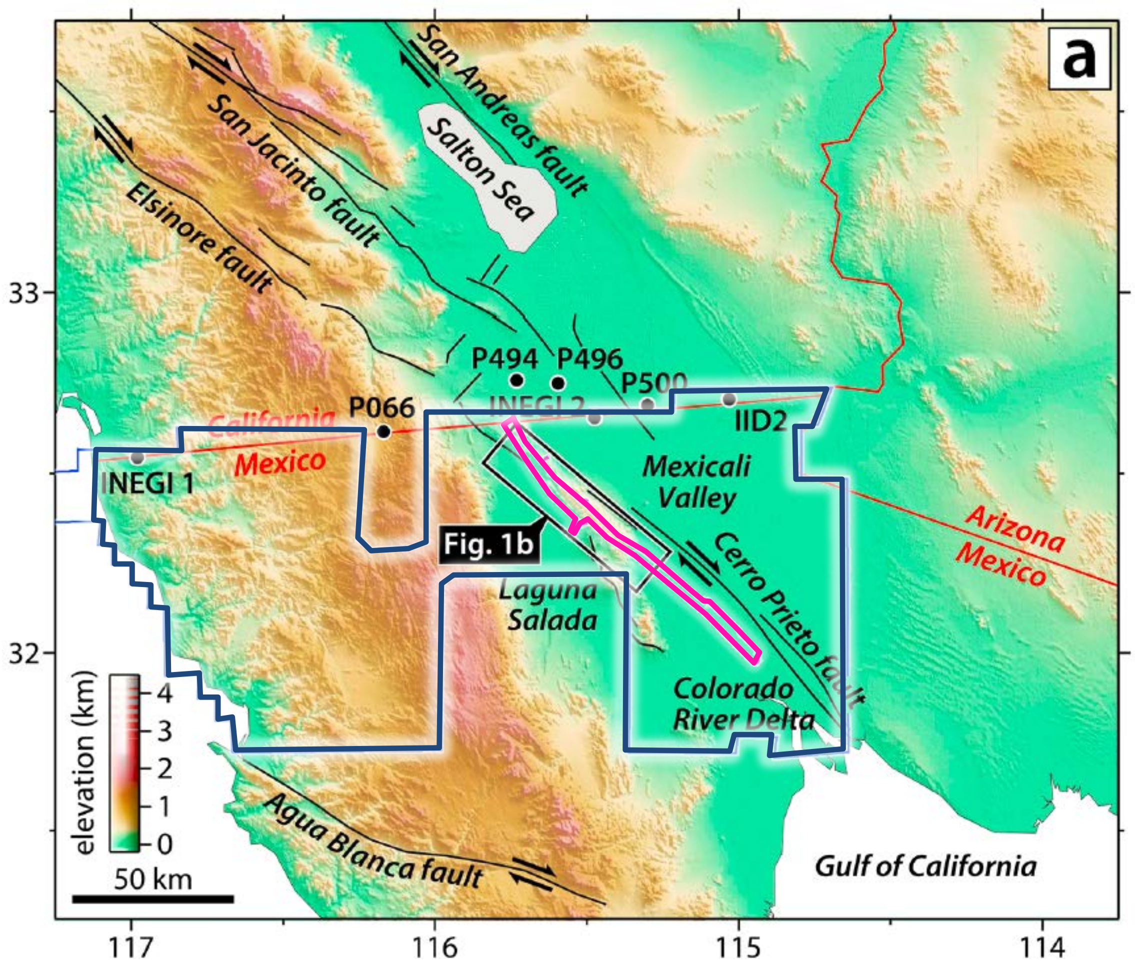

- First complete earthquake rupture with pre-event LiDAR coverage
- Regional lidar flown by INEGI in 2006 at high elevation (6 km AGL) with 0.01 pts/m^2
- Post-event lidar flown by NCALM along a 3 x 100 km strip in August 2010, with ~9 pts/m^2

4 April 2010 El-Mayor-Cucapah earthquake

Wei *et al.* (2011), *Nat. Geosci.*

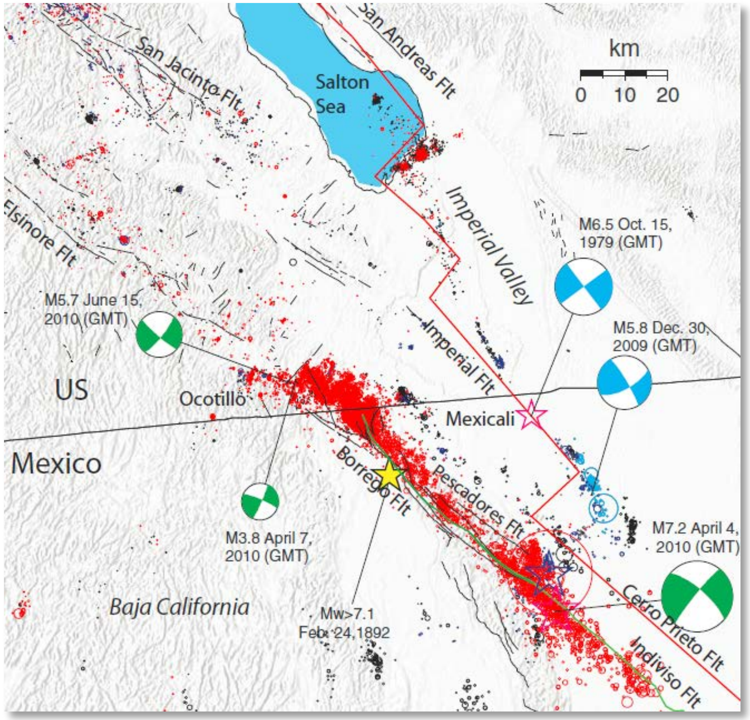

• Geodetic and seismological modelling supports steep dips of 60° – 90°

Wei *et al.* (2011), *Nat. Geosci.*

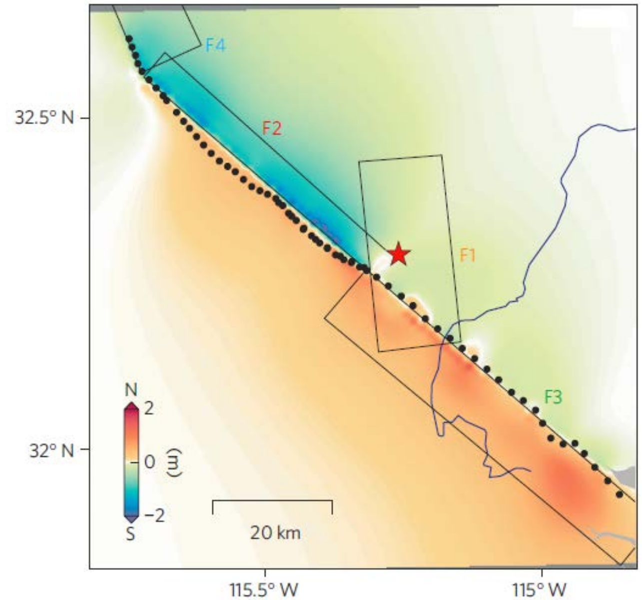

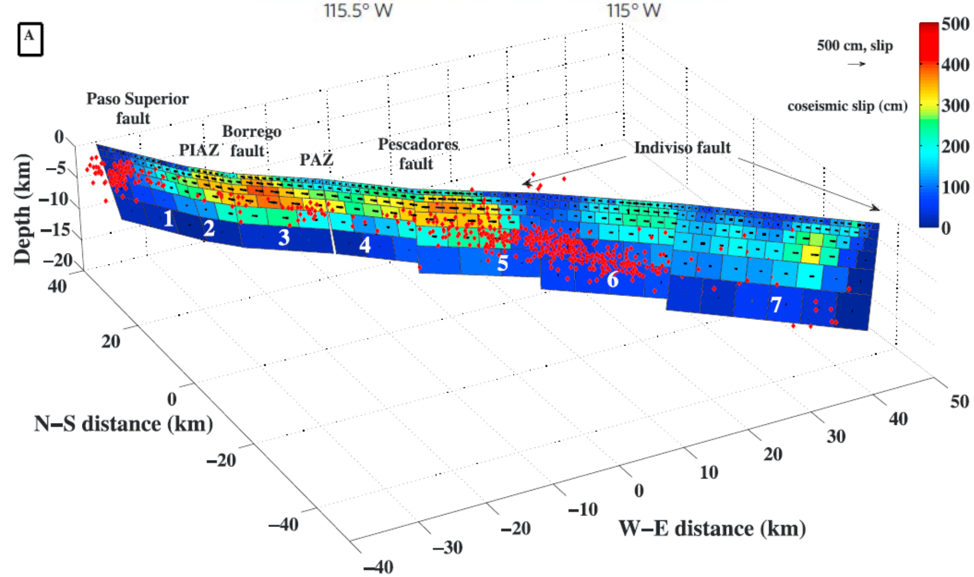

Fialko *et al.* (2010), *AGU Fall Meeting*

4 April 2010 El-Mayor-Cucapah earthquake

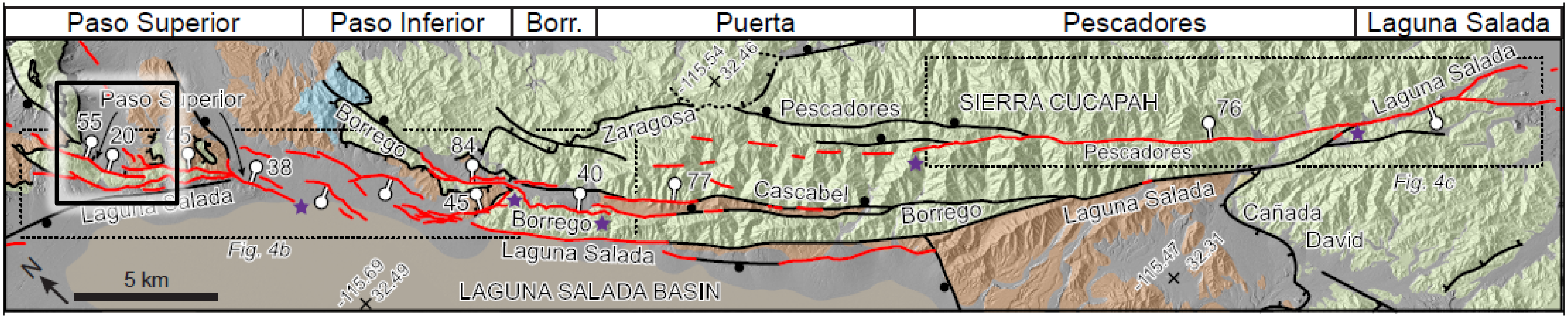

Teran *et al.* (2014), *Geosphere*

- Geodetic and seismological modelling supports steep dips of 60° – 90°
- Field observations support a much wider range of dips and imply slip on low-angle detachment faults with dips of ca. 20°

4 April 2010 El-Mayor-Cucapah earthquake

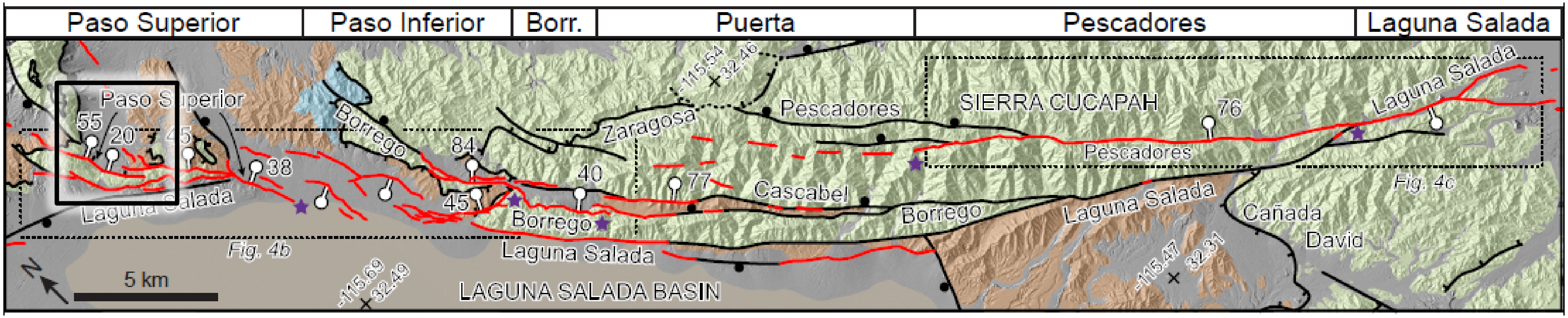

Teran *et al.* (2014), *Geosphere*

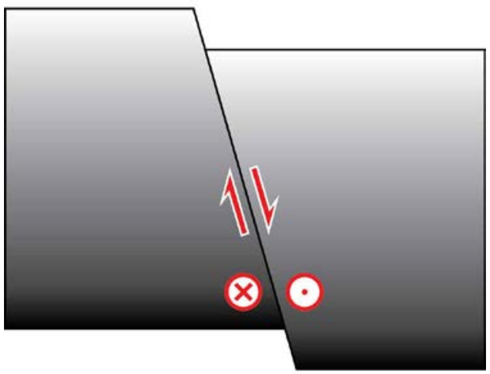

For high-angle slip, vertical motions dominate over fault-perpendicular motions

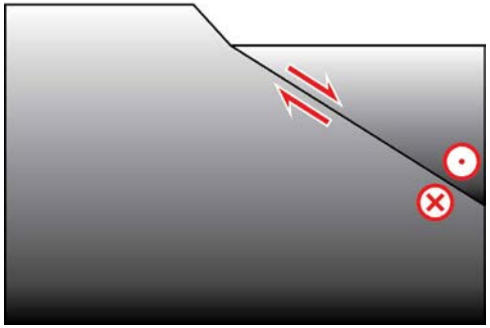

For low-angle slip, fault-perpendicular motions dominate over vertical motions

4 April 2010 El-Mayor-Cucapah earthquake

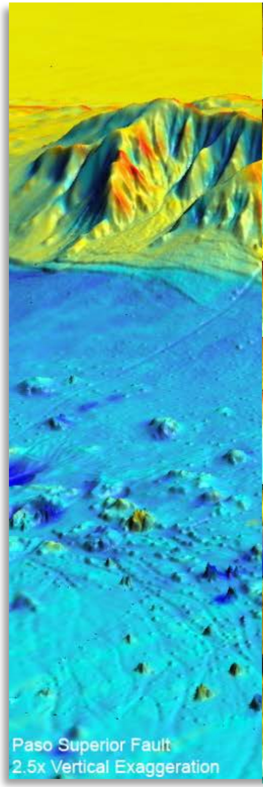

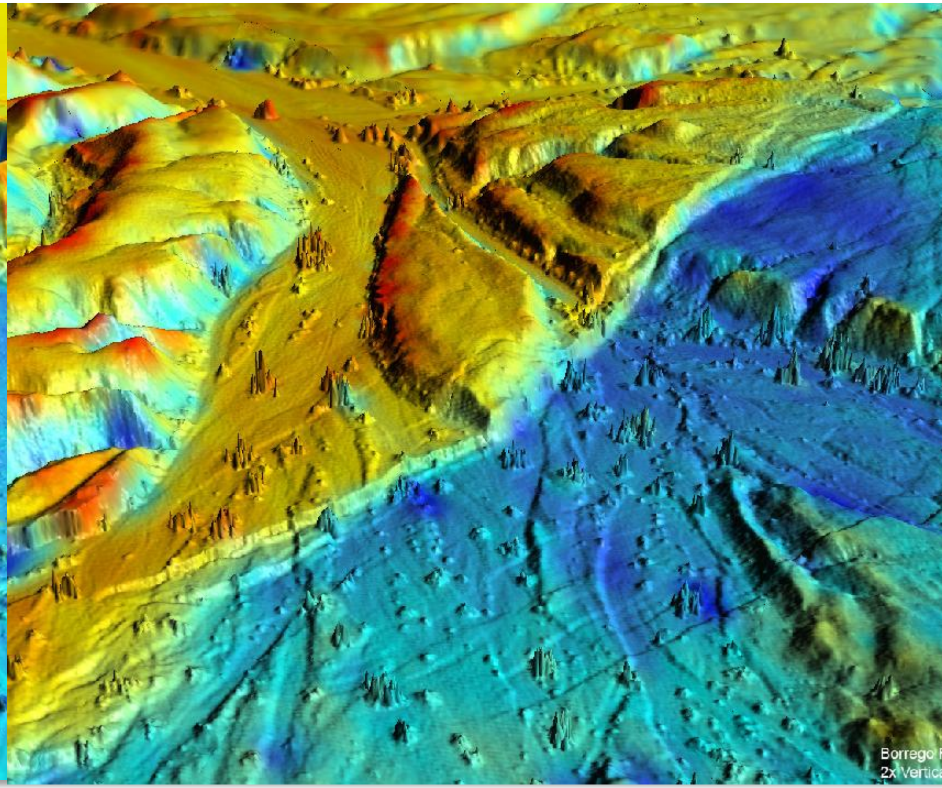

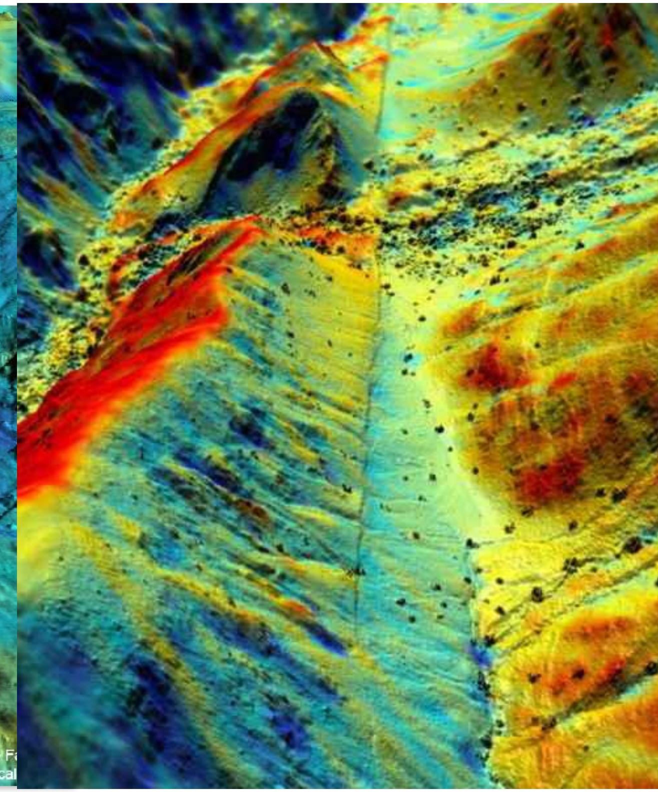

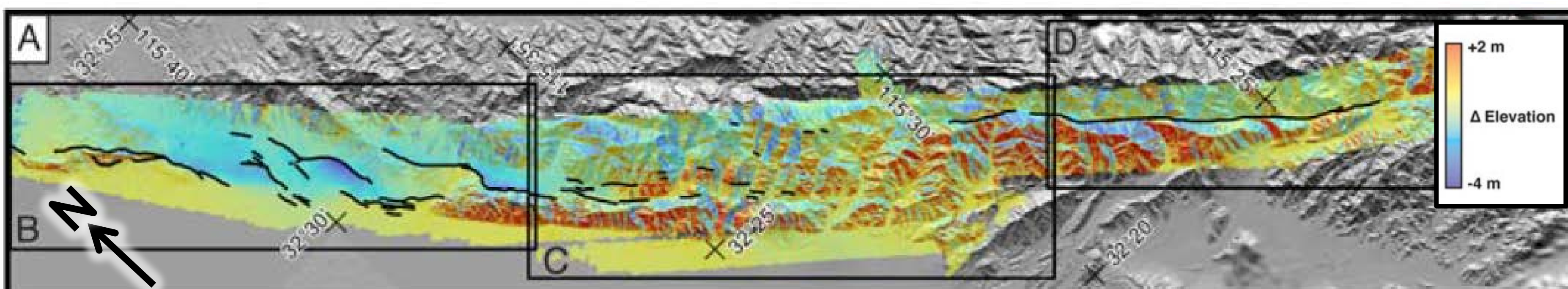

Near-Field Deformation from the El Mayor–Cucapah Earthquake Revealed by Differential LIDAR

Michael E. Oskin,[1*] J Ramon Arrowsmith,[2] Alejandro Hinojosa Corona,[3] Austin J. Elliott,[1] John M. Fletcher,[3] Eric J. Fielding,[4] Peter O. Gold,[1] J. Javier Gonzalez Garcia,[3] Ken W. Hudnut,[5] Jing Liu-Zeng,[6] Orlando J. Teran[3]

10 FEBRUARY 2012 VOL 335 SCIENCE

4 April 2010 El-Mayor-Cucapah earthquake

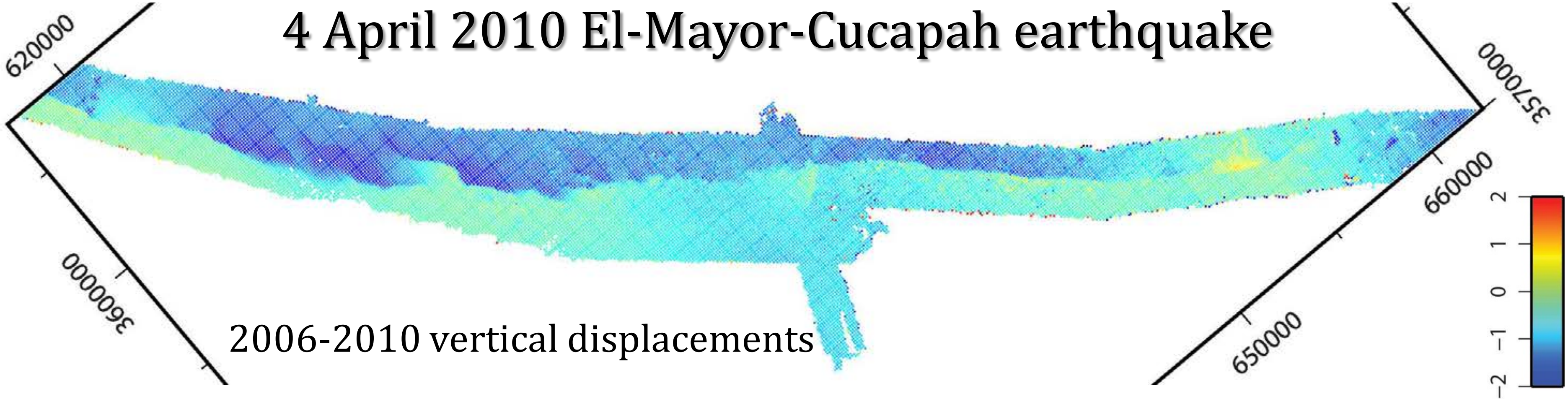

2006-2010 vertical displacements

Geophysical Research Letters

Optimization of legacy lidar data sets for measuring near-field earthquake displacements

Craig L. Glennie[1], Alejandro Hinojosa-Corona[2], Edwin Nissen[3], Arpan Kusari[1], Michael E. Oskin[4], J. Ramon Arrowsmith[5], and Adrian Borsa[6]

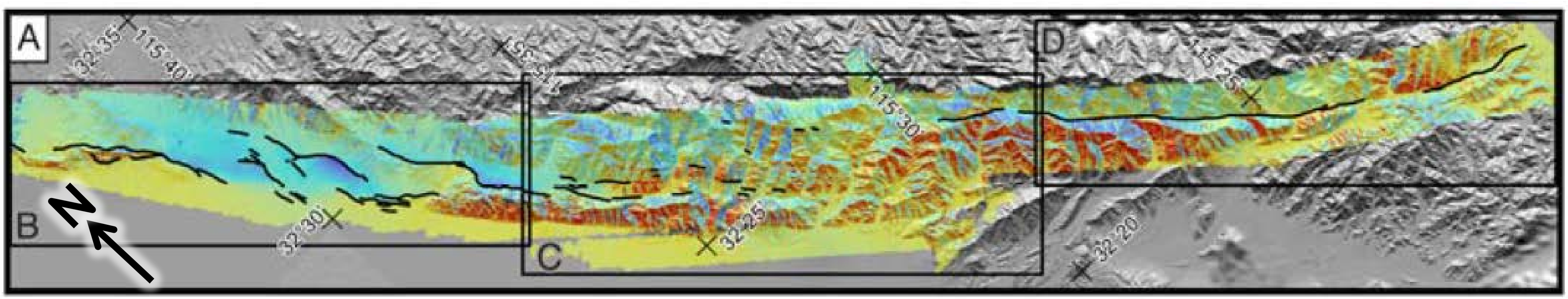

Near-Field Deformation from the El Mayor–Cucapah Earthquake Revealed by Differential LIDAR

Michael E. Oskin,[1*] J Ramon Arrowsmith,[2] Alejandro Hinojosa Corona,[3] Austin J. Elliott,[1] John M. Fletcher,[3] Eric J. Fielding,[4] Peter O. Gold,[1] J. Javier Gonzalez Garcia,[3] Ken W. Hudnut,[5] Jing Liu-Zeng,[6] Orlando J. Teran[3]

10 FEBRUARY 2012 VOL 335 SCIENCE

4 April 2010 El-Mayor-Cucapah earthquake

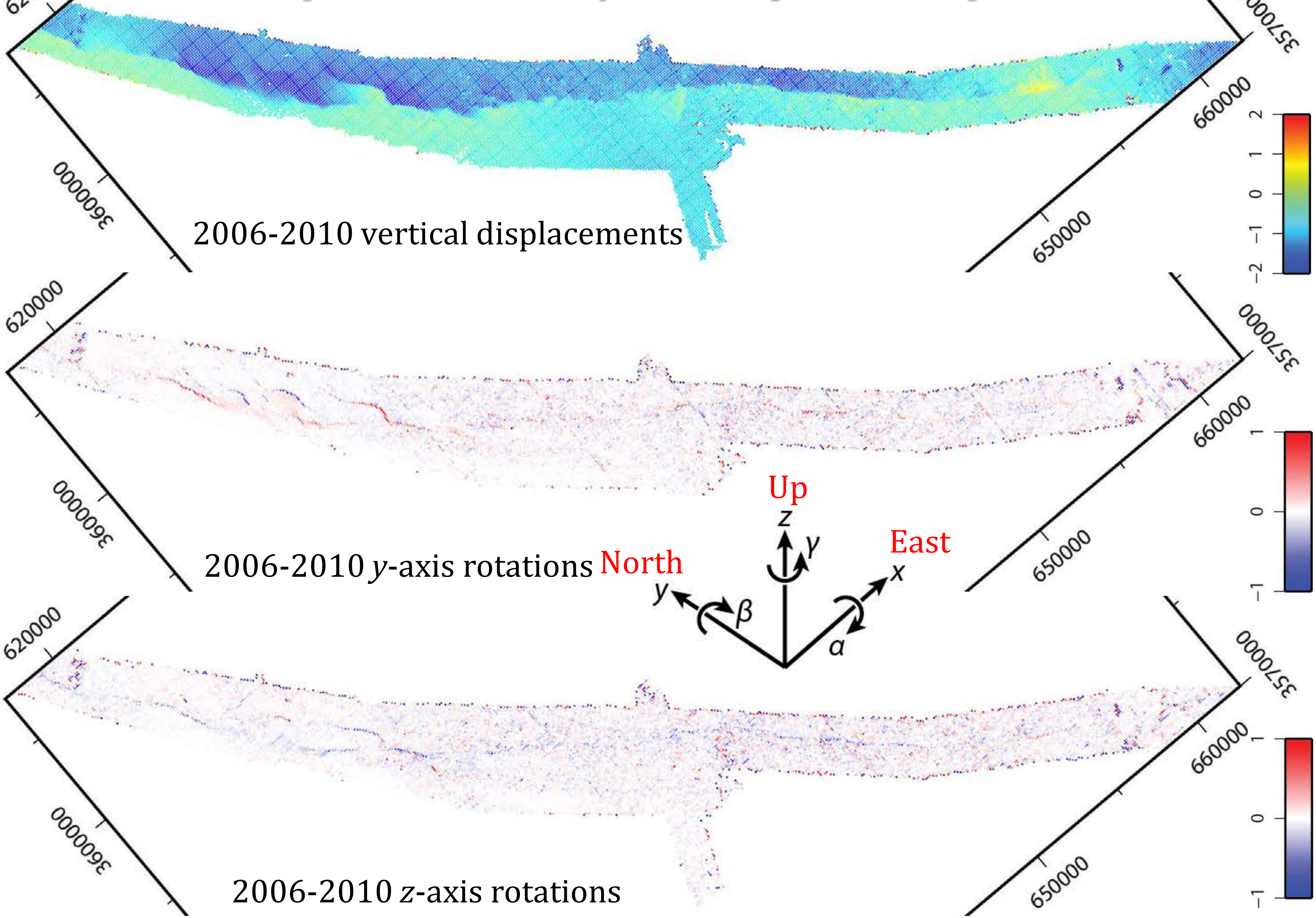

4 April 2010 El-Mayor-Cucapah earthquake

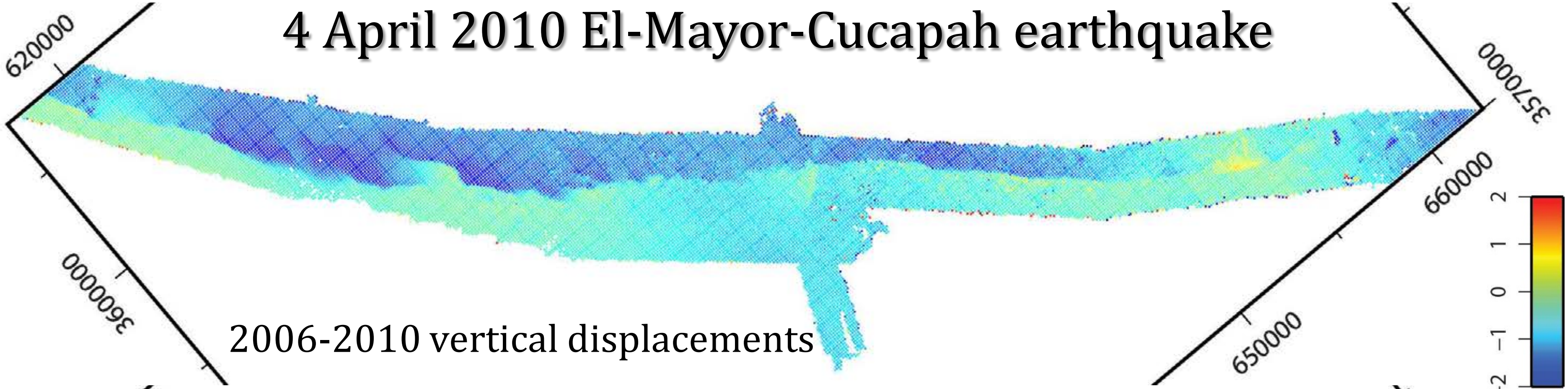

2006-2010 vertical displacements

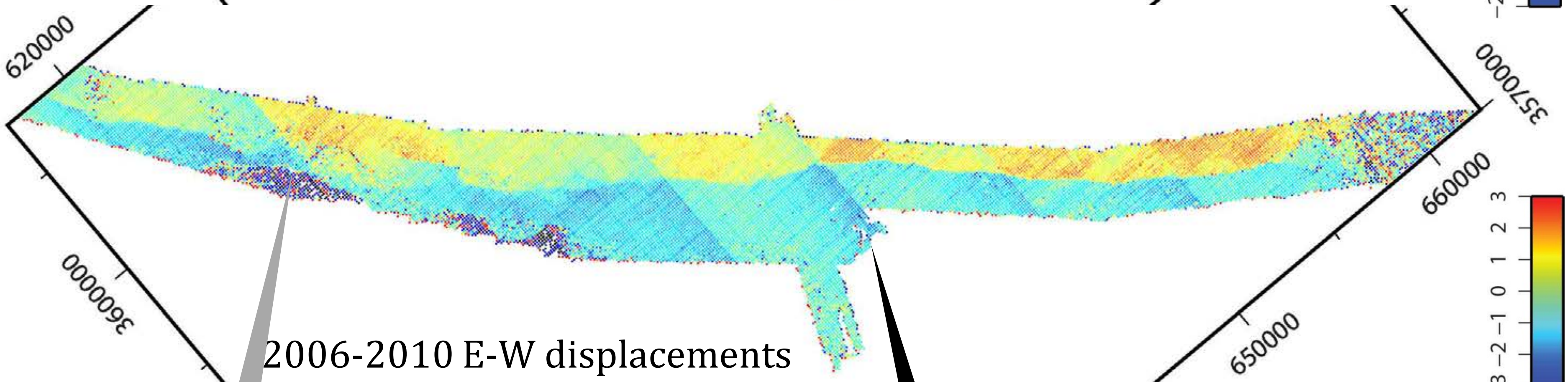

2006-2010 E-W displacements

Lidar instrument errors correlate with pre-event flight lines (see Glennie *et al.*, 2014, *Geophys. Res. Lett.*)

4 April 2010 El-Mayor-Cucapah earthquake

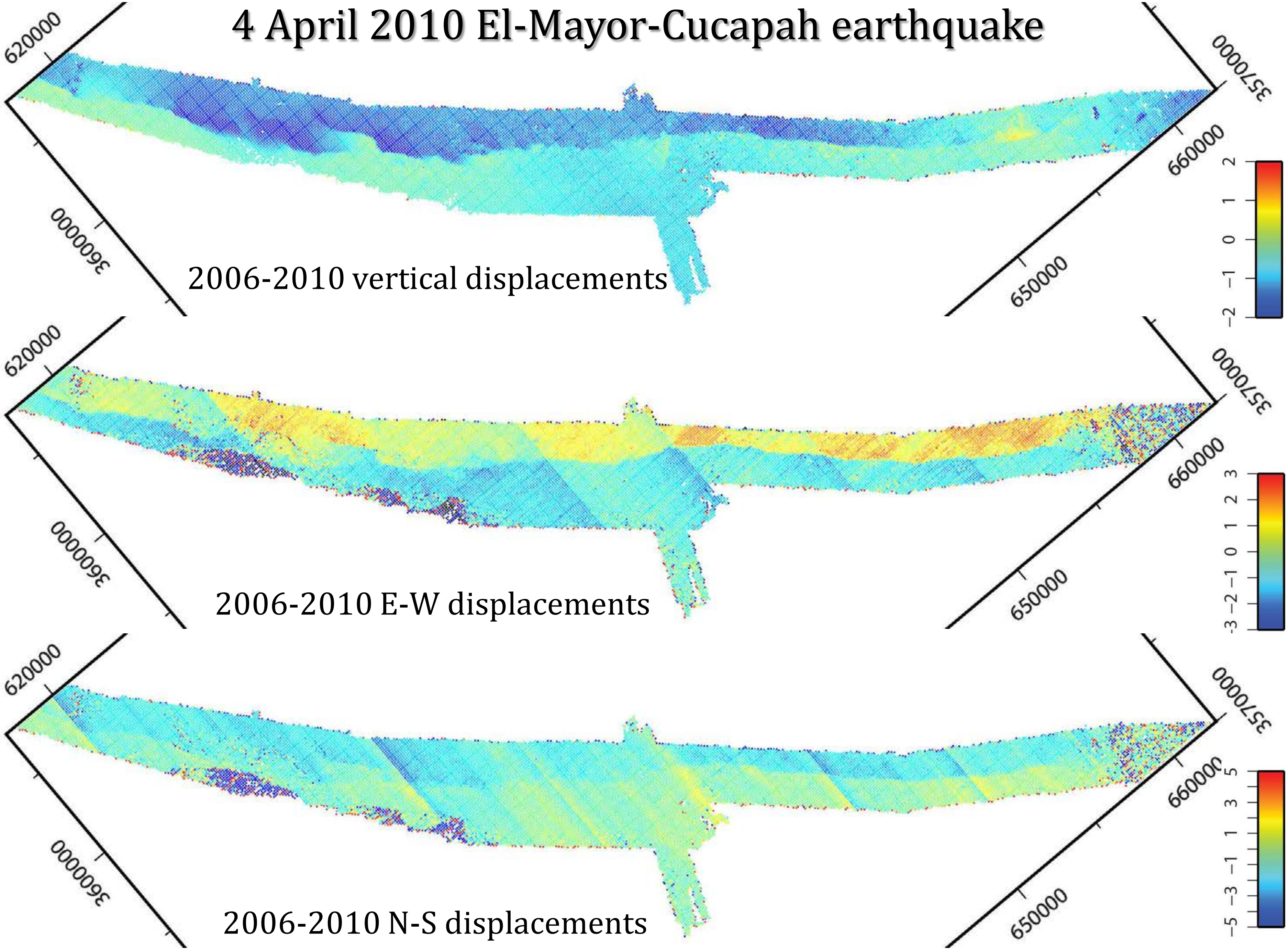

4 April 2010 El-Mayor-Cucapah earthquake

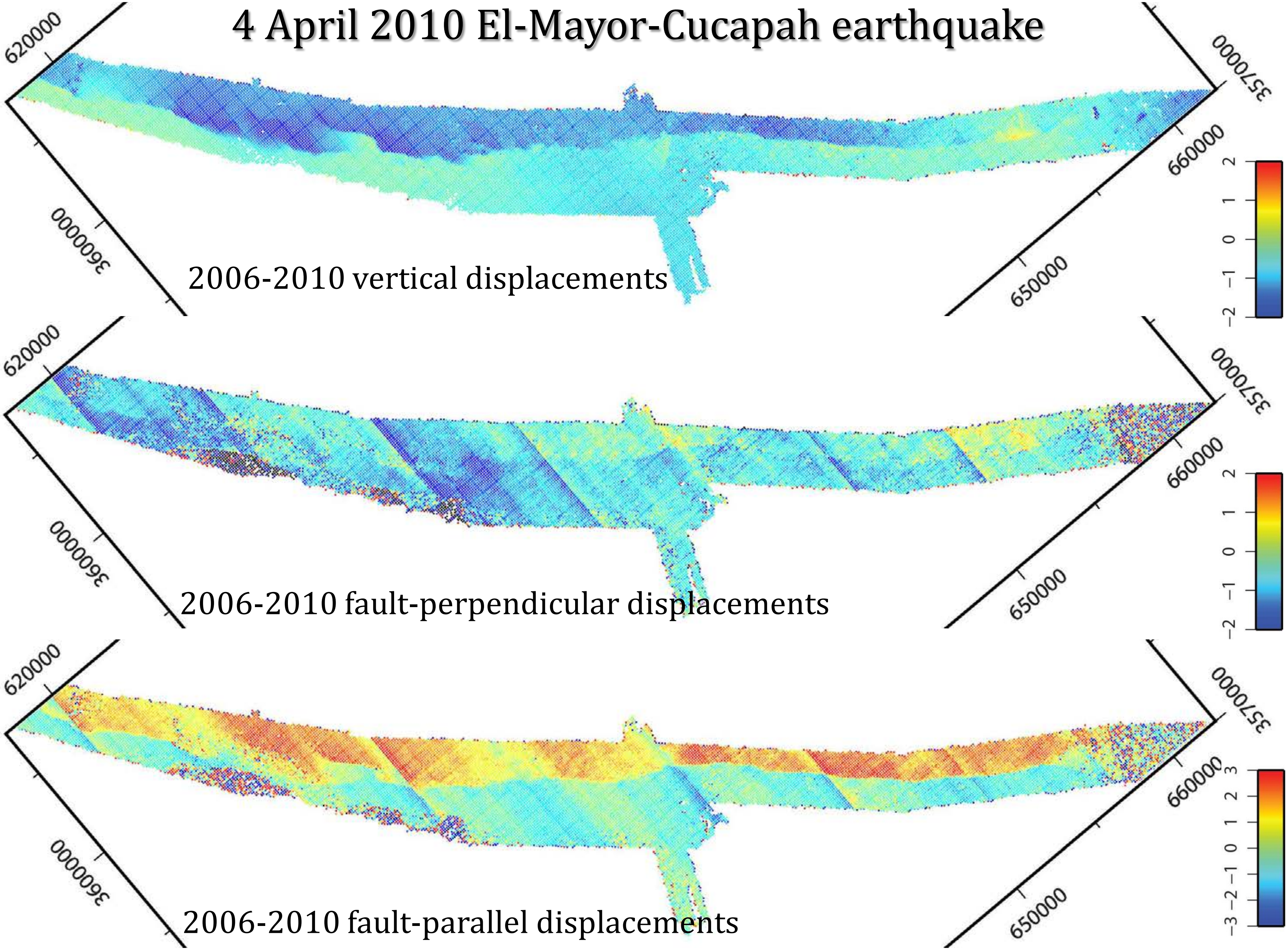

4 April 2010 El-Mayor-Cucapah earthquake

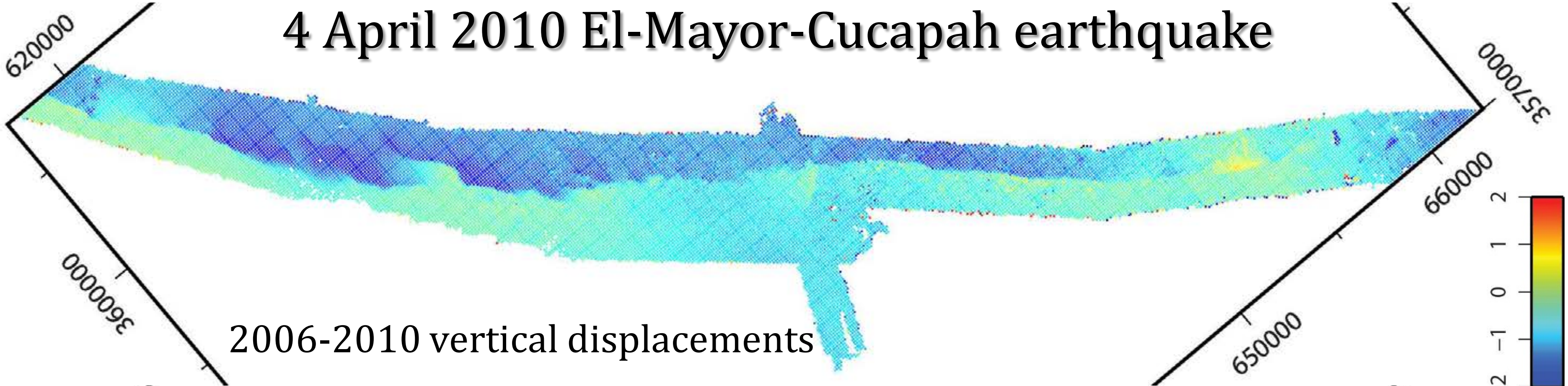

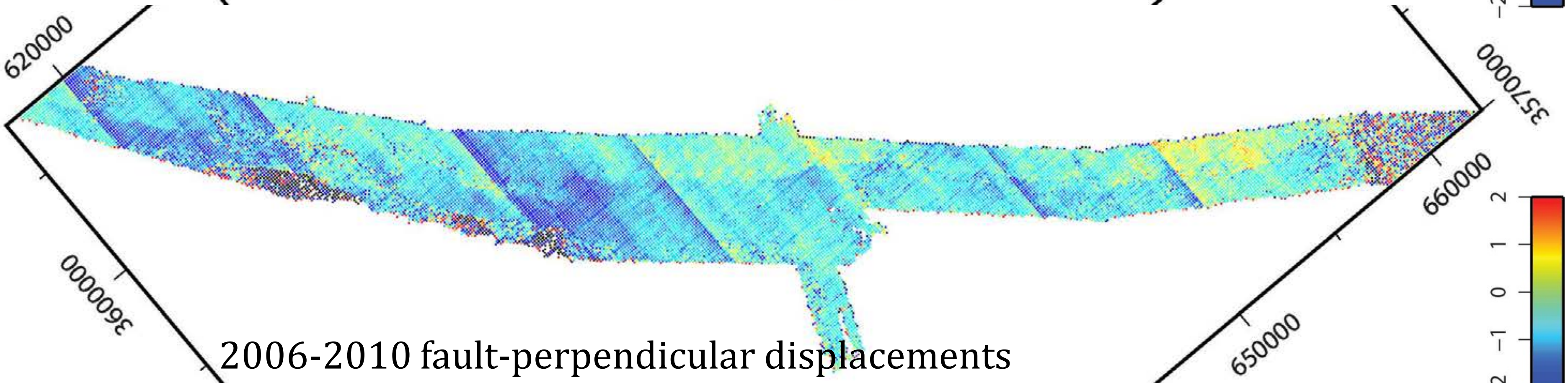

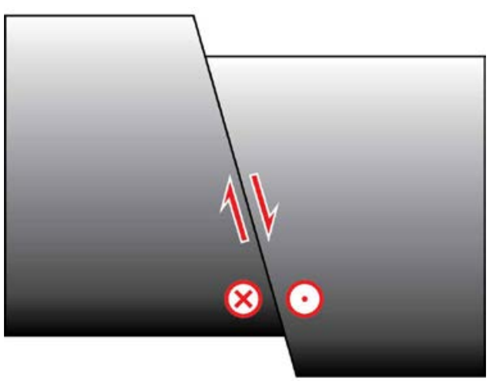

For high-angle slip, vertical motions dominate over fault-perpendicular motions

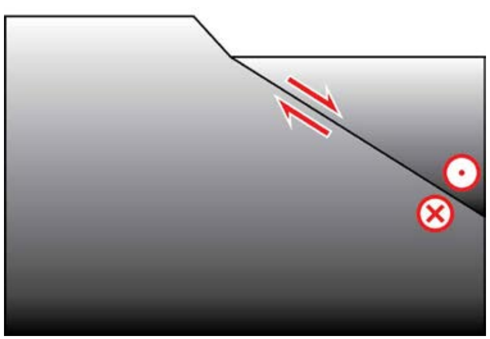

For low-angle slip, fault-perpendicular motions dominate over vertical motions

Lidar differencing vs other methods

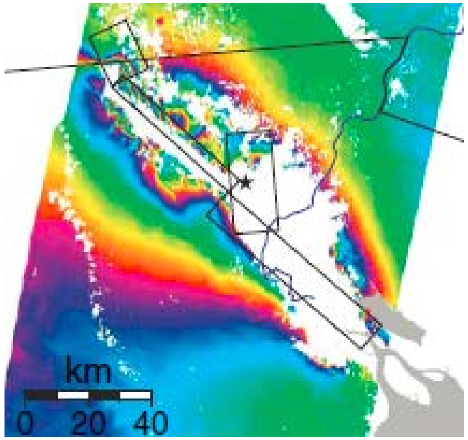

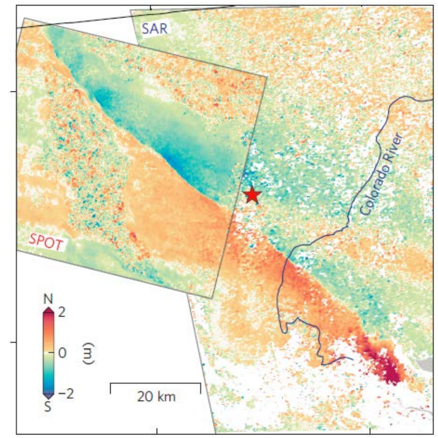

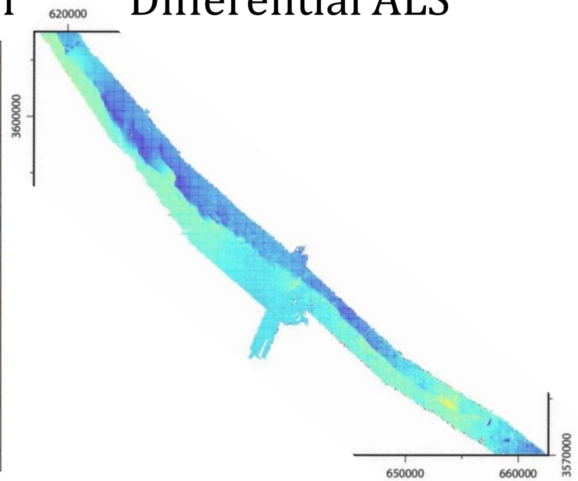

	InSAR	Sub-pixel correlation	Differential ALS
Temporal resolution?	Good	Good	Limited, will get better
Temporal coherence?	Limited	Variable	Good
Far-field deformation?	Good	Limited	Poor
Near-field deformation?	Limited	Good	Good
Dense vegetation?	Limited	Poor	Good
3-D displacements?	Limited	Good	Good – with potential to measure strain, rotations

Degradation of the 2010 El Mayor-Cucapah earthquake scarp

Austin Elliott, UC Davis/Oxford

Degradation of the 2010 El Mayor-Cucapah earthquake scarp

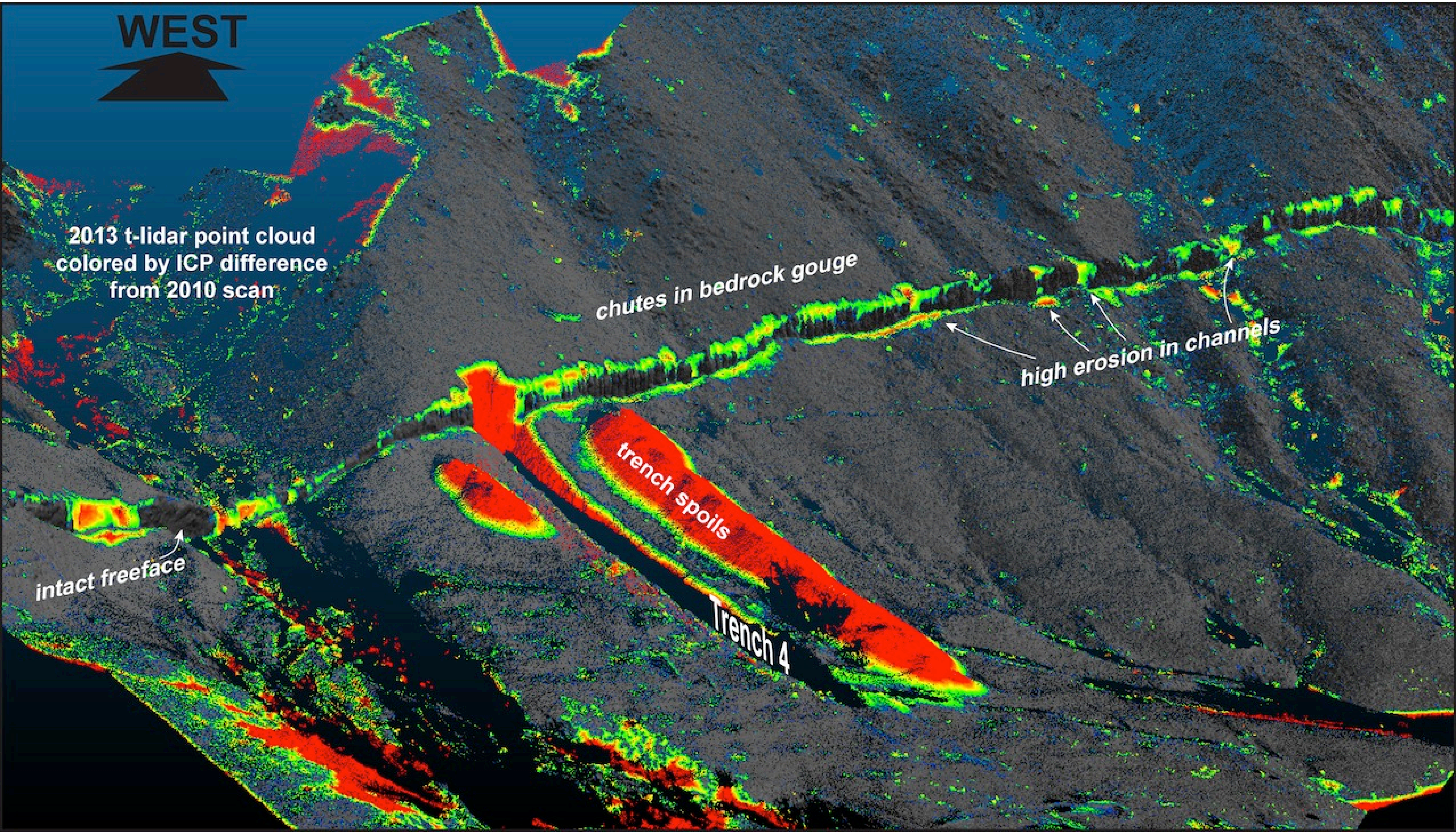

Austin Elliott, UC Davis/Oxford

Degradation of the 2010 El Mayor-Cucapah earthquake scarp

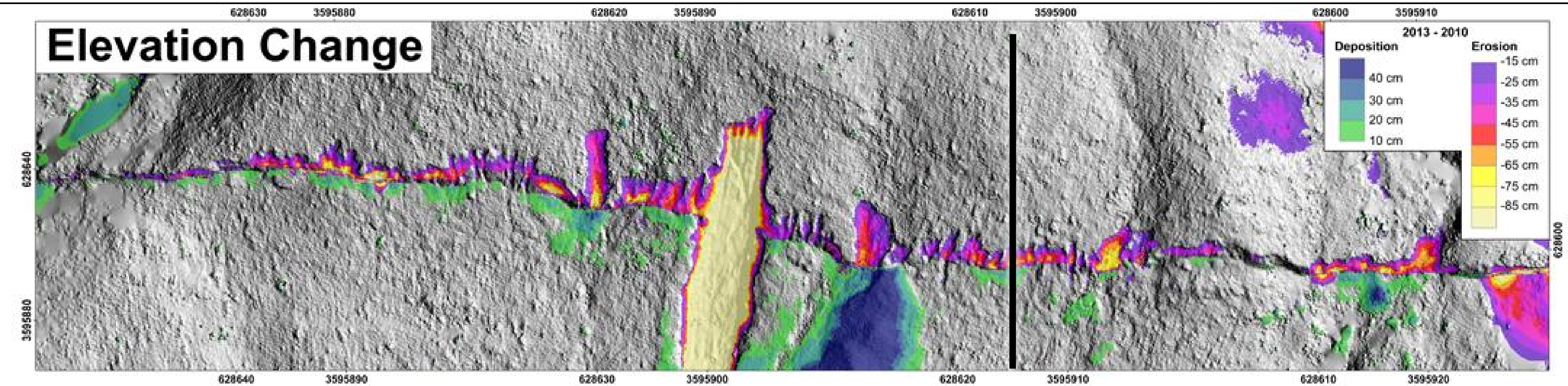

10 m

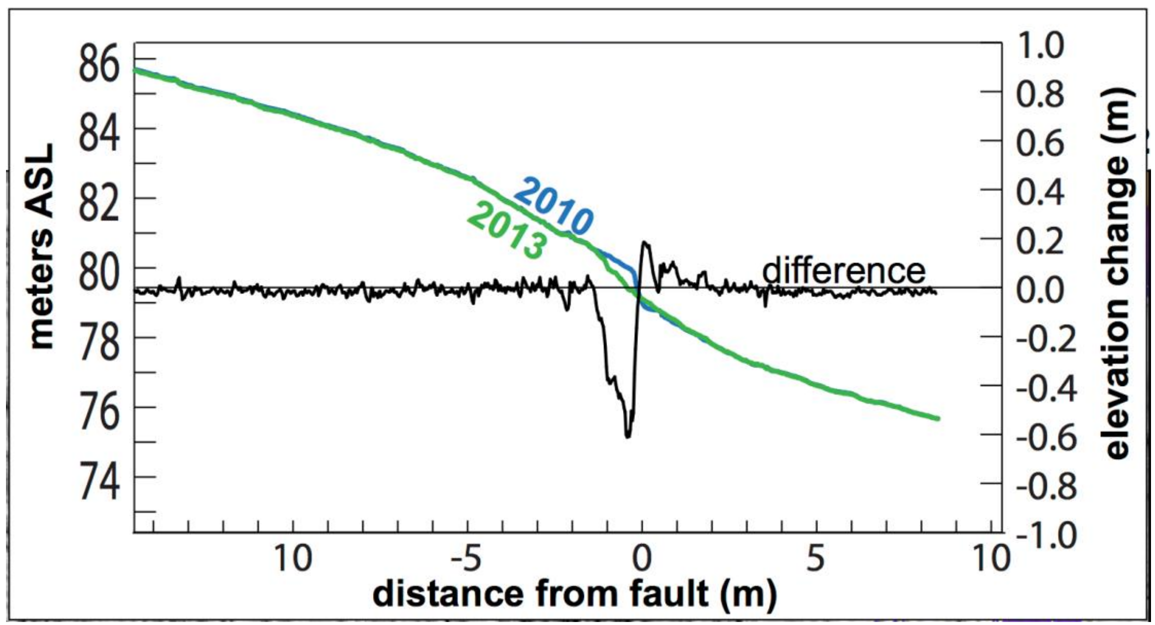

Austin Elliott, UC Davis/Oxford

Degradation of the 2010 El Mayor-Cucapah earthquake scarp

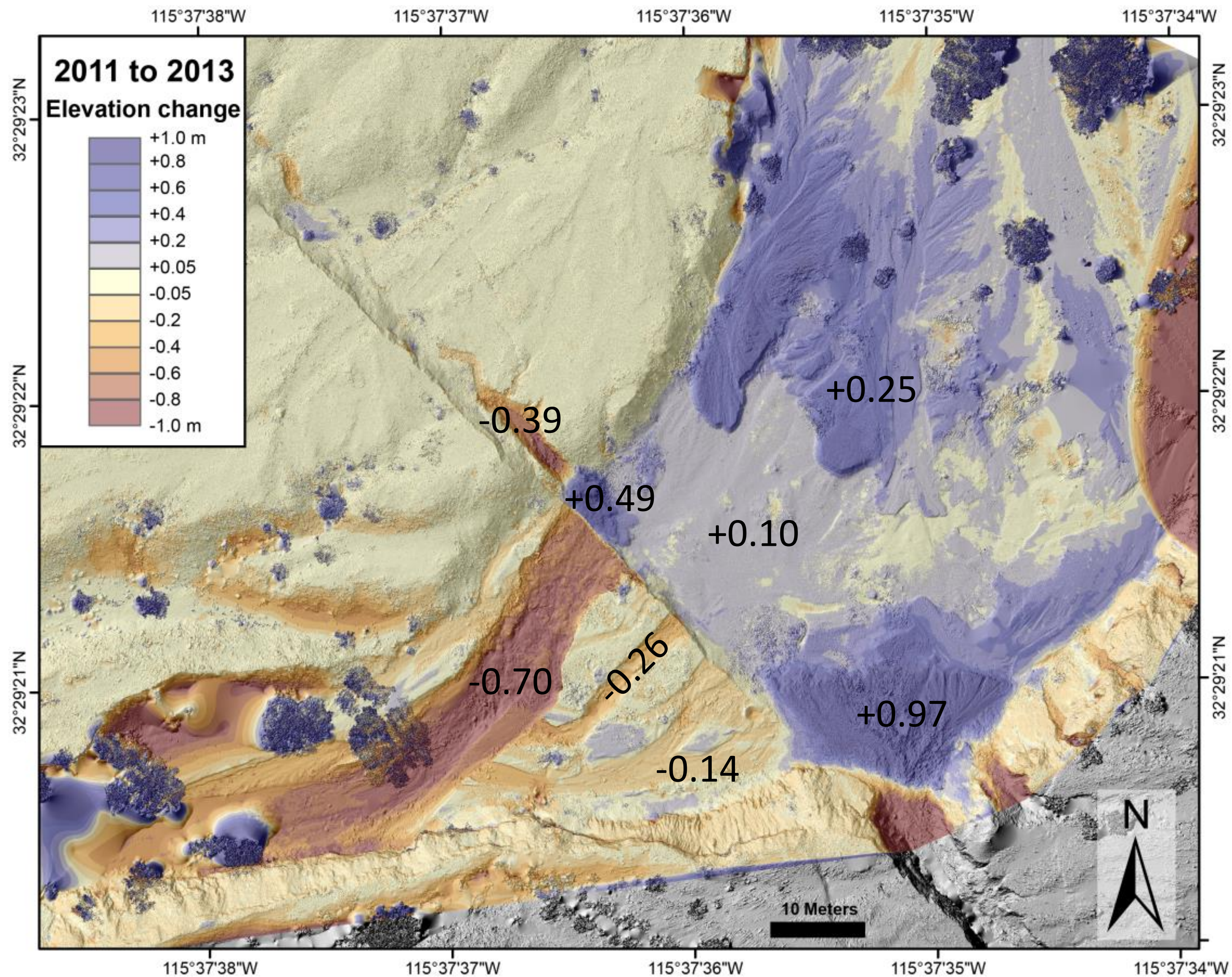

Austin Elliott, UC Davis/Oxford

Aligning point clouds and topographic change detection

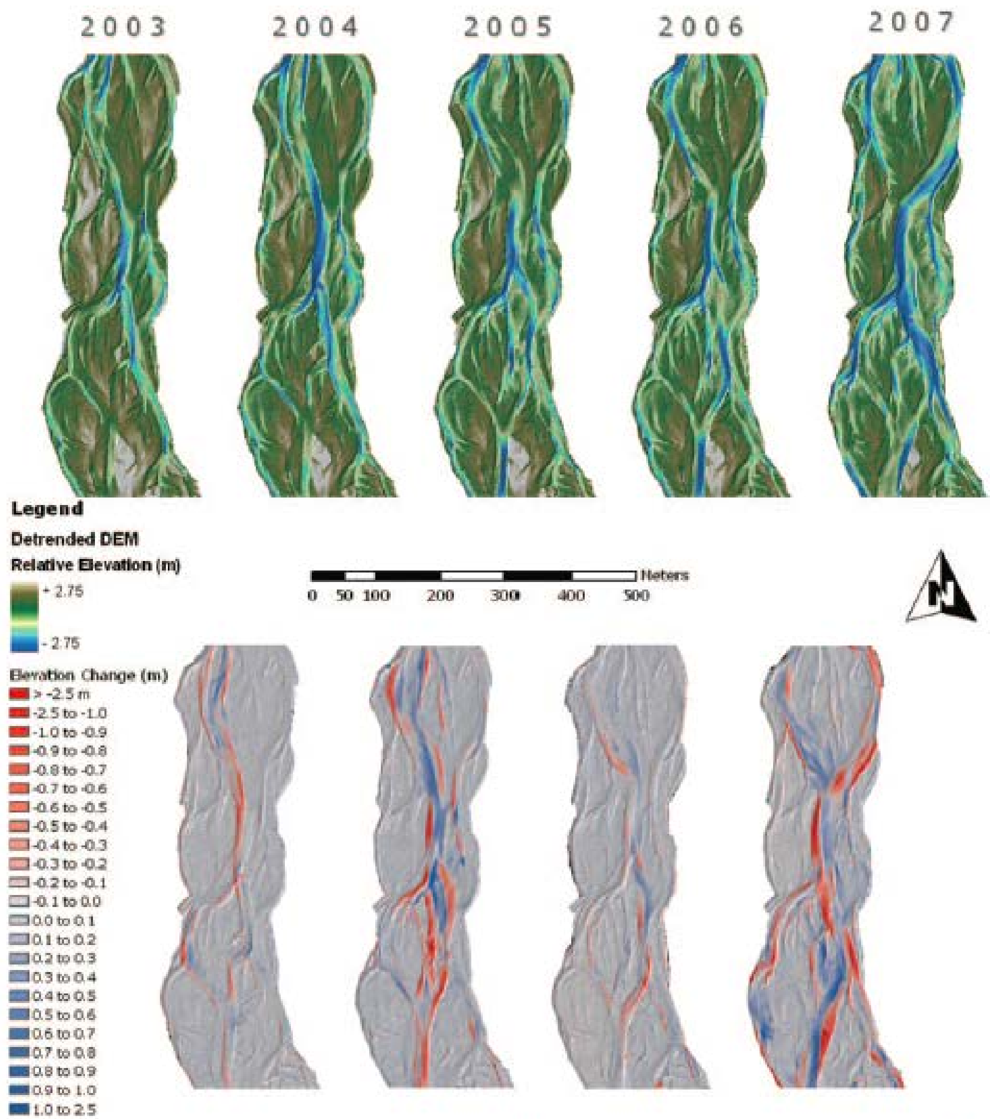

Figure 2. Detrended DEMs and DoD for 2003 to 2007. Note that the hillshades from the more recent year in the DoD are shown behind the DoD for context. This figure is available in colour online at www.interscience.wiley.com/journal/espl

RTK dGPS surveys tied to base stations occupying the same known point.

Point clouds are in exactly the same reference frame from the start.

DEMs are generated and pixel values subtracted: "DEM of Difference" of DOD

Wheaton *et al.* (2010), Accounting for uncertainty in DEMs from repeat topographic surveys: improved sediment budgets, *Earth Surface Processes and Landforms*

Aligning point clouds and topographic change detection

Repeat SfM surveys tied to ground control points surveyed with real-time kinematic GPS (2 – 4 cm accuracy).

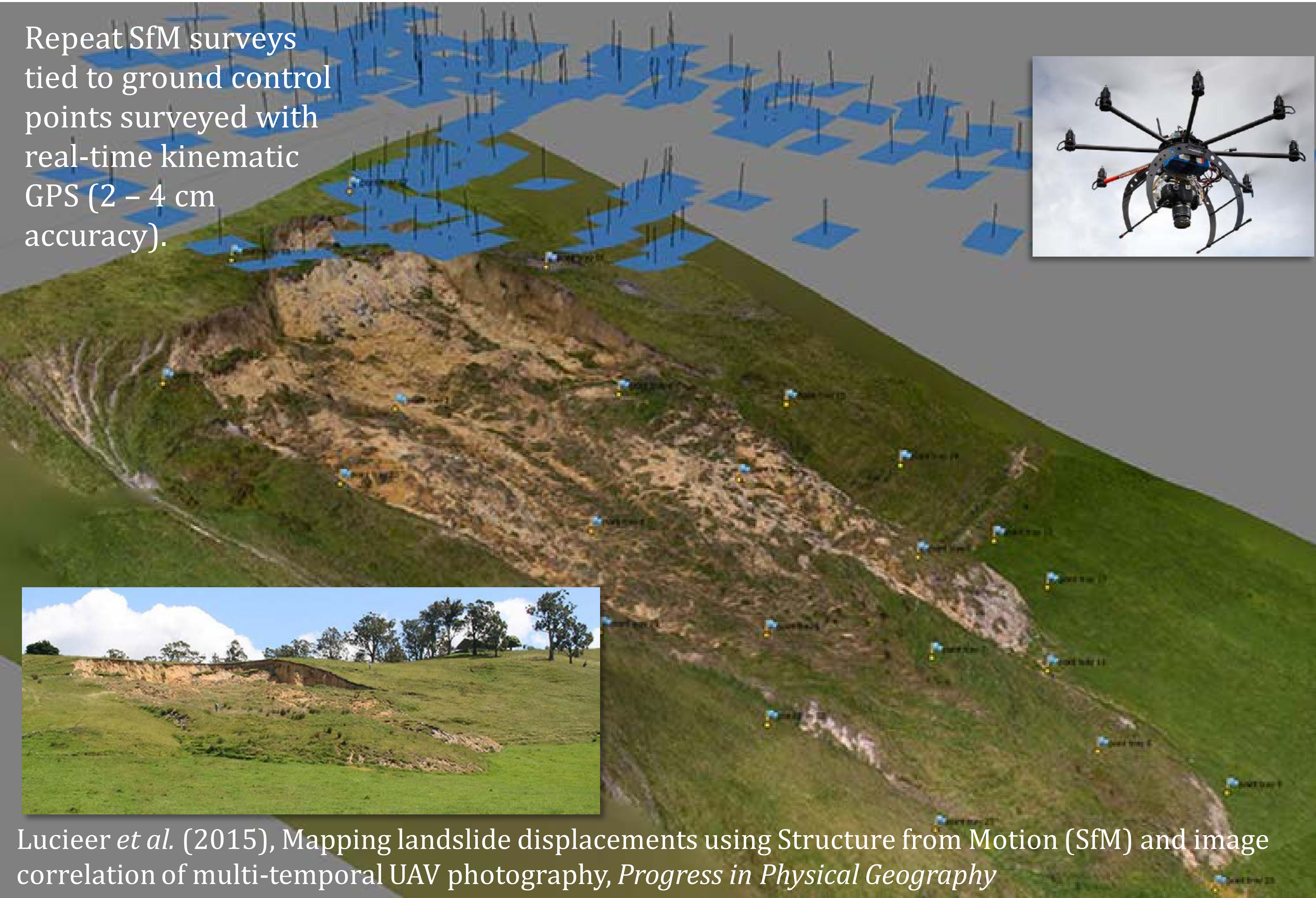

Lucieer *et al.* (2015), Mapping landslide displacements using Structure from Motion (SfM) and image correlation of multi-temporal UAV photography, *Progress in Physical Geography*

Aligning point clouds and topographic change detection

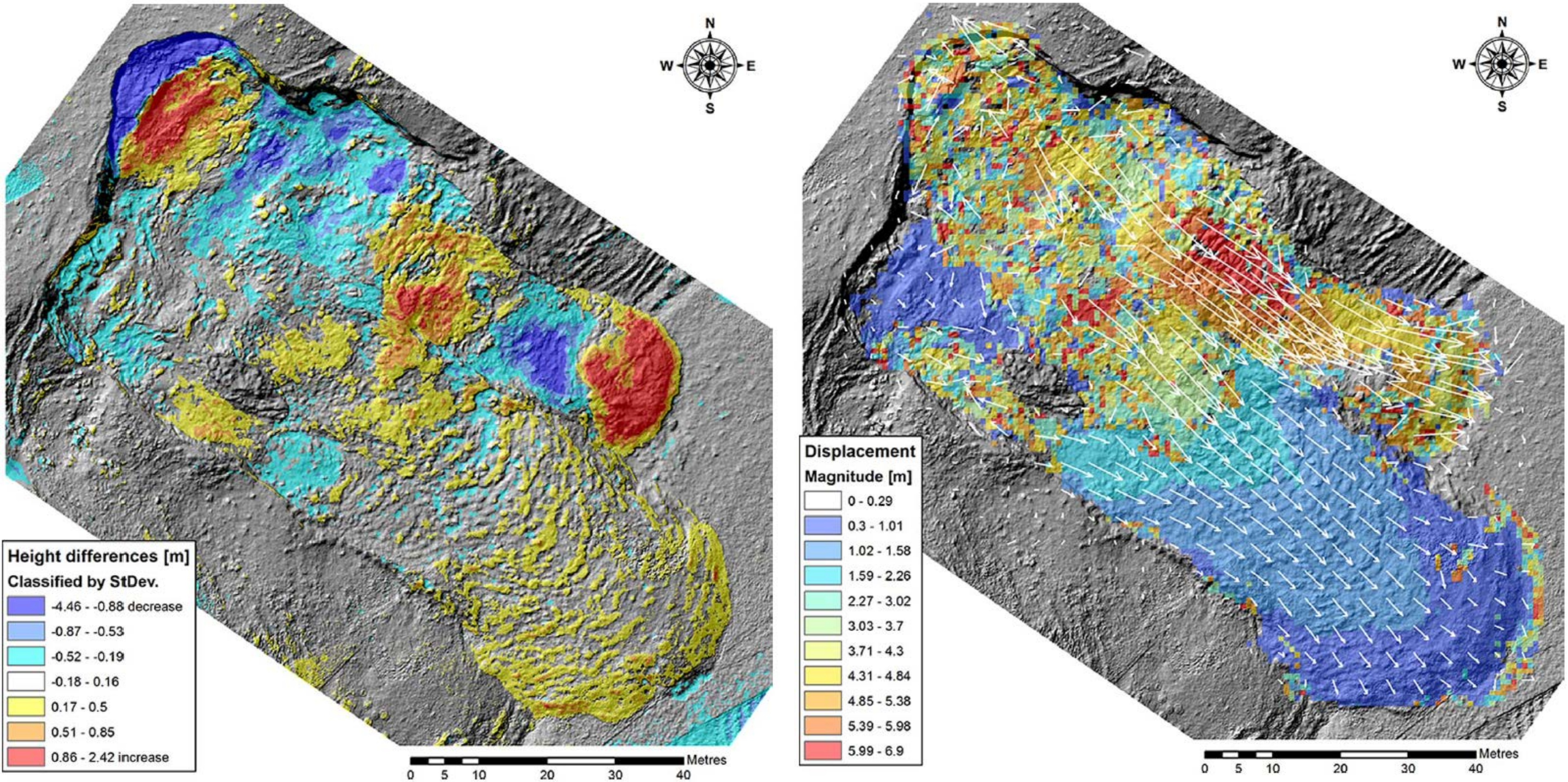

- DEM of Difference (left) and horizontal displacement field from pixel cross-correlation (right)

- Caltech COSI-Corr package: Co-registration of optically-sensed images and correlation
http://www.tectonics.caltech.edu/slip_history/spot_coseis/index.html

Lucieer *et al.* (2015), Mapping landslide displacements using Structure from Motion (SfM) and image correlation of multi-temporal UAV photography, *Progress in Physical Geography*

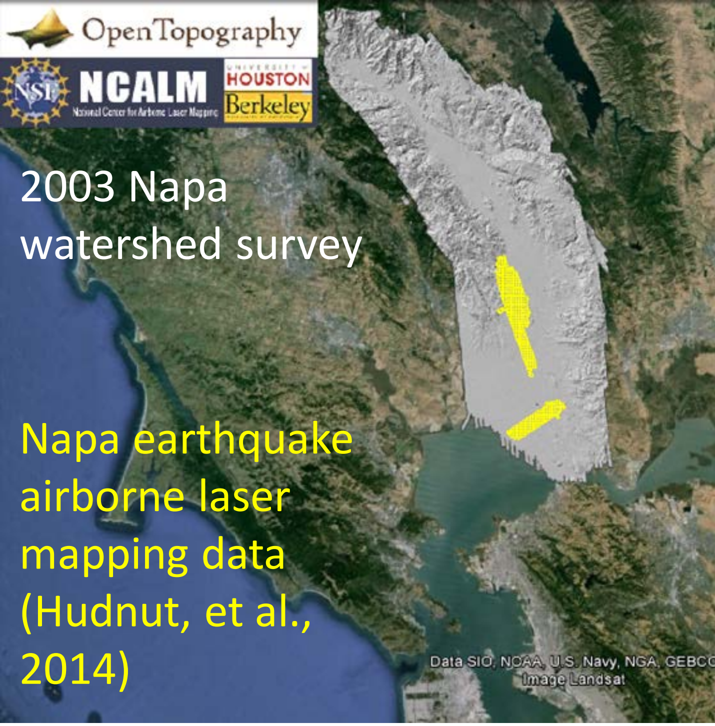

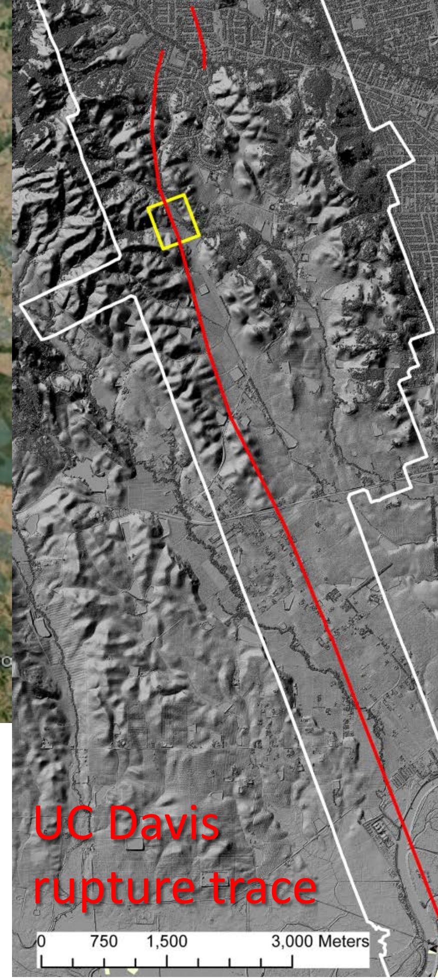

2003 = 2 pts/m^2
2014 = 40 pts/m^2

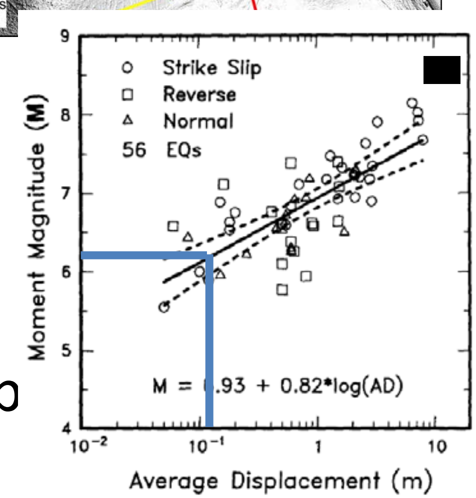

Pre event acquired for watershed management
Post event challenging to fund and acquire
Open data
Data processing: project & clip (post event data >19Gb
Alignment problems; low signal to noise

August 24, 2014 South Napa Earthquake

Overview:
The August 24, 2014, South Napa earthquake (M6.0) produced significant damage resulting from shaking, fault rupture, fault afterslip, and ground deformation. Lidar data were collected to aid specialized work on the South Napa earthquake including: (1) fault afterslip, especially in the Browns Valley residential neighborhood; (2) shaking and correlation to damage such as red- and yellow-tagged structures, especially in the downtown Napa area; (3) seismic hazards of the West Napa Fault System, especially in residential areas; and (4) geospatial analysis and imagery support (such as post-processing of lidar and other imagery that has already been acquired).

Airborne lidar data and imagery were collected on September 9, 2014 as part of multi-agency/institutional response to the August 24, 2014 South Napa Earthquake. Details of the scientific response to this earthquake including the lidar acquisition can be found in Hudnut et al., 2014: USGS Special Open-File Report 2014-1249. Data were collected and initially processed by Towill and are available both as raw files and products as initially delivered by the vendor, as well as the USGS re-processed version of re-classified point clouds and 0.25 meter DEM's from the USGS HDDS Explorer. Point clouds available from USGS and OpenTopography were reclassified (metadata) by the US Geological Survey; this re-processing was funded by FEMA. Orthoimagery were collected by Towill on September 9, 2014, and by Google on August 24, 2014.

Platform: Airborne LiDAR | *Survey Date*: 09/09/2014 | *Survey Area*: 78.00 km^2 | *Point Density*: 22.56 pts/m^2

Full Metadata | Dataset Acknowledgement | *Funders*: CGS, DWR, FEMA, GEER, PEER, USGS | *Collector*: Towill

As high resolution topography data become increasingly ubiquitous, a critical cyberinfrastructure challenge will be to provide processing and analysis solutions that enable rapid extraction of information from these datasets.

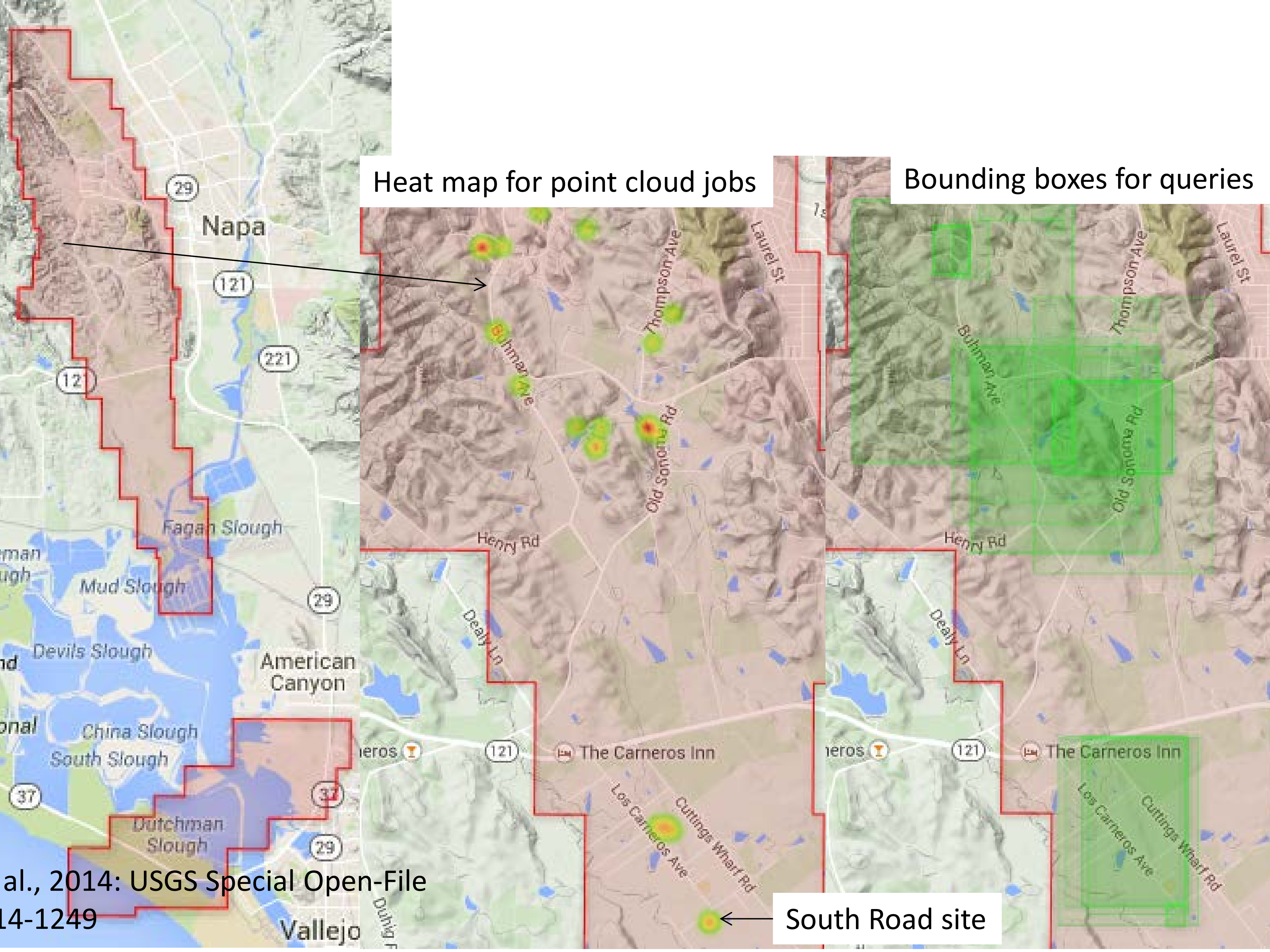

Heat map for point cloud jobs
Bounding boxes for queries
South Road site
al., 2014: USGS Special Open-File
14-1249
Napa
Fagan Slough
Mud Slough
Devils Slough
China Slough
South Slough
Dutchman Slough
American Canyon
Vallejo
Thompson Ave
Laurel St
Buhman Ave
Old Sonoma Rd
Henry Rd
Dealy Ln
The Carneros Inn
Los Carneros Ave
Cuttings Wharf Rd
29
121
221
37

All point cloud data

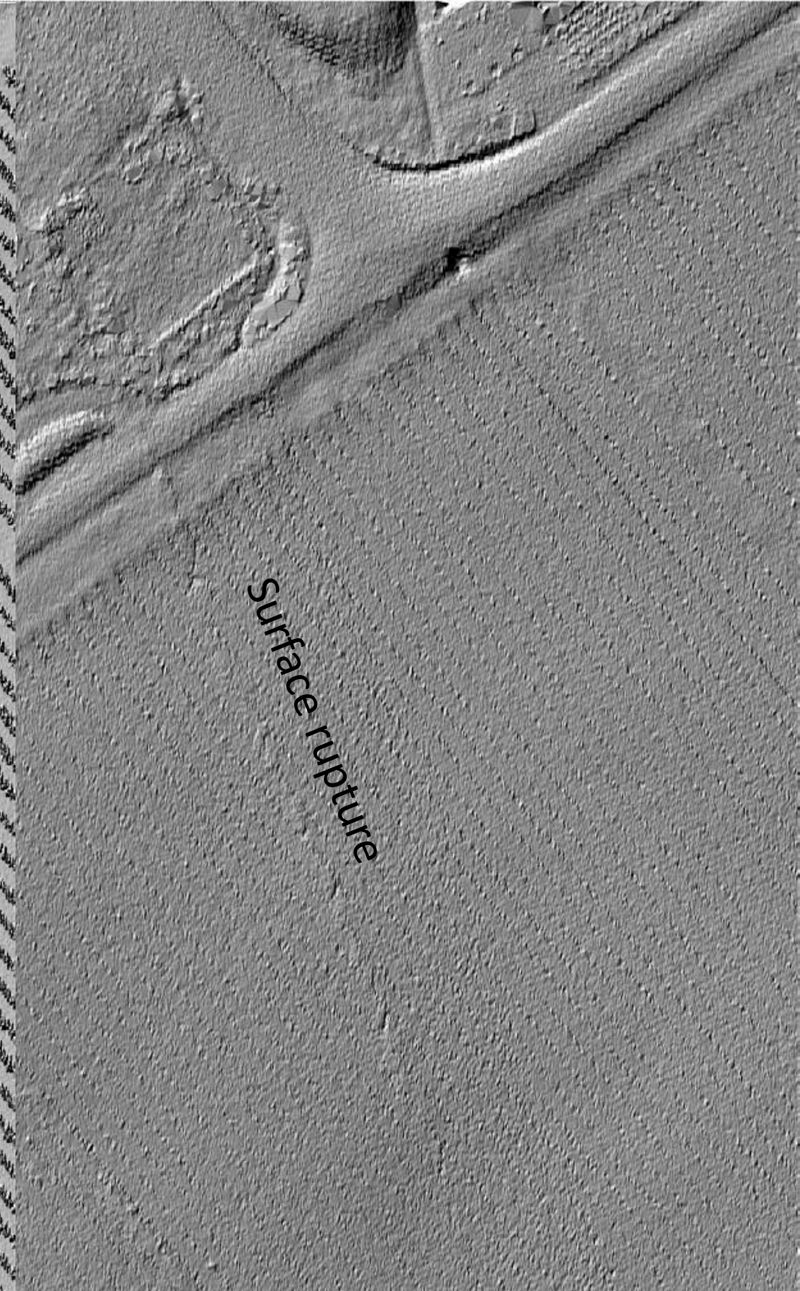

S. Delong and colleagues (USGS) ground classified point cloud data

2003 points white; 2014 colored by time: swath edges evident

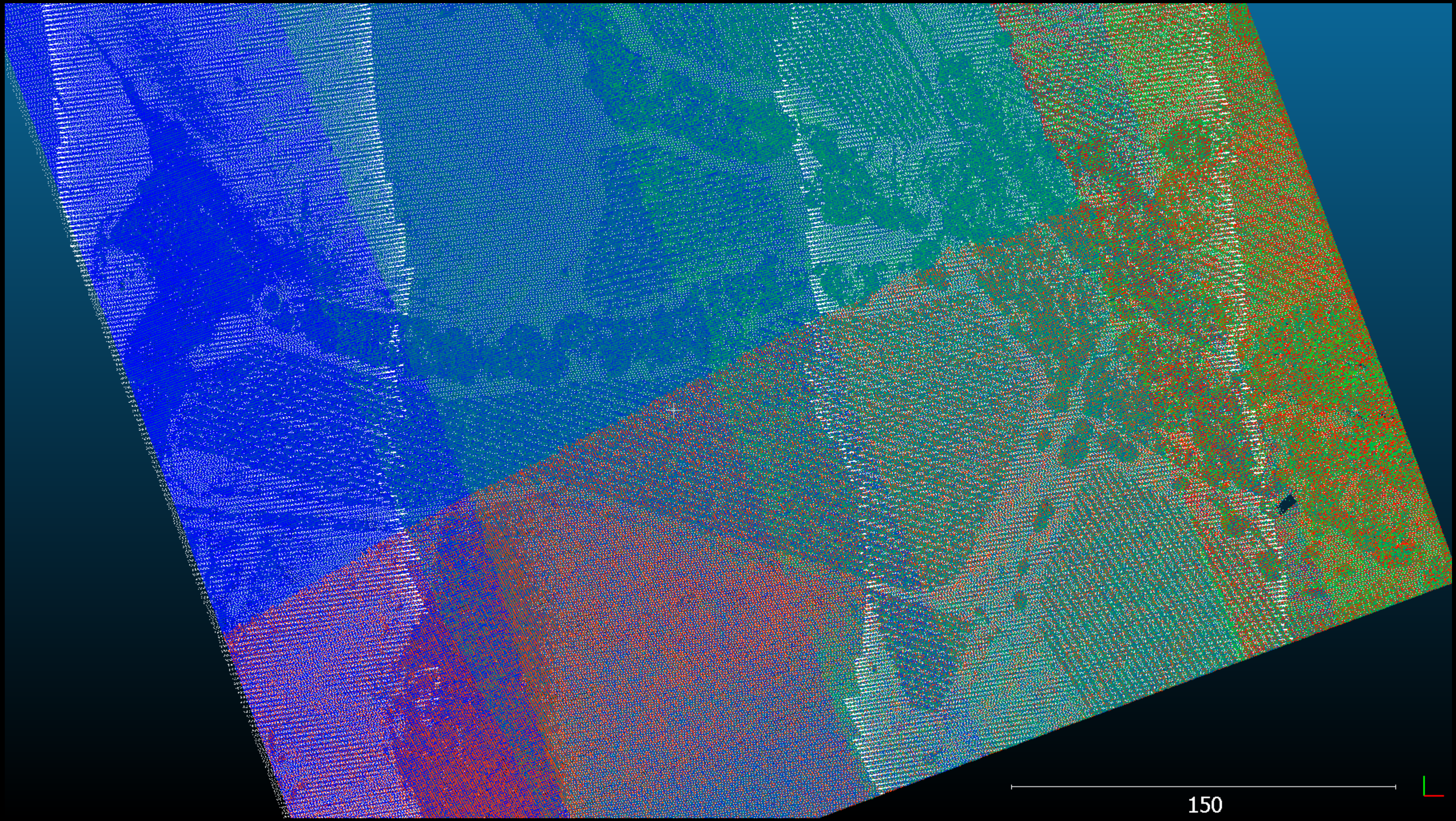

Cloud to cloud difference (using CloudCompare software)

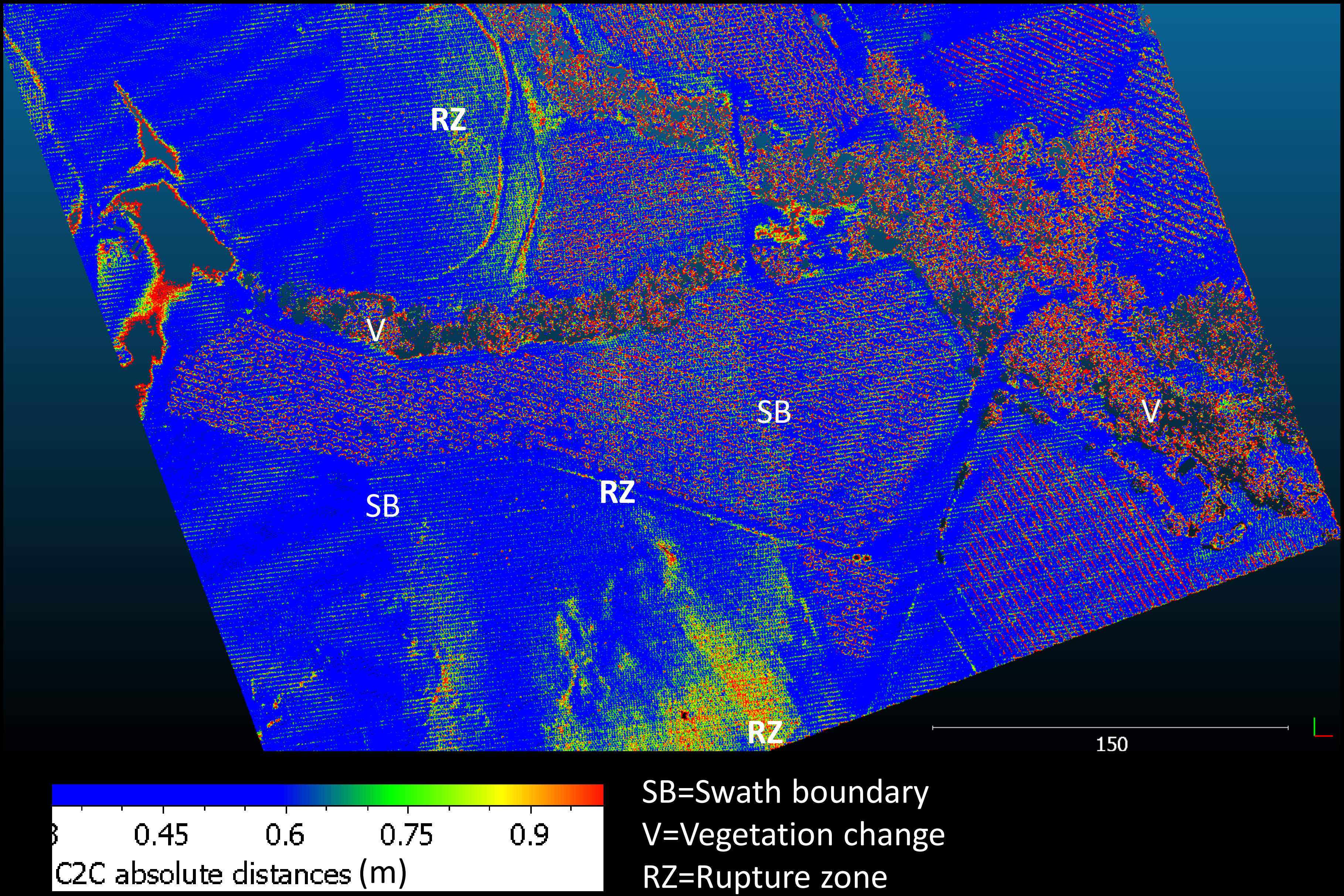

SB=Swath boundary
V=Vegetation change
RZ=Rupture zone

Liquefaction impact on critical infrastructure in Christchurch, NZ (Bray, et al., 2012) Pipeline responses to permanent ground deformation measured by differential topography

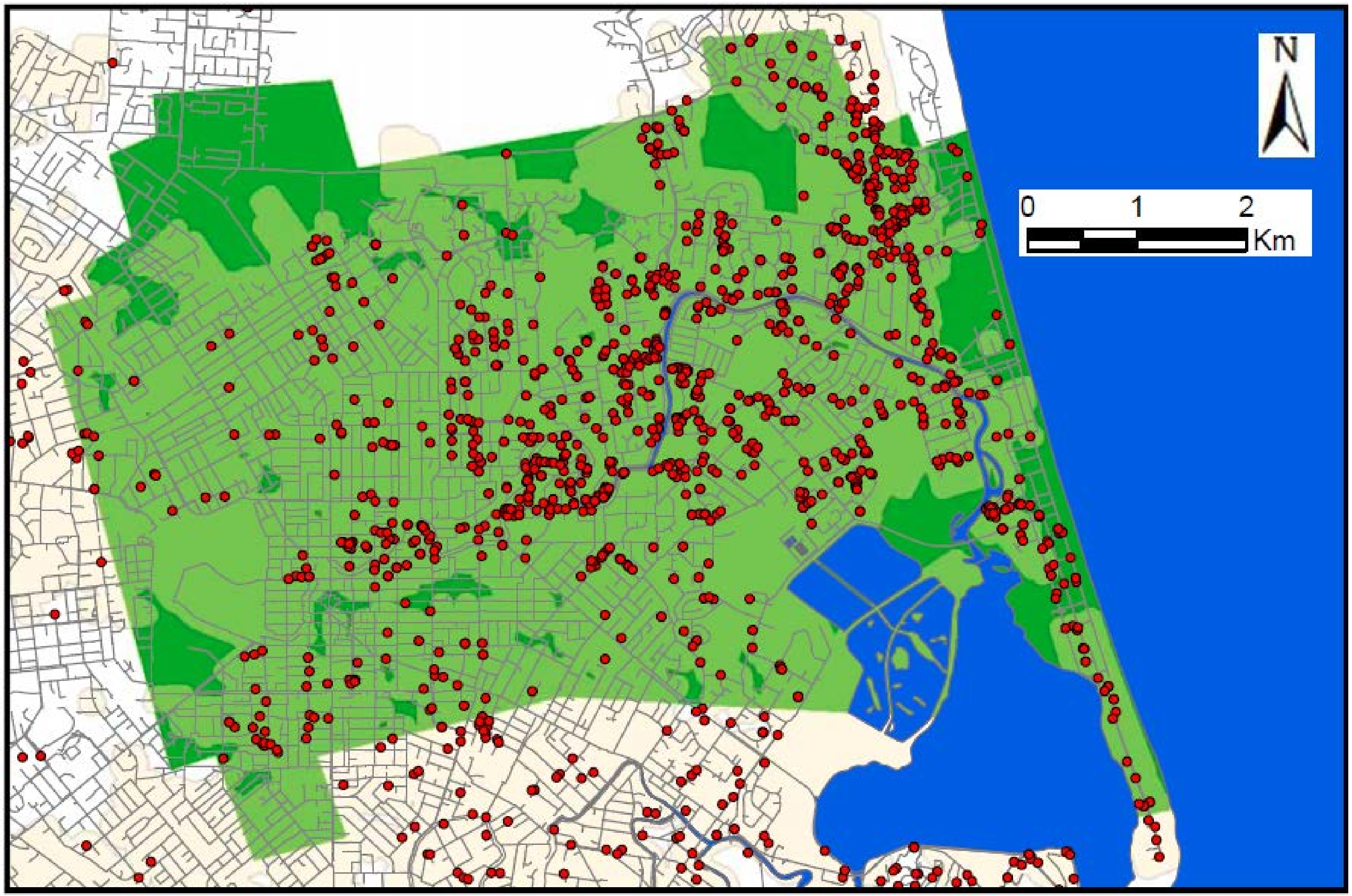

22 Feb. 2011 earthquake; $\beta = (dv_1 - dv_2)/l$ [angular distortion from vertical difference; l = 5 m]

Repairs — Pipelines ■ water □ Liquefaction ■ Measured LiDAR Vertical Displacment

Repeat topography survey from Canterbury Earthquake Recovery Authority [CERA] (2012)

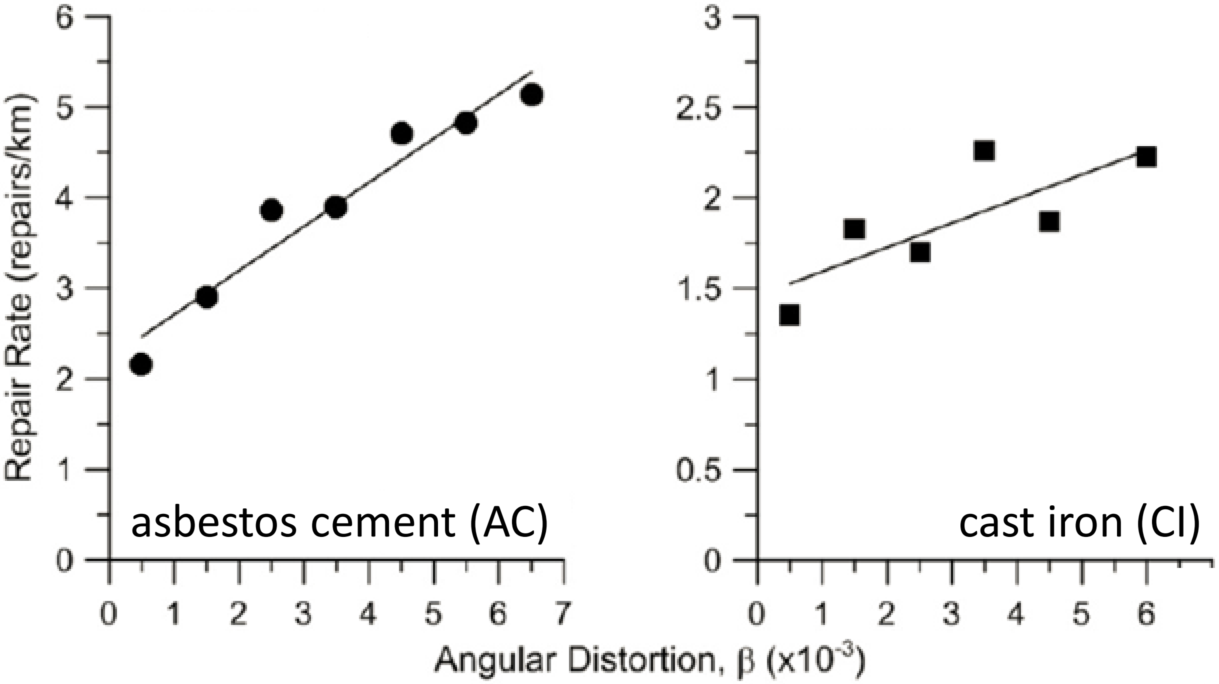

polyvinyl chloride (PVC)
earthenware (EW)
reinforced concrete pipe with rubber rings (RCRR)
concrete (CONC)

AC uses a weak collar that is susceptible to cracking in response to rotation due to differential settlement

CI has additional wall thickness at the joints

Repair rate as a function of angular distortion for different pipe types